THESIS FOR THE DEGREE OF DOCTOR OF PHILOSOPHY (PHD)

Organization of extracellular matrix macromolecules in the vestibular nuclear complex of the rat and frog, and their possible role during compensation

by BOTOND GAÁL

SUPERVISOR:
PROF. DR. MATESZ KLÁRA

UNIVERSITY OF DEBRECEN
DOCTORAL SCHOOL OF DENTAL SCIENCES
DEBRECEN, 2014.

CONTENTS

LIST of ABBREVIATIONS

bHABP:	biotinylated Hyaluronan Binding Protein
BSA:	Bovine Serum Albumin
bWFA:	biotinylated *Wisteria floribunda* agglutinin
CNS:	Central Nervous System
CS:	Chondroitin Sulfate
CSPG:	Chondroitin Sulfate Proteoglycans
DAB:	3, 3'-diaminobenzidine-tetrahyrdochloride
DVN:	Descending Vestibular Nucleus
ECM:	Extracellular Matrix
EGF:	Epidermal Growth Factor
GAG:	Glycosaminoglycan
HA:	Hyaluronan
HAPLN:	Hyaluronan and Proteoglycan Link Protein
HAS:	Hyaluronan Synthase
HC:	Histochemistry
IHC:	Immunohistochemistry
LP:	Link Protein
LTD:	Long Term Depression
LTP:	Long Term Potentiation
LVN:	Lateral Vestibular Nucleus
MMP:	Matrix Metalloproteinase
MVN MC:	Magnocellular part of Medial Vestibular Nucleus
MVN PC:	Parvocellular part of Medial Vestibular Nucleus
NGS:	Normal Goat Serum
NHS:	Normal Horse Serum
NRS:	Normal Rabbit Serum
PBS:	Phosphate Buffered Saline
PNN:	Perineuronal Net
RT:	Room Temperature
SVN:	Superior Vestibular Nucleus
TN-C:	Tenascin-C
TN-R:	Tenascin-R
UL:	Unilateral Labyrinthectomy
VNC:	Vestibular Nnuclear Complex
VOR:	Vestibulo-Ocular Reflex
WB:	Western blot

1. INTRODUCTION

„a delicate covering, mainly reticular in structure, but also in the form of tiny tiled scales or an interrupted envelope which sorrounds the cell body of all nerve cells and continues along their protoplasmic extension…" Golgi

Since the recognition of Camilo Golgi, published in 1898, it is known that the extracellular space of the nervous tissue contains different macromolecules that form a net-like composition covering nerve cell bodies, dendrites and axon initial segments. The first period of enthusiastic pericellular net investigation was started by Golgi and ended by Ramon y Cajal, who claimed in 1911 that *"…the pericellular net is not nervous; …this net is due to the coagulation of a substance dissolved in the pericellular fuild"* (Vitellaro-Zuccarello et al. 1998). In the early 1900s a diffuse and pericellular net was defined. During this time in Italy, a neurologist and psychiatrist, Carlo Besta developed a modified methylene blue staining to visualize the nets. He successfully mapped the pericellular nets of neurons in various mammals and human, and stressed first that the morphology of pericellular net varies with animal species and cell types. His experiments suggested that the net is not modified after lesions, thermal variations or starving. Later in the 1931 Belloni found interesting alterations of pericellular and diffuse nets in human cerebropathies like dementia, diffuse gliosis and psychiatric diseases, by that supporting the theory of Nissl, or Alzheimer. First Held, then Belloni proposed the net's glial origin.

But the authority of Cajal's claims against the existence of the pericellular nets had strong impact; therefore no further interest was there for the pericellular net in the next fifty years. The first scientific acknowledgement revealing that the molecular assembly of the network is close to that of connective tissues' extracellular matrix (ECM) was in the early 1970s (Tani and Ametani 1971). Due to the lack of advanced techniques at that age, only a few of the macromolecular components (incl. chondroitin sulfate proteoglycans (CSPG), hyaluronan (HA), fibronectin, collagens) were known to be present in the nervous ECM, until the 1990's (Margolis et al. 1975; Rutka et al. 1988; Carbonetto 1984; Sanes 1989). Today, in the new wave of perineuronal matrix research, high resolution laboratory methods, like lectin histochemistry or immunohistochemistry, microscopic imaging, or electron microscopy are available. Until today, a growing number of evidence proves that these molecules play important regulative roles in morphogenetic processes, substance transportation, cell

signaling, cell migration, plasticity events, axon regeneration etc., in the nervous tissue, under both physiological and pathological conditions.

One open problem of neurological medicine is the treatment of patients suffering from disturbances caused by unilateral deficit of the vestibular apparatus. Such conditions occur for example in Meniere syndrome or after the schwannoma of the 8^{th} cranial nerve, and neurodegeneration. The unilateral deafferentation of the brainstem vestibular nuclear complex (VNC) results in various static and dynamic symptoms due to the disturbance of wide spreading connections of the VNC. After time the static symptoms will be restored, but the dynamic disturbances only settle, but never get completely normalized (Dieringer 1995; Precht et al. 1966; Curthoys and Halmagyi 1999). This is the phenomenon of vestibular compensation, the process involving the plasticity of the nervous system adjusting neuronal activity to the changed conditions. Plastic events involve various changes in the synaptic transmission and reorganization, axonal sprouting, neurogenesis, glial reaction (Dityatev and Schachner 2003; Dityatev and Rusakov 2011). Increasing number of evidence is reported on the role of ECM macromolecules in neuronal plasticity, regeneration and inhibition of regeneration after lesions (Rhodes and Fawcett 2004; Dityatev and Schachner 2003).

The present thesis is devoted to provide better understanding of the possible roles of extracellular matrix macromolecules in the vestibular system during physiological state in rat and frog, and after unilateral labyrinthectomy in rats.

2. SCIENTIFIC BACKGROUND

2.1 Molecules of the extracellular matrix in the central nervous system

In the central nervous system (CNS), the intercellular space between neurons and glial elements is approx. 10-20% of the total brain volume (Zimmermann and Dours-Zimmermann 2008). This extracellular gap contains the network of extracellular molecules providing the working environment for neurons. The ECM molecules are produced intracellularly and secreted to form a dense network of proteins and carbohydrate-like glycans. Structurally the ECM provides neural cells with points of anchorage and may allow migration of cells to distinct CNS regions. Chemically, it is a source of diverse molecular signals that guide cellular growth, differentiation, activity in pathological conditions, and survival.

2.1.1 Overview on the function of extracellular matrix molecules in the CNS

(**1**) In the adult nervous system the ECM molecules are involved in *trafficking soluble and membrane-bound molecules*. Maintenance of the steady state extracellular environment is essential for physiological neuronal activity, especially for fast reacting neuronal circuits. (**2**) By accumulating around neuron cell bodies, proximal dendritic segments, axon hillock or preterminal axons, the ECM is an *important stabilizer of synaptic connections*. (Blosa et al. 2013; Frischknecht et al. 2009). (**3**) ECM molecules *influence neuronal activity* during normal and pathological conditions, and neuronal activity influences ECM appearance. (Dityatev and Fellin 2008; Dityatev and Rusakov 2011; Dityatev and Schachner 2003; Hartig et al. 1999; Morita et al. 2010; Sykova and Nicholson 2008). (**4**) The different ECM molecular components are associated to several membrane bound receptors or synthases. Anchoring to the cytoskeleton they are *involved in molecular cascades* controlling synaptic trafficking, or they can restrict mobility of neurotransmitters and postsynaptic receptors (Dityatev and Rusakov 2011). (**5**) In the past decade ECM molecules are considered as the *fourth component of synapses*, termed as '*tetrapartite'* synapses (Dityatev and Rusakov 2011). They are shown to interact with the pre- and postsynaptic membranes and astroglia, and they are able to regulate the activity of synaptic receptors and ion channels (Dityatev and Rusakov 2011; Dityatev and Schachner 2006). (**6**) *During development*, specific ECM components are secreted in spatial and temporal timing, to *facilitate the migration and engagement of newly born neurons*, to promote steps of differentiation, or to provide guidance cues for axonal growth and target finding (Galtrey and Fawcett 2007b; Oohira et al. 2000), as well as

regulating synaptogenesis and synaptic activity. (**7**) Clinically important to note that by CNS gliomas the perivascular or periaxonal invasion of *tumor cells* triggers the release of extracellular proteases which, by cleaving, will modify the original ECM composition and surface receptors, to facilitate their own diffuse *spreading* (Dityatev and Fellin 2008; Dityatev and Rusakov 2011; Dityatev and Schachner 2003; Hartig et al. 1999; Morita et al. 2010; Sykova and Nicholson 2008; Mentlein et al. 2011).

2.1.2 Organization of ECM in the CNS

Molecules of the ECM are present in various extracellular compartments of the brain tissue. (**1**) Basement membrane is a sheet-like plate that lies under endothelial cells of the cerebrovascular system, and provides boundary between vessels and CNS parenchyme. It is also found in the subpial layer. The molecules composing it are collagen, entactin, fibronectin, distroglycan and perlecan (Lau et al. 2013). (**2**) The perineuronal net (PNN) that is a dense layer of mesh-like network, built up by accumulations of matrix molecules around the neuronal soma, proximal segments of dendrites, and the axons' initial segments. The PNN, if labeled, demarcates the neuron somas, proximal parts of neuronal processes, and can be well distinguished from the less condensed neuropil. Principal molecular constituents are the hyaluronan, CSPGs, tenascin-R and various link proteins (Celio et al. 1998; Zimmermann and Dours-Zimmermann 2008; Kwok et al. 2011). During development PNN appears at critical times of synaptogenesis, where it is believed to fulfill cation buffering, neuroprotective, axonal guiding, and structural roles (Soleman et al. 2013). PNNs are generally present embracing GABA-ergic neurons and pyramidal cells, as well as some populations of motoneurons in the brainstem and spinal cord, and various other neurons in the sensory systems (Galtrey et al. 2007; Soleman et al. 2013). The formation of PNN is activity dependent, it surrounds synapses of only a selected neuronal subpopulation (Dityatev and Schachner, 2003, 2006). (**3**) The neural interstitial matrix consists of ECM molecules in the interneuronal compartment of the parenchyme that are not tightly associated to basement membranes or perineuronal nets, but considered just in the neuropil. It shows a highly area dependent expression, which, as mentioned above, is activity dependent (Sykova and Nicholson 2008). Molecular components are the hyaluronan, CSPGs, tenascins and link proteins. (**4**) Recently, a new compartment, the preterminal segment of axons and boutons has been distinguished to be enwrapped by ECM accumulation, termed as the axonal coat (AC). It was first described by Brückner et al. (2008). (**5**) Along white matter bundles, in nodes of

Ranvier, accumulation of mainly lecticans and link proteins are reffered as the nodal ECM (Dours-Zimmermann et al. 2009; Bekku et al. 2010).

In the present study we focused on the following ECM molecules in the CNS the (**1**) HA, consisting of repeating non-sulfated disaccharide chains, being the backbone of ECM; (**2**) the CSPGs, mainly lecticans, having various number of sulfated GAGs on the core protein, and by N- and C- terminal domains interact with hyaluronan and tenascins, to form the molecular meshwork; (**3**) glycoproteins which are the link proteins, small sized stabilizers of lecticans to hyaluronan bond, and tenascins, the adhesive molecule to interact with CSPGs, laminin or fibronectin.

Hyaluronan

The HA is a non-sulfated polymer of repeating dimers composed of D-glucuronic acid and N-acetylglucosamine, producing chains up to 25,000 dimers (see for review Fraser et al. 1997; Vigetti et al. 2014). Despite the simple basic structure, hyaluronan forms complex secondary and tertiary structures, with differing size and conformation being the key organizer of ECM, especially in the PNN. HA is a GAG that does not bind to other proteins covalently, thus doesn't build proteoglycans. It is ubiquiter in most of the tissues in various amounts, and its structure is conservative in vertebrates. It carries strong negative charge that traps cations, water, or other extracellular trafficked molecules.

Until today there isn't a known specific HA receptor expressed by neurons, but, their transmembrane hyaluronan synthase (HAS) enzymes are responsible for double roles (Weigel et al. 1997). Firstly, they synthesize HA into the extracellular space, secondly, they are the cell surface receptors for HA by anchoring the molecules. In mammals, HA is produced by either of the three isoenzymes, the HAS1, HAS2, and HAS3. The HA content of a tissue is adjusted by active balance, where anabolism and catabolism is regulated by neighboring cells. The latter is controlled by hyaluronidase enzyme mediated fragmentation, or by oxygen free radicals followed by diffusion through lymph. In the juvenile brain HA is ubiquitous and is present in large amount, but later in development it gradually downregulates, although it is present throughout life. HA has permissive role to axon growth during development or after injuries (Margolis and Margolis 1997; Bausch et al. 2006).

The ability of HA to activate intracellular signaling cascades requires interactions with cell-associated hyaluronan-binding proteins, such as CD44 or RHAMM (receptor for hyaluronan mediated motility). These mediate HA dependent biological functions, depending on cell and tissue type, like cell migration, proliferation and transformation, phosphorilation,

or tumor cell invasion (Lindwall et al. 2013; Hall and Turley 1995). The CD44 binds to hyaluronan through an extracellular linker domain, whereas an intracellular domain provides a direct link between hyaluronan, cytoskeletal proteins and signal transduction pathways. The RHAMM is present, as cell surface protein and receptor binding hyaluronan, but also in the cytoplasm, interacting with cytoskeleton, and nucleus (Hamilton et al. 2007).

Chondroitin sulfate proteoglycans

CSPGs are built of a core protein of variable composition, covalently binding to chondroitin sulfate glycosaminoglycans. The core proteins are assemblies of molecules composed of multiple domains that serve their integration into the ECM. There are four major groups of CSPGs: (**1**) lecticans, including aggrecan, versican, brevican, and neurocan; (**2**) phosphacan or receptor-type protein-tyrosine phosphatase ß; (**3**) small leucine rich proteoglycans (decorin, biglycan); (**4**) others (neuroglycan-C) (Galtrey and Fawcett 2007a). Our research focuses on lectican family, as detailed below (Fig. 1).

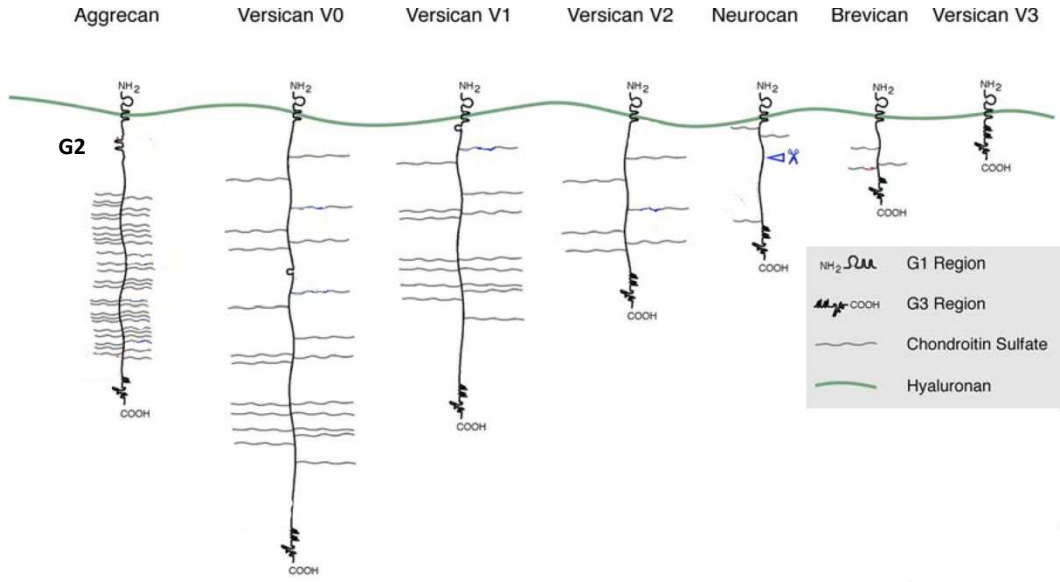

Figure 1. Schematic structure of lecticans. In the mautre CNS aggrecan, versican V2, neurocan, and brevican are present. They bind to HA with N-terminal G1 domain, and to tenascins by C-terminal. Arrowhead shows cleavage site on neurocan. (modified after Zimmermann and Dours-Zimmermann, 2008)

The chondroitin sulfate GAG chains are long linear molecules; they are formed by repeating disaccharide units of D-glucuronic acid and N-acetyl galactosamin, linked by ß-glycosidic bonds. During matrix assembly GAG chains are linked to serine residues in the core proteins via xylose, by the xylosiltransferase enzyme. After xylose addition, a linkage tetrasaccharide is generated by addition of N-acetyl-ß-galactose. The disaccharides are polymerized into long chains by the human chondroitine synthase and chondroitin

polymerizing factor. In the next step GAGs are modified by sulfation. The position of the sulfating substituent determines the type of the chondroitin sulfate. CSs can be monosulfated in the 4 (CS-A) or 6 (CS-B) postion of the galactose, or disulfated on 2 and 6 positions of glucuronic acid and galactosamin (CS-D), or on 4 and 6 positions of galactosamin (CS-E). The enzymes chondroitin sulfotransferases are responsible for sulfation patterns. The sulfation of the GAG chains at certain positions and patterns determines their ability to bind other molecules (Galtrey and Fawcett 2007a).

The number of GAG chains connected to a core protein is one considerable difference among lecticans.

Aggrecan

The structure of the articular cartilage aggrecan is well corresponding to the one found in the nervous system (see for review Morawski et al. 2012; Fig. 1). The aggrecan isolated from tissues is polydisprese due to its giant molecular size ranging at 1-3 MDa molecular weight, due to variations in the number and length of GAGs attached. It consists of a linear core protein, 300 kDa in size, with glycosylated serine residues. The core protein has 3 globular domains, the G1, G2 and G3. It is only the aggrecan that carries the G2 domain. GAG chains are connected at the long segment between G2 and G3 domains. Two types of GAG chains, the chondroitin sulfate and keratan sulfate can substitute. The first one containing 40-50 GAG repeats and present up to 100 chains per core, while the latter one only consists of 20-25 repeats, having only 30 chains attached, intermittent to GAGs there are 8-10 short O-linked oligosaccharides, reaching the length of up to 90 nm. The disaccharide building blocks of GAGs carry sulfate or carboxylate groups, which are negatively charged at physiological pH. Each disaccharide has two negative charges, approx. 3000 per “bottlebrush”, thus a polyelectrolyte.

In cartilage, as well as in the nervous extracellular space the aggrecan binds to hyaluronan via loops of the G1 domain, worn on the N-terminal end of the core protein. On HA, aggrecans are in 12 nm distance forming long and relatively wide aggregates, being able to trap water, and counter charged soluble substances, like ions or growth factors (Chandran and Horkay 2012; Schwartz and Domowicz 2004).

The aggrecan is produced by neurons (Matthews et al. 2002; Carulli et al. 2006), and have a non-permissive effect on neural circuitry development, and on post-lesional axon regrowth. The cleaving off of GAGs by chondroitinase ABC, the restricting effect disables (Wang and Fawcett 2012; Galtrey and Fawcett 2007b).

Brevican

As all lecticans, the brevican comprises of an N-terminal globular G1 domain, being able to bind HA, a C-terminal domain carrying a G3 domain, and between is the chondroitin sulfate attachment region (see for review Frischknecht and Seidenbecher 2012; Fig. 1). Brevican is only expressed in the nervous system, and has no G2 domain. The G1 has immunoglobulin-like loops, followed by two link-protein-like modules. The G3 has an epidermal growth factor (EGF)-like module, a C-type lectin-like domain, and a complement regulatory protein (RP)-like module, having great affinity to binding to tenascin-R. The central part comprises a non-homologous region, where just a small number of chondroitin sulfates (1-5) attaches, at the molecular weight of 140 kDa. Brevican is a part time proteoglycan, with a significant portion of the molecule being in not proteoglycan state. Brevican has been reported to be in an alternatively spliced GPI form, as rare variant. Brevican is localized at the outer surface of neurons, it contributes to PNN formation, particularly present at perisynaptic sites (Blosa et al. 2013; Frischknecht and Seidenbecher 2012), and it has also been shown to surround axon initial segments *in vivo* and *in vitro*. It has been found in a selected group of the Ranvier nodes (Bekku et al. 2009).

Brevican is mainly expressed by glial cells, but in situ hybridization says that neurons produce it in smaller amount in the soma, and travels via axon transport to presynaptic sites, where it empties (Carulli et al. 2006).

The consensus of papers shows that brevican provides a non-permissive environment for regrowing axons, and its enzymatic removal is necessary for enabling recovery (Beggah et al. 2005).

Neurocan

The neurocan wears the general structure of all CSPGs, having the N-terminal G1 domain with the hyaluronan binding globular module and a double Ig-like sequence. The C-terminal G3 domain has an EGF-like sequence, C-type lectin module, ‘sushi’ module and a terminal extension of 45 amino acid. The central part of the molecule carries 3 sulfated GAG substituents, with chain sizes of 22-32 kDa. Additionally there are 40 O-linked oligosaccharides bond to the core protein providing mucin-like appearance. The full length neurocan (245 kDa) is present only in the developing nervous system, but during maturation central part of the core protein is cleaved, then further a 150 kDa N-terminal fragment (recognized by antibody 1F6) and a 130 kDa C-terminal fragment (recognized by antibody

1D1) remains in the extracellular space (Fig. 1). Another 90 kDa cleavage product can remain, after cleaving the core protein at the minor cleavage point, also recognized by the antibody 1F6. After cleavage, N-terminal fragment has 2 GAGs, and C-terminal has 1 GAG substituent (see for review Rauch et al. 2001).

The neurocan is anchored to HA via the N-terminal domain, or by the C-terminal fragment to N-CAM, Ng-CAM (cytoskeleton), axionin-1, tenascin-C and tenascin-R for linking the matrix structure.

Neurocan is believed to play role in nervous tissue development and in tissue remodeling processes parallel with other ECM molecules and cell surface proteins (Friedlander et al. 1994). Full length form is permissive and forms cues for axon guidance. Cleavage products are rather non-permissive. In adults, neurocan is expressed by neurons and contributes in PNN accumulations, but also accumulates in nodes of Ranvier (Bekku and Oohashi 2010).

Versican

Versican is a lectican present in various soft tissues (see for review Wight 2002). The core protein structure follows the general assembly of CSPG lecticans, for it binds to HA by its globular G1domain found on the N-terminal, and at the C-terminal it has two EGF modules, a C-type lectin, and a complement regulatory region. The middle region of the core is encoded by two large exons, in which RNA splicing specifies the chondroitin sulfate attachment regions, determining the types of GAGs binding. The region encoded by exon 7 is called αGAG, the region encoded by exon 8, ßGAG. The mRNA product will give rise to four variants. (1) V0 carries both exon 7 and 8, having 17-23 GAGs of both α- and ßGAGs; (2) V1 possesses only exon 8, carrying 12-15 ßGAGs; (3) V2 resembles only to exon 7, but not 8, carrying 5-8 αGAGs; and (4) V3 possesses neither exon 7 or 8, with no GAG attachment sites, thus carrying no GAG substituent. The length of the molecule severely decreases from V0 until V3 isoforms.

According to versican isoform dynamics the V0/V1, with neurocan, are the first detected in prenatal rat brain, which are then replaced by V2, brevican and aggrecan. The V2 versican (and neurocan, brevican) is exclusively expressed in the CNS, at about 400kDa. The core protein adheres to CD44 receptor, facilitated by C-terminal and by CS-GAG chains, triggering inflammatory progress. Also by the C-terminal G3 domain it can be attached to ß1-integrin receptors of glioma cells promoting invasion. Via N-terminal domains versican attaches to HA. As a biologically active molecule, it is involved in signaling of cell

proliferation, including breast, nervous or prostate cancers, or melanoma, suspectedly through EGF of the G3 domain (Schmalfeldt et al. 2000).

In the adult nervous system versican V2 has a characteristic punctuate occurrence by immunohistochemical labeling. Specific places of accumulations are perisynaptic spaces, myelinated tracts, or nodes of Ranvier, alongside with brevican, tenascin-R and link proteins, providing ion reservoir for saltatory action potential propagation (Bekku et al. 2010). The V2 isoform, represented in the adult CNS, has inhibitory effect on axon outgrowth after CNS mechanical traumas. The cellular origin is oligodendrocytes and NG2 positive cells, a precursor of oligodendrocytes and astrocytes, secreting NG2 proteoglycan (Zimmermann and Dours-Zimmermann 2008).

Glycoproteins

Tenascins

Tenascins are very large multimeric glycoproteins reperesenting a well conserved structure throughout vertebrates (see for review Anlar and Gunel-Ozcan 2012; Fig. 1). In mammals, the group has four members, the tenascin-C, -R, -X, -W, (and –N). The different tenascins have similar macromolecular structure as they follow the same modular arrangement. They have an N-terminal cystein rich oligomerization region composed of 3-4 α-helical heptad repeats, EGF-like parts, fibronectin type-III repeats, and a C-terminal fibrinogen-like globular domain. The heptad domains allow an N-terminal association of the individual subunits that primarily form homotrimers. In tenascin-C and –W an additional cysteine dock permits these trimers to further aggregate into hexameric or '*hexabrachion*' structure. In tenascin-R the cysteine residue is also present, but it only allows trimers to be formed. The number of EGF-like repeats and fibronectin-III domains vary, being subjects of alternative splicing, so different isoforms of tenascins are produced. Tenascin-R contains 4,5 EGF and 9 fibronectin-III repeats, and has two splice variants with 180 kDa and 160 kDa of molecular weights per subunit. The tenascin-C has 14,5 EGF and 17 fibronectin-III, 9 of which can be spliced alternatively, providing 27 different transcripts, at 180-300 kDa. The differences depend on the presence of supplementary fibronectin-III modules between fibronectin 5 and 6. The tenascin-W and –N seems to express from the same gene, and tenascin-X also has various splice variants, but they don't reach significant levels in the CNS.

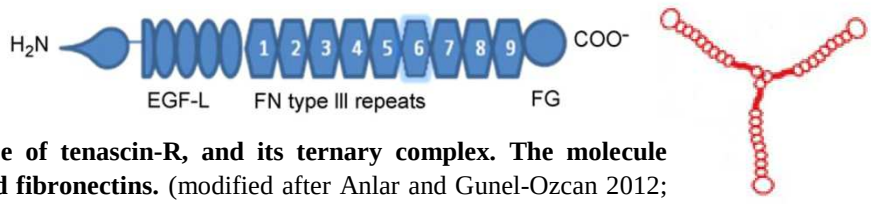

Figure 2. Schematic structure of tenascin-R, and its ternary complex. The molecule contains EGF-like repeats and fibronectins. (modified after Anlar and Gunel-Ozcan 2012; and Rauch 2007).

Tenascins in the CNS bind to a number of ECM and cell surface ligands, mediated by the fibronectin-III modules. Tenascin-R and –C mainly binds to integrins, heparin sulfate proteoglycans (syndecan, glypican), and to cell adhesion molecules of the immunoglobulin superfamily (contactin F11 F3, axonin TAG-1, neurofascin). Other cell surface located binding molecules are the annexin II and receptor protein tyrosine phosphatase. EGF-like sequences of tenascin-C were reported to bind to EGF receptors, but with unknown biological functions. There is strong connection to other ECM partners, particularly to lecticans like the C-terminal G3 domain of aggrecan, brevican, neurocan, forming the ternary network unit composed of HA, lecticans and tenascin-R. Versican, phosphacan and fibronectin may bind to TN-R as well (Zimmermann and Dours-Zimmermann 2008).

Link proteins

Link proteins (LP) belong to the family of glycoproteins that establish binding between lectican and HA in the ECM, stabilizing their aggregates. The group of LPs counts four members: the HAPLN1 (hyaluronan and proteoglycan link protein 1, CRTL1); HAPLN2 (Bral1 – brain derived link protein 1); HAPLN3 (present in smooth muscle and vessels, but not in CNS); and HAPLN4 (Bral2) (Cicanic et al. 2012; Galtrey and Fawcett 2007b; Zimmermann and Dours-Zimmermann 2008).

According to structure, HAPLN1 is a short polypepdite, sharing highly conserved amino acid sequences among vertebrate species. They have 3 modules: Ig like fold at the N-terminal, and two proteoglycan tandem repeats. Its interaction to large CSPG molecules is complex, both by the Ig fold (aggrecan) and by the proteoglycan repeats (versican). The molecular weight is 41, 44 or 48 kDa, differing in their degrees of glycosylation (Cicanic et al. 2012; Zimmermann and Dours-Zimmermann 2008).

LPs are essential constituents of the PNN formation, and are present in relatively larger amounts in the nodes of Ranvier and axonal coats. HAPLN1 glycoprotein is expressed by neurons (Carulli et al. 2006), at the very time prior to PNN assembly. There are growing number of publications about the function of link proteins in the PNN, nervous development, and plasticity.

Other ECM molecules

Other ECM constitutents are present in the CNS, but at spatially or temporally different compartments.

The **phosphacan** is a non-lectican-like proteoglycan. It has two variants determined by their glycosylation. The phosphacan is also considered as the extracellular domain of protein-tyrosin-phosphatase (RPTPζ/β). It binds to cell adhesion molecules, and interacts during the development of the CNS, being either permissive or non-permissive molecule for axon outgrowth or regeneration (Maurel et al. 1994; Faissner et al. 2006).

The **heparan sulfate proteoglycan** family has two subgroups, the syndecans and glypicans. *Syndecans* have 4 isoforms discovered in various tissue types. Syndecan 1 is mainly present in hepatocytes and white blood cells, syndecan 2 is in the nervous tissue activating matrix metalloproteinases (MMP), and also during angiogenesis, syndecan 3 is the most abundant in the CNS, active in development, synaptic plasticity, and appetite regulation in the hypothalamus. Syndecan 4 does ECM-cell adhesion to the cytoskeleton triggering cell signaling pathways (Leonova and Galzitskaya 2013). *Glypicans* have six members having important role in the morphogenesis of tissues regulating through various signaling pathways. It is present during development of the CNS, axon growth, and dendritic spine formation (Svensson et al. 2012).

The *agrin* molecule was widely described in the formation of neuromuscular junction during embryogenesis. It's involved in aggregating acetylcholine receptors and is released at the growing axon's terminal, anchoring to skeletal muscle fiber membrane, where the synaptic contact will be established (Hubbard and Gnanasambandan 2013).

The **glycoprotein family** has the laminins, fibronectins, and reelin molecules as well. *Laminins* are found in variants differing in their α-, β-, and γ subunits, presenting approx 10 different molecules. They are present not only in basal laminas of vessels forming blood brain barrier, but are active parts of synaptic stability, plasticity, and form a sheath for peripheral nerves and neuromuscular junctions (Colognato and Yurchenco 2000). *Fibronectins* have around 20 splice variants, and are present at sites of intensive axon growth. They establish nexus between neuron-ECM or ECM-ECM, regulating axon growth and neuronal adhesion (Meland et al. 2010). *Reelin* plays crucial role in development of the nervous system, regulating neuronal migration in an inside-outside manner. The lack of reelin produces motor abnormalities in the so called reeler mice (Aboitiz and Zamorano 2013).

2.1.3 Assembly of the PNN

The ability to form ECM accumulations at the brain's extracellular space is one of the hallmarks of vertebrate tissue development. The timing of the formation of these aggregates suggests their important properties in the adult brain functions, influencing synaptic plasticity, and maturation of the brain.

During the development of PNN the filamentous HA chains bond to neuronal cell membranes, then associate to G1 domains of distinct lecticans. Their connection is stabilized by LP subtypes, and PNN assembly cannot be executed before LP expression. The G3 domian on lecticans' C-terminal engage to one arm of tenascins, either being TN-R having three or TN-C having six arms. This produces a HA-lectican-tenascin aggregate (Fig. 3). Throughout ontogeny the expression of lecticans changes. The full length neurocan, and versican V0/V1 is present prenatally and early postnatlly, then V2 isoform takes over. On the other hand aggrecan and brevican builds up gradually after birth. Consequently the amount of negatively charged molecules increase, attracting water and cations. This hydrated substance fills the ~20% total brain volume (Schwartz and Domowicz 2004; Zimmermann and Dours-Zimmermann 2008).

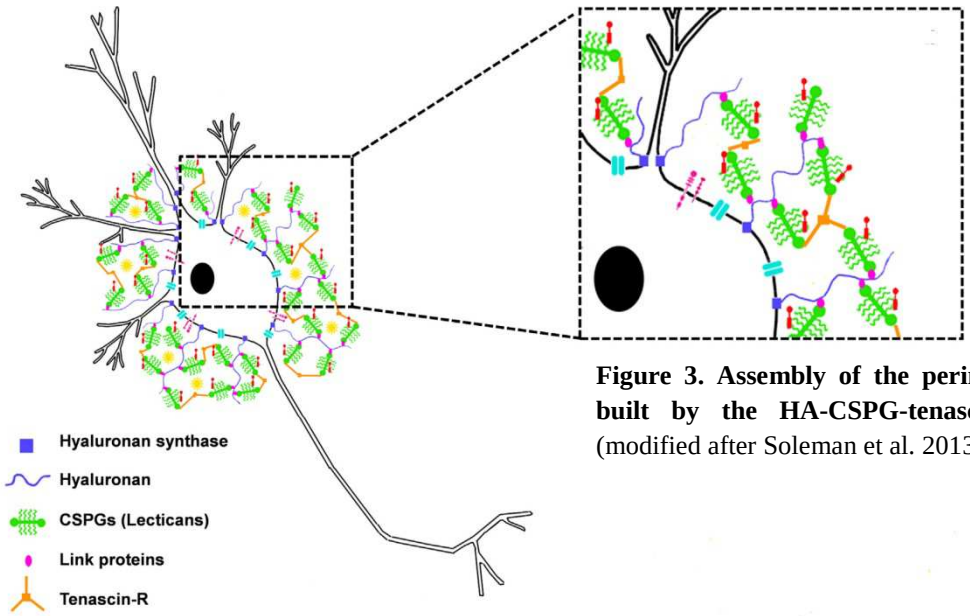

Figure 3. Assembly of the perineuronal net, built by the HA-CSPG-tenascin complex. (modified after Soleman et al. 2013)

2.2 The vestibular system

The vestibular system is the circuit for the sensation of motion, head position, and spatial orientation to gravity. Over the motion sensation, the vestibular system regulates balance, posture, gaze, and vision stabilization by extraocular muscles, paravertebral and limb muscles, or autonomic functions via wide spreading connections in the brainstem, cerebellum,

thalamus, and spinal cord. The peripheral parts of the system are in the inner ear. They are located either in the macula of *utricle* and *saccule*, or in the *crista ampullaris* of the semicircular canals, or the *lagena* of phylogenetically lower vertebrates. Vestibular receptor cells, the sensory hair cells, are able to transform physical motion of the head into electric signals. In all hair cells, receptor potential releases glutamate to transduce signals to the peripheral branch of the vestibular ganglion neurons (Scarpa), and their central processes terminate in the vestibular nuclear complex (VNC) of the brainstem.

2.2.1. The vestibular nuclear complex of the rat; central connections and functions

The vestibular nuclear complex (VNC) of the rat has many parallel characters to other mammalian species, as it remained relatively conservative in vertebrates (Brodal and Brodal 1981;Voogd, J. 1998). It is located in the *pons* and *medulla oblongata*, starting rostrally at the lateral recess of the fourth ventricle, extending caudally until hypoglossus nucleus. The nuclei of the VNC consisting of the superior (SVN), lateral (LVN), medial (MVN), and the descending (DVN) vestibular nuclei. Some smaller neuron groups are also functionally related to the VNC, the interstitial nucleus (IN), group 'F' (GF), group 'X' (GX), group 'L' (GL), and group 'Y' (GY). Although the vestibular nuclei share common functions, different contributions of the individual nuclei in the vestibulo-ocular, vestibulo-spinal reflexes, spatial cognition, and responses has been reported (for details see McCall and Yates, 2011) (Fig. 4).

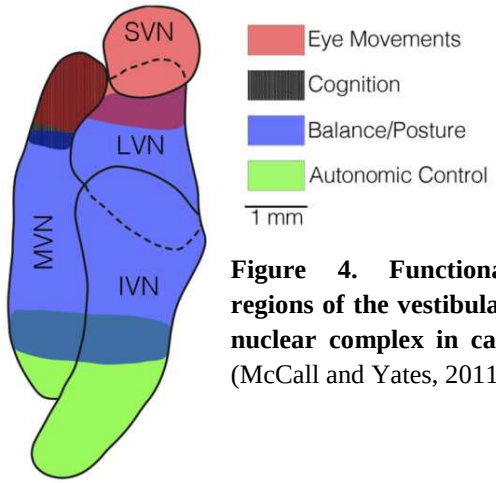

Figure 4. Functional regions of the vestibular nuclear complex in cat. (McCall and Yates, 2011)

Superior vestibular nucleus (Bechterew)

The nucleus begins rostrally at level of the mesencephalic trigeminal nucleus and extends caudally until the abducens nucleus. Medium-sized neurons provide two-third of SVN, and only a minor group of large or giant neurons is present. Large neurons are located centrally, medium and small-sized ones are found mostly in the peripheral part of the nucleus (Suarez et al. 1993). The large-sized neurons establish inhibitory synapses with the oculomotor and trochlear neurons (Ito et al. 1970; McCrea et al. 1987b; Mitsacos et al. 1983a). In contrast, the small-sized neurons project to the cerebellum and reticular formation and establish commissural connections with the contralateral vestibular nuclei (Ladpli and Brodal 1968; Mitsacos et al. 1983b).

Lateral vestibular nucleus (Deiters)

The LVN lies ventrocaudal to the SVN. It begins at the facial genu and extends caudally until its replacement by the DVN. LVN accumulates the largest perikarya within the VNC, nearly half of neurons being large or giant sized, and only a minor portion is small-sized. The neurons with different sizes are evenly distributed throughout the nucleus (Suarez et al. 1993).

The rostral part of LVN receives afferents from the utricle and cristae ampullares, project to the oculomotor nuclei, and establish reciprocal connection to cerebellum. The caudal part of the LVN receives spinal originating afferents relayed in the inferior olive or the reticular formation. The entire nucleus sends somatotopically organized projecting fibers towards the spinal cord, dominantly to its cervical region (Brodal and Brodal 1981; Epema et al. 1988; Donevan et al. 1992; Matesz et al. 1997; Bacskai et al. 2002).

Medial vestibular nucleus (Schwalbe)

The MVN begins slightly caudal and medial to SVN, its rostrocaudal extension is the longest in the VNC. The large and medium sized neurons form the magnocellular part (MVN MC), located ventrolaterally in the MVN, whereas the parvocellular part is located in the dorsomedial position of the nucleus. The neurons of the parvocellular region (MVN PC) are GABAergic having regular firing rate, receiving input from the otolith organs, sending projections to the inferior olive, and have reciprocal connection with the cerebellum and spinal cord (Suarez et al. 1993). The neurons of the magnocellular division have irregular firing rate, and they are glutamate-, or glycinergic (Bagnall et al. 2007; Eugene et al. 2011; Kodama et al. 2012). The primary input of the MVN is from the semicircular canals and cerebellum. Its efferents contribute to VOR by projecting to oculomotor neurons, and caudally give rise to the vestibulo-spinal pathways (Holstege 1988; Mitsacos et al. 1983b, a; McCrea et al. 1987b; McCrea et al. 1987a; McCall and Yates 2011). These pathways are involved in spatial recognition by projecting to the mammillary body (Brown et al. 2005; Shinder and Taube 2010).

Descending vestibular nucleus (Roller)

The DVN is the second longest vestibular nucleus. Approx. two-thirds of neurons are medium sized, and only a minority belongs to large-or giant sizes (Suarez et al. 1993). Between the rostral and caudal parts there is great difference in neuron morphology and function. The rostrally located large and giant cells project to the eye movement nuclei, and to the spinal

cord (Peterson and Coulter 1977). The small neurons in the caudal part receive inputs from a number of areas like spinal grey matter connected with limbs and GI tract sensation, pontomedullary reticular formation, inferior olive, medullary raphe, spinal and principal sensory trigeminal nucleus, and nucleus of solitary tract, prepositus hypoglossi nucleus and are in connection with solitary tract, the dorsal motor nucleus of vagus, rostral and caudal ventrolateral medulla (Balaban and Beryozkin 1994; Ruggiero et al. 1996; Matesz et al. 1997; Jian et al. 2005). Extensive connection with the latter areas suggests the involvement of DVN in cardiovascular, respiratory, and digestive regulation by vestibular stimulus (Suarez et al. 1993; McCall and Yates 2011). The characteristic appearance of DVN is the longitudinally running axon bundles between islets of neurons.

2.2.2 Vestibular nuclear complex of the frog

Although the frog's VNC is not entirely characterized until today, but still the afferentation from the sensory end organs and the central projections show considerable overlap with mammalian species (Opdam et al. 1976; Matesz 1979; Birinyi et al. 2001).

The structural organization of frog VNC corresponds with the mammals, composed of four nuclei, the superior, lateral, medial, and descending vestibular nuclei. Functional divisions are also close to mammals. The lateral part of SVN, rostral part of both LVN and MVN project to the oculomotor nuclei, the medial and lateral vestibulo-spinal tracts originate in the caudal part of LVN, MVN and DVN (Montgomery 1988; Matesz et al. 2002; Fanardjian et al. 1999). Extensive cerebellar connection is also established (Racz et al. 2006; Precht and Llinas 1969; Matesz 1979), most probably regulating in vestibulo-spinal and vestibulo-ocular circuits. Indirect experimental evidence suggests the conserved functional properties of frog VNC, being comparable to mammals (Dieringer 1995).

Lesion in the inner ear or in the central apparatus, either by mechanic or vascular trauma, will severely affect the above mentioned functions, triggers a series of plastic events compensating the imbalance of the vestibular circuit.

2.3 Plasticity of the nervous system

2.3.1 Plasticity in the normal brain, and relations to extracellular matrix

It has long been stated that functional circuits of the brain change throughout life with experience (Chklovskii et al. 2004), which is called as plasticity of the brain. It has been shown that ECM molecules are involved in the regulation of synaptic plasticity, therefore

being essential components of learning and memory. Besides the homeostatic roles of the ECM molecules, the activity-dependent modification of the ECM affects the formation of dendritic filopodia and the growth of dendritic spines. Thus, turnover of ECM, as a degradable stabilizer of neural microcircuits, is a promoter of structural and functional plasticity (Dityatev et al. 2010).

Another important property of the ECM in the mature brain is the non-permissive environment provided by its molecular components (Galtrey and Fawcett 2007b; Dityatev et al. 2010), the CSPGs. Although ECM molecules limit structural plasticity, they do promote different forms of functional plasticity, including long term potentiation (LTP) and long term depression (LTD), homeostatic plasticity[1], or metaplasticity[2]. ECM regulates activity of N-methyl-D-aspartate (NMDA) receptors and L-type Ca^{2+} channels, perisomatic GABAergic inhibition, and a number of the properties of astrocytes (Dityatev and Schachner 2006; Dityatev and Fellin 2008). Many of the studies emphasize the non-permissive role of ECM molecules on structural plasticity, although some of its components are promoting for growth and regeneration. Therefore, the balance between repellent and growth-promoting constituents determines the overall effect of ECM on structural plasticity (Dityatev et al. 2010; Pizzorusso et al. 2002).

In the extracellular space, there are proteolytic enzymes responsible for the cleavage of ECM core proteins and their membrane bound receptors (Chaturvedi and Kaczmarek 2014). These molecules are the MMPs, a family of Zn^{2+} dependent endopeptidases capable of degrading ECM, considered to be the major executors of tissue remodeling in all tissues of the body, both in physiological and pathological conditions (Szepesi et al. 2013; Michaluk et al. 2011; Chaturvedi and Kaczmarek 2014). Their expression and activity are tightly regulated in accordance with the cell activity. They can be inhibited by tissue inhibitors of metalloproteinases, as well as their activity is regulated by glycosylation and internalization (Yong 2005). In the family of MMPs, the MMP9 is involved in physiological plastic processes of the brain (Nagy et al. 2006). In the hippocampus the MMP9 expression is regulated during development and later during reorganization induced by experience. MMP9, by cleaving perisynaptic ECM molecules and releasing signaling molecules, has effect on dendritic turnover and dendritic spine morphology (Michaluk et al. 2011; Nagy et al. 2006).

[1] *homeostatic plasticity:* the scaling of synaptic efficacy counterbalancing destabilizing influences, like changes in synapse number and strength during learning and development, and to adjust balance between excitation and inhibition network wide (Turrigiano 2012).

[2] *metaplasticity:* the higher understanding of synaptic plasticity or 'plasticity of synaptic plasticity', meaning the modifications of those ways, how synaptic efficacy can transform (Abraham and Bear 1996; Dityatev et al. 2010).

Taking the results above mentioned into deeper consideration, the MMP9 and ECM molecules possible have crucial role in the molecular onset of psychiatric disorders like drug and alcohol addiction, major depression, bipolar disorder or schizophrenia (Knapska et al. 2013). In physiological conditions MMP9 enzyme is enhanced after appetitive training in the amygdala, around the excitatory synapses. But opposite effect was seen by introducing external *tissue inhibitor of MMP 1* (TIMP1), or in aversively motivated trained animals, and in MMP9 -/- KO mice (Knapska et al. 2013).

2.3.2 Plasticity in the lesioned brain, and relations to extracellular matrix

Recently a number plasticity experiments were initiated in different areas of the CNS, which suggested the important role of ECM molecules in the success and time lapse of plastic events and functional recovery. Results demonstrated that either anatomical repair or compensation of lost function by neighboring areas taking over, both influenced the intact state ECM assembly, temporarily or permanently.

After experimental deafferentation of the rat's phrenic nucleus by C2-hemisection, the lesion site becomes invaded by immune cells, meningeal cells, reactive astrocytes, that get upregulated for the secretion of CSPGs; all forming the glial scar tissue (Seil and Webster 2010). This milieu provides a physical barrier and molecular inhibition for the newly sprouting axons across the section site. Introducing chondroitinase ABC into the lesion site could, without other intervention, promotes the restoring of a limited activity to the paralysed diaphragm (Alilain et al. 2011). Similar effect on glial scar formation was made by the treatment of the lesion site with HA gel, on rat cortex. After 12 weeks of treatment, the thickness of the scar and GFAP immunopositivity was significantly less in HA gel treated groups (Lin et al. 2009). HA enrichment at the lesion site reduces CSPG production at acute time points, and also in cultures of astrocytes (Khaing et al. 2011). Opposite effect was experienced when hyaluronan was experimentally cleaved at the site of nigrostriatal tract injury. By degrading HA the inhibiting CSPGs become released from the ECM providing non-permissive effect on axon growth through the scar (Moon et al. 2003). Degradation of CSPGs by extrinsic chondroitinase ABC treatment has enhancing effect on neural plasticity. An induced focal ischemic stroke in rat's forelimb motor cortex appears in the loss of skilled movements. A series of local chondroitinase ABC injection into the perilesional area degraded the CSPG molecules in the ECM, thus the local plastic modification of the excitatory cortical circuitry is less limited, promoting earlier recovery. By degrading CSPGs in the penumbra and applying skilled reaching training on the forelimb, rehabilitation was

more sufficient, enhancing motor functional recovery (Gherardini et al. 2013), which indicated close functional characteristics with ECM in the rat VNC.

2.3.3 Vestibular compensation

Lesion in the inner ear, or in the central **vestibular networks, either by mechanic injury, vascular disorder, virus infection, or as a side effect of some antibiotics, results impaired balance.** The symptoms may include postural deficit, nystagmus and may be accompanied by dizziness, vertigo, vision problems, nausea, as well as changes in heart rate and blood pressure. The collection of these symptoms is called as vestibular disorder classified by static and dynamic symptoms. Many, but not all of these symptoms regain spontaneously in a process of behavioral recovery known as vestibular compensation (Darlington and Smith 2000; Curthoys and Halmagyi 1995, 1999; Dieringer 1995; Vidal et al. 1998). Since the lesioned primary vestibular axons do not regenerate in mammalian species, vestibular compensation is attributed to the plasticity of vestibular nuclei and related neuronal circuits. On the other hand, successful morphological and functional regeneration has long been demonstrated in lower vertebrates following the surgically sectioned and reunited vestibular nerve (Newman et al. 1986; Sperry 1945; Zakon and Capranica 1981).

The term compensation collects a number of simultaneous processes setting on soon after an injury of a CNS pathway. Neuronal circuits have the ability to take over the function of a lesioned area, involving a series of synaptic plastic events, which will eventually change the prelesional functional map of the area. Compensation processes are crucial elements of neurological rehabilitation.

In the background of vestibular compensation *many possible neural mechanisms* are suggested. *Presynaptic* theories have suggested axonal sprouting to the vestibular nuclei and changes in the efficacy of synaptic inputs from the existing non-labyrinthine pathways to the deafferented second order vestibular neurons (Dieringer 1995; Ris et al. 1995; Ris and Godaux 1998; Vidal et al. 1998). *Postsynaptic* factors include either change in the postsynaptic receptors or in the intrinsic properties of VNC neurons (Dieringer 1995; Straka et al. 2005; Vibert et al. 1995; Dutheil et al. 2013). As a result of glial reaction, the secreted growth factors and cytokines could promote the survival of deafferented vestibular neurons and contribute to their resting discharge recovery (Li et al. 1999). Recent studies have demonstrated reactive neurogenesis in the vestibular nuclei as one of the possible mechanisms of vestibular compensation (Dutheil et al. 2013). During these presumably interrelated mechanisms the intrinsic properties of neurons are working in concert with a variety of

different macromolecules in the extracellular matrix (ECM) produced by the neurons and glia cells. Since the vestibular compensation does occur in case of the permanent loss of vestibular input, it is an excellent model for studying the deafferentation-induced plasticity of CNS. According to theories in the relation of synaptic plasticity and ECM alteration, we may expect changes in the ECM composition following UL in the VNC, especially in the structure and molecular composition of PNNs.

3. AIMS

It has long been confirmed experimentally, that the CNS of phylogenetically lower vertebrates has much higher ability to regenerate and reorganize, than mammalian species. Injured cranial nerves of frogs, or fish, e.g. optic nerve or vestibulocochlear nerve, can regrow into the CNS and reestablish anatomical contacts, and restore function. Our purpose was to get deeper understanding whether there is any association between, phylogenetic levels, and ECM, especially the PNN construction, and the better regenerative capacity of the vestibular system.

The VNC is rather conservative throughout evolution regarding its nuclei, hodological and functional organization. On the basis of this, we stated the following aims:

1, In intact rat VNC:

* Provide a comprehensive mapping of ECM molecular composition in each nucleus and subnucleus of the rat VNC, by using histochemical and immunohistochemical methods. ECM molecules to be labeled are: hyaluronan; CSPGs generally, and specifically aggrecan, versican, neurocan, brevican; tenascin-R; HAPLN1.

*Evaluate the intensities of PNN staining for each studied molecule by semiquantitative scoring, in each nucleus and subnucleus of the rat VNC.

* Illustrate the distribution of PNN-bearing neurons in nuclei and subnuclei of the rat VNC by Neurolucida reconstruction.

2, In rat VNC following UL:

* Deafferentation of the VNC by UL, and follow the changes in staining pattern/intensity of HA and CSPGs in 1^{st}, 3^{rd}, and 7^{th} postoperational days in the LVN of rat.

* Observe whether repair of UL caused symptoms shows temporal correspondence with reestablishment of PNN around neurons of LVN.

3, In intact frog VNC:

* To make a comprehensive mapping of ECM molecules in the VNC of the frog, by labeling HA, TN-R, CSPGs generally, and aggrecan, for comparative and future application/experimental CNS regeneration purposes.

4. MATERIALS and METHODS

The applied experimental protocols, relating live animals or their fixed tissues, were revised and licensed by the Animal Care Committee of the University of Debrecen, Debrecen, Hungary, considering national laws and European Union regulations [European Communities Council Directive of 24 November 1986 (86/609/EEC)], and was properly conducted under the control of the University's Guidelines for Animal Experimentation (license number: 11/2011/DEMAB).

4.1 Animal and tissue processing for histochemistry and immunohistochemistry

For purposes of ECM mapping in the VNC, we used female adult Wistar rats (12-14-week old; 250-300 g; n=6), from Charles River Laboratory (Strain Crl: WI); and adult water frogs (n=12) (*Rana esculenta* L.), taken from natural fishpond environment. We used male adult Wistar rats (n= 9) for unilateral labyrinthectomy, to investigate alterations of ECM expression during compensation in subnuclei of the VNC,.

The normal rats used for ECM mapping were terminally anesthetized by intraperitoneal injection of 10% urethane (1,3 ml/100 g body weight; Reanal, Budapest, Hungary). Frogs, used for the same purpose, were terminally anesthetized by 0.1% ethyl 3-aminobenzoate methanesulfonate salt (MS 222, Sigma–Aldrich, St. Louis, MO, USA). Animals were transcardially perfused with physiological saline, 0,9 m/v % NaCl for rat, 0,65 m/v % for frog. Approach to the brainstem was by opening a vault of the skull in rat, or by sagittally opening the palatine mucosa and cranial base in case of frog. Brainstems were immediately removed, and immersed into Sainte Marie's fixative (99% absolute ethanol and 1% glacial acetic acid) for 24 h at 4 ºC, a non cross-linking fixative ideal for connective tissue preservation, according to earlier experiences. Following fixation, specimens were dehydrated by ascending series of ethanol and embedded into paraffin. Transverse sections of 8 µm were made and collected on silane coated slides, and left to dry at 37 ºC, overnight. Histochemical and immunohistochemical protocols were carried out on the sections as follows.

In case of all reactions, deparaffination and rehydration was followed by rinsing in 3 % H_2O_2 in distilled water for 10 min at room temperature (RT), for blocking endogen peroxidase. Then, specimens were washed in phosphate buffered saline (PBS), pH 7.4.

4.1.1 Histochemistry

Sections gained from intact rats, frogs and labyrinthectomized rats were incubated applying the same histochemical protocol, see detailed below.

Before histochemical reactions, specimens were blocked against aspecific lectin or probe binding for 30 min at RT in 1% bovine serum albumin (BSA), diluted in PBS (Sigma-Aldrich).

The biotinylated Hyaluronan Binding Protein (bHABP; kindly provided by R. Tammi and M. Tammi, Dept. of Anatomy, University of Kuopio, Kuopio, Finland) is the isolated HA binding N-terminal G1 domain from bovine nasal cartilage aggrecan, that specifically recognizes HA. The biotinylated *Wisteria floribunda* agglutinin (WFA) lectin (bWFA, Sigma-Aldrich) is a general marker of most of the CSPGs, specifically binding to N-acetylgalactosamine residues of chondroitin sulfate GAGs (Härtig et al, 1992) (see Table 1). Sections were overnight incubated with bHABP and bWFA markers at dilutions of 1:50 (bHABP) or 1:500 (bWFA) in PBS, containing 1 % BSA, at 4 ºC.

4.1.2 Immunohistochemistry

For specifically detecting the local expression of ECM molecules we used the following primary antibodies and immunohistochemical protcols: anti-aggrecan (rabbit, polyclonal IgG, Merck Millipore, AB1031, Billerica, MA, USA), anti-versican (mouse, monoclonal IgG1, Developmental Studies Hybridoma Bank, DSHB, clone 12C5, Iowa City, IA, USA), anti-neurocan (mouse, monoclonal IgG1, DSHB, 1F6), anti-brevican (mouse, monoclonal IgG1, BD Biosciences, 610894, San Jose, CA, USA), anti-tenascin-R (TN-R, goat, polyclonal IgG, R&D Systems, AF3865, Minneapolis, MN, USA), and anti-Hyaluronan and Link Protein Binding Protein 1 (HAPLN1, goat, polyclonal IgG, R&D Systems, AF2608) (see Table 1).

Table 1. Summarizing Table of Primary Probe, Lectin and Antibodies Used in Rat and Frog

	Supplier, cat. No.	Species of origin, type	Immunogen	Dilution HC, IHC[e]/***WB***[f]	Characterization	Controls
Rat – VNC[a]						
bHABP[b]	Provided by R. Tammi and M. Tammi; Kuopio, Finland	HA-binding region of aggrecan isolated from bovine articular cartilage; biotinylated	-	1:50 (0,2 µg/ml)	By HC (Midura et al., 2003)	HC on rat sternal cartilage
bWFA[c]	Sigma-Aldrich, L1516	Lectin isolated from *Wisteria floribunda;* biotinylated	-	1:500	By HC (Härtig et al., 1992)	HC on rat sternal cartilage; HC pattern on cerebellum identical to Carulli et al., 2006
Anti-aggrecan	Merck Millipore, AB1031	rabbit, polyclonal, IgG	GST fusion protein containing amino acids 1177-1326 of mouse aggrecan	1:500/***1:400***	By WB (Afshari et al., 2010): single band of 60 kDa	WB in our laboratory on rat brain, band of approx. 60kDa (not shown)
Anti- versican	DSHB, 12C5	mouse, monoclonal, IgG1	Hyaluronate-binding region of human versican	1:100	By WB (Asher et al., 2002): single band of approx. 400 kDa	IHC pattern on rat cerebellum identical to Carulli et al., 2006
Anti-neurocan	DSHB, 1F6	mouse, monoclonal, IgG1	PBS-soluble CSPGs from rat brain	1:100	By WB (Asher et al., 2000): one band for core protein (270 kDa), other band for neurocan-N (130 kDa)	IHC pattern on rat cerebellum identical to Carulli et al., 2006
Anti-brevican	BD Biosciences, 610894	mouse, monoclonal, IgG1	Rat Brevican aa. 232-394	1:200	By WB (factory datasheet): single band of 140 kDa	IHC on rat cerebellum pattern identical to Yamada et al., 1997
Anti-tenascin-R	R&D Systems, AF3865	goat, polyclonal, IgG	Mouse myloma cell line NS0-derived recombinant human Tenascin-R isoform 1, Glu34-Phe1358	1:300/***1:500***	By WB: in our laboratory, single band of 180 kDa (not shown)	WB in our laboratory, on rat brain and articular cartilage, band of approx. 180 kDa (not shown)
HAPLN1[d]	R&D Systems, AF2608	goat, polyclonal, IgG	Mouse myeloma cell line NS0-derived recombinant human HAPLN1, Asp16-Asn354	1:300	Used successfully for IHC by Carulli et al., 2007	IHC pattern on rat cerebellum identical to Carulli et al., 2007
Rat – UL[g]						
bHABP	Provided by R. Tammi and M. Tammi; Kuopio, Finland	see above	-	1:10 (1 µg/ml)	By HC (Midura et al., 2003)	HC on rat sternal cartilage
bWFA	Sigma, L1516	see above	-	1:500	By HC (Härtig et al., 1992)	see above
Frog - VNC						
bHABP	Provided by R. Tammi and M. Tammi; Kuopio, Finland	see above	-	1:10 (1 µg/ml)	By HC (Szigeti ZM et al., 2006)	HC (see text)
bWFA	Sigma, L1516	see above	-	1:500	By HC (see text)	HC (see text)
Anti-tenascin-R	R&D Systems, AF3865	see above	see above	1:40/***1:500***	By WB: 180 kDa	WB (see text)
Anti-CSPG clone Cat-301	Chemicon (Millipore), MAB5284	mouse, monoclonal, IgG1	Feline spinal cord fixed gray matter	1:100/***1:250***	By WB: 500kDa	WB (see text)

a, vestibular nuclear complex; b, biotinylated Hyaluronan Binding Protein; c, biotinylated *Wisteria floribunda* agglutinin; d, Hyaluronan and Proteoglycan Link Protein 1; e, histochemistry, immunohistochemistry; f, Western blot; g, unilateral labyrinthectomy.

Antibodies against aggrecan, versican, and brevican were raised to recognize segments of the core protein, therefore to better expose the antibody binding sites sections were pre-incubated with chondroitinase ABC (0,02 U/ml; Sigma-Aldrich; C2905). Chondroitinase ABC is an enzyme that acts on chondroitin-4-sulfate, chondroitin-6-sulfate, and dermatan sulfate at pH 8.0, and acts slowly on hyaluronan as well, at pH 6,8, by eliminative degradation of polysaccharides containing 1,4-β-D-hexosaminyl and 1,3-β-D-glucuronosyl or 1,3-α-L-iduronosyl linkages to disaccharides containing 4-deoxy-β-D-gluc-4-enuronosyl groups of GAG chains anchored on core proteins of CSPGs, thus it makes the core protein exposed for antibodies to recognize. Using manufacturer's instructions, we incubated in specific TRIS-sodium-acetate buffer, pH 8 for 1 hour at 37 ºC.

For the blocking of aspecific binding sites we applied 1 % BSA and 10 % normal goat serum (NGS) for aggrecan; 2 % BSA (versican and HAPLN1); 3 % normal horse serum (NHS), (neurocan); 1 % BSA and 10 % NHS (brevican); and 1 % BSA and 10 % normal rabbit serum (NRS) (TN-R). All blocking serums were diluted in PBS, and incubated for 30 min at RT. After blocking serum, sections weren't rinsed in PBS.

Primary antibodies utilized on rat were dissolved with 1 % BSA and 3 % NGS (aggrecan, 1:500), 2 % BSA (versican, 1:100), 1 % NHS (neurocan, 1:100), 1 % BSA and 3 % NHS (brevican, 1:200), 1 % BSA and 3 % NRS (TN-R, 1:300), or 1 %BSA (HAPLN1, 1:300), all diluted in PBS, incubated overnight at 4 ºC.

Primary antibodies used on frog were the anti-CSPG clone Cat-301 (recognizing aggrecan core protein, mouse, monoclonal IgG1, Merck Millipore, MAB5284) and anti-tenascin-R (R&D Systems, AF3865).

4.1.3 Visualization

For ECM mapping on rat, we chose the avidin-biotin-complex (ABC) reaction for visualizing. Following bHABP and bWFA primary markers, sections were incubated with ExtrAvidin Peroxidase (1:500; Sigma-Aldrich; E2886) dissolved in PBS, for 1 h at RT, which was followed by specific staining with 3, 3'-diaminobenzidine-tetrahyrdochloride (DAB, Sigma-Aldrich), diluted in TRIS-HCl buffer, pH 7.6 with H_2O_2. Sections were dehydrated and coverslipped with DPX mounting medium (Sigma-Aldrich). Against primary antibodies used for IHC, secondary antibodies were the biotinylated goat-anti-rabbit IgG (Vector Laboratories, Burlingame, CA, USA; BA-1000) (aggrecan), biotinylated horse-anti-mouse IgG (Vector Labortatories; BA-2000)(versican, neurocan, brevican), or biotinylated rabbit-anti-goat IgG (Vector Laboratories; BA-5000)(TN-R, HAPLN1), all diluted in 1: 200, in PBS,

incubated for 1 h at RT (Table 2). After incubation with the biotinylated secondary antibodies, sections were incubated with ExtrAvidin Peroxidase (Sigma-Aldrich, 1:500) dissolved in PBS, for 1 h at RT, and finally were stained with DAB (Sigma-Aldrich), in TRIS-HCl buffer, pH 7.6 with H_2O_2. After dehydration, sections were coverslipped with DPX mounting medium.

On rat tissues taken from labyrinthectomized animals we used bHABP and bWFA labeling. Both reactions were visualized by DAB reaction, as described above, and by Streptavidin Alexa 555 (Invitrogen Life Technologies, Grand Island, NY, USA, S32355, 1:1000) diluted in PBS and dark incubated for 1h at RT. Sections were coverslipped by Vectashield mounting medium for fluorescens, with DAPI (Vector Laboratories).

For the ECM mapping on frog we used the secondary reagents Streptavidin Alexa 488 (bHABP; Invitrogen, S32354, 1:1000), Sterptavidin Alexa 555 (WFA, 1:1000, Invitrogen), Alexa Fluor 647 anti-goat IgG (TN-R, 1:500) (made in chicken, Invitrogen), and Fluorescein anti-mouse IgG (Cat-301, 1:500) (made in horse, Vector Laboratories, FI-2000)(Table 2). All diluted in PBS and incubated for 1h at RT. Sections were coverslipped by Vectashield mounting medium for fluorescens, with DAPI (Vector Laboratories).

Table 2. Summarizing Table of Secondary Reagents Used in Rat and Frog

Rat - VNC	**Species of origin, type**	**Supplier, cat. No.**	**Dilution**
ExtrAvidin Peroxidase	-	Sigma-Aldrich; E2886	1:500
biotinylated anti-rabbit IgG (aggrecan)	goat	Vector Laboratories, BA-1000	1:200
biotinylated anti-mouse IgG (versican, neurocan, brevican)	horse	Vector Laboratories, BA-2000	1:200
biotinylated anti-goat IgG (TN-R, HAPLN1)	rabbit	Vector Laboratories, BA-5000	1:200
Rat - UL			
ExtrAvidin Peroxidase	-	Sigma-Aldrich; E2886	1:500
Streptavidin Alexa 488 (bHABP)	-	Invitrogen, S32354	1:1000
Streptavidin Alexa 555 (WFA)	-	Invitrogen, S32355	1:1000
Frog - VNC			
Streptavidin Alexa 488 (bHABP)	-	Invitrogen, S32354	1:1000
Streptavidin Alexa 555 (WFA)	-	Invitrogen, S32355	1:1000
Alexa Fluor 647 anti-goat (TN-R)	chicken, IgG	Invitrogen, A21469	1:500
FITC anti-mouse (Cat-301)	horse, IgG	Vector Laboratories, FI-2000	1:500

4.1.4 Specificity of reactions

Special care was taken on the specificity of reactions. Therefore we choose antibodies applied and cited by referred laboratories, experienced in ECM research.

Most of the markers and antibodies were already applied on rat brain, so testing of specificity was either by HC and IHC reactions, by comparing staining pattern with the ones published on rat cerebellum by Carulli et al., (2006) (bHABP, bWFA, anti-versican, anti-neurocan, anti-brevican, and anti-HAPLN1), or by Western Blot (WB) analysis for those not yet tested on rat nervous tissue (anti-aggrecan (Merck Millipore) and anti-tenascin-R (R&D)). Staining pattern was identical to rat cerebellum found by Carulli et al., (2006), and for WB, bands appeared at appropriate molecular weights (Table 1).

On frog tissues the specificity of bHABP was tested by Szigeti et al., (2006), in our laboratory. The bWFA, anti-aggrecan Cat-301, and anti-tenascin-R were not yet used on amphibian nervous tissue, therefore specificity was tested. Frog specimens were parallel incubated with rat cerebellum sections, for comparison with the pattern found by Carulli et al., (2006), as detailed above. We made positive control reactions as well for the bWFA, by incubating frog sternum sections with nervous ones. In the sternum the CSPG rich hyaline cartilage showed positivity in the matrix. The Cat-301 and TN-R antibodies were checked for positivity by WB on frog sternal cartilage and brain, rat knee joint cartilage and brain tissues.

For the WB reactions samples were collected from frogs (n=4) and rats (n=3), right after anesthesia. The brain and sternal cartilage from the frogs, or brains and knee joint cartilages from the rats were freshly taken from the animals. Samples were homogenized in 100 µl of buffer containing 50 mM Tris–HCl buffer (pH 7.0), 10 µg/ml Gordox, 10 µg/ml leupeptine, 1 mM phenylmethylsulphonylfluoride (PMSF), 5 mM benzamidine, 10 µg/ml trypsin inhibitor as protease inhibitors. The tissue samples were then mechanically homogenized and were collected in 100 µl PBS, pH 7.4. For exposure of antigen, extract was incubated in 10% chondroitinase AC (Sigma Aldrich) and suspensions were sonicated by pulsing burst for 30 s, at 40 A (Cole-Parmer, Illinois, USA), then centrifuged for 10 min on12,000 rpm, at 4 ºC. The supernatant was removed, aliquoted. The 20 µg/lane of extract was separated in 7.5% SDS polyacrylamide gel, then electrophoretically transferred (Trans-Blot Turbo® transfer system, Bio-Rad Laboratories, Hercules, CA, USA) onto a nitrocellulose membrane (Bio-Rad Laboratories). After blocking with 5% non-fat dry milk in PBS with 0.1% Tween 20, membranes were incubated with primary antibodies overnight at 4 ºC (for dilutions see Table 1). Later membranes were incubated with anti-rabbit IgG, anti-mouse IgG (Bio-Rad Laboratories), in 1:1500, and anti-goat IgG, 1:2000 dilution (DAKO, Glostrup, Denmark).

Finally, membranes were developed using enhanced chemiluminescence (Merck Millipore) according to the protocol provided by the manufacturer. Bands were visible at 180 kDa for TN-R, and at 500 kDa for Cat-301 antibodies, corresponding to the previously published data (Table 1, Figure 14). Based on these control reactions, the used markers showed to be specific in amphibians.

4.1.5 Semiquantitative analysis of results

During ECM mapping in rat the presence and intensity of reactions was an important detail of our results, especially in the perineuronal nets, therefore a semiquantitative analysis was made scoring by non-instrumental observation. Scorings of PNN are as follows: -: no staining; +: weak staining; ++: moderate staining;+++: strong staining; ++++: very strong staining. The characteristic punctuate appearance of versican staining suggested separate symbolizing with crosses (Table 3). Analysis was done according to Carulli et al., (2006).

4.2 Neurolucida reconstruction

In rat, to further describe and compare the distribution differences of PNN-bearing neurons between the nuclei of the VNC and different ECM molecule labelings, a Neurolucida reconstruction was made on all nuclei and subnuclei of the VNC. Representative sections were chosen for reconstruction, being characteristic for each subnucleus. The reconstruction was drawn on Neurolucida 8.0 program (MBF Bioscience Inc., Williston, VT, USA). Nuclear boundaries were reconstructed using 4-10x objectives. For identification of PNN bearing neurons the same 4-10x objectives were used, or 20-40x ones, if recognition of PNNs demanded. PNN bearing neurons were illustrated with dots in the LVN, SVN, and magnocellular part of MVN, or rings in MVN parvocellular part. The specific punctuate appearance of versican labeling was separately labeled by solid or empty triangles.

The position, boundaries and rostrocaudal extension of the vestibular nuclei were identified on native sections using the stereotactic atlas of The Rat Brain by Paxinos and Watson, (1998). Measurement of neuronal somas was done at the widest diameters using the cellSense Entry 1.5 software (Olympus), following the descriptions on VNC by Suarez et al. (1993). In the frog the appropriate brainstem sections were chosen according to the Atlas of the Frog's Brain, by Kemali and Braintenberg, (1969), Matesz, (1979), and Birinyi et al. (2001).

Images were recorded using Nikon Eclipse E800 conventional light microscope, or by Olympus FV1000 confocal laser scanning microscope. Contrast and background color was minimally adjusted with Photoshop CS4 v11.0 (Adobe Systems Inc., San Jose, CA, USA).

4.3 Unilateral labyrinthectomy

We used 9 adult male Wistar rats for unilateral labyrinthectomy (UL) according to Hitier et al, (2010). The animals were anesthetized with intraperitoneal injection of urethane, with dosages described above.

For the ventrolateral approach of the middle ear cavity the incision of the skin was made just behind the left auricle, slightly ventrally. Subcutaneously the parotid gland was exposed and prepared to the rostral direction, preserving parotid duct. Unlike in human, the facial nerve doesn't penetrate the parotid gland, but runs dorsally to it. During the procedure the facial nerve was spared. Following the anterior border and retracting caudally the sternomastoid muscle, preparation reaches the posterior belly of digastric muscle, which attaches on the paramastoid process. Anterior to the paramastoid process the tympanic bulla is found which is analogue of the middle ear cavity. It can be palpated with blunt probe between the mentioned muscles, and provides orientation point. The other guide for orientation is the external auditory meatus, through which a wooden probe could be driven until the tympanic membrane. After separating the muscles by fascia and retracting with blepharostat, the tympanic bulla can be opened dorsolaterally. The tympanic membrane is also removed. We use small malleotome to open the bulla. Inside there are the auditory ossicles, stapedial artery, tensor tympani muscle, and the promontory is also visible. Special care was taken to keep the stapedial artery intact, to avoid causing fatal bleeding. The *malleus* and *incus* were removed and through the promontory the inner ear was accessed by breaking bone with sword shaped scalpel. A surgical hook was used to mechanically damage the membraneous labyrinth. After ensuring that no bleeding was left, the area was rinsed with saline, and the skin was sutured. Animals were left to survive for 1, 3, and 7 postoperative days.

After the lesioned animals returned to awake state, they produced static (ocular and postural) and dynamic vestibular symptoms, due to the wide spreading connections of the VNC; symptoms are best described by Hitier et al. (2010). The ocular signs were the skew deviation (eye on lesion side goes ventrally, opposite rose dorsally – Hertwig-Magendie phenomenon, caused by otolithic deafferentation), and nystagmus (rapid phase rostral and dorsal on lesioned side, caudal and ventral on contralateral). The postural signs were present in resting animals as well. The head tilted to unoperated side, with the operated ear closer to

ground, neck also bent with snout closer to lesioned side shoulder. The body spirally twisted around longitudinal axis, and limb asymmetry occurred. On lesioned side limbs were in flexion and adduction (losing antigravity muscle tone), while limbs were extended and abducted on the intact side. The tail rotated counterclockwise. Dynamic signs occurred as the imbalance or uncoordination during motion of the animal. Animals rolled toward the operated side starting with head torsion, followed by further rotation in the vertebral axis (Fig. 5a, b). Animals also have autonomic imbalances, causing gastrointestinal, or cardiovascular and respiratory malfunctions.

After UL operation the animals were let to survive for 1, 3, or 7 days, while this time static signs mostly, and dynamic disturbances also gradually settle. Postural signs were still recognized at all survival days, as reported by Dieringer et al., (1995). At the proper days of survival animals were sacrificed, then in their lateral vestibular nucleus alteration of HA and CSPGs expression in the PNNs were visualized by fluorescent microscopy.

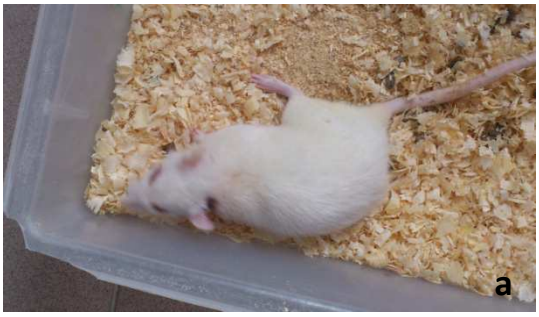

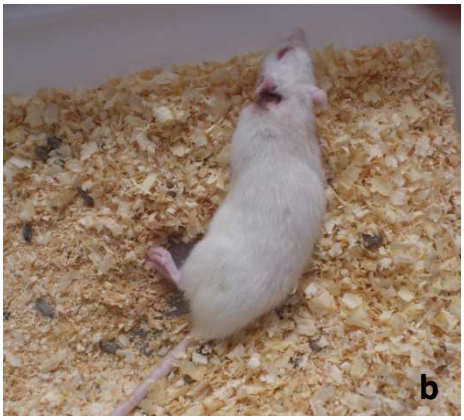

Figure 5. Rat showing limb asymmetry and postural deficits as a result of UL.

5. RESULTS

Considering the localization of ECM molecules we could distinguish four compartments. ECM molecules accumulated surrounding a distinct group of neurons, identified as PNN, or they were present in a diffuse reticular form in the neuropil. In addition, within the stained neuropil, darker ovoid or round shaped structures of 2-4 µm in diameter were observed with all ECM reactions studied. These structures were first described by Brückner et al. (2008), as axonal coats. Finally, small dot-like accumulation was seen in the neuropil perisomatically and in the white matter.

Below, results on the distribution pattern and intensity of histochemical and immunohistochemical staining in normal rat and normal frog is detailed in each nucleus of VNC evaluating PNNs and neuropil, and results are further illustrated with Neurolucida reconstruction. A semiquantitative assessment was made by scoring PNN staining intensities and summarized for each subnucleus of the rat VNC in a Table 3. Alterations of ECM staining patterns after unilateral labyrinthectomy in the LVN of rat are presented. Last, results of ECM mapping in the frog VNC is presented.

5.1 Distribution of matrix molecules in the vestibular nuclear complex of the rat

To associate certain neuron types of the VNC to the PNNs observed in the immunohistological sections, we categorized neurons according to their sizes. Measurements were made by Suarez et al, (1993) were taken as reference, thus making the categories of: small neurons having maximal diameter below 20 µm; medium size neurons of 21-35 µm; large neurons of 36-49 µm; and giant neurons of 50-80 µm.

	SVN	LVN	MVN*	DVN rostral	DVN caudal
Hyaluronan	+++	+++	+++	++	-
WFA	++	++	++	++++	-
Aggrecan	++++	++++	+++	++++	-
Versican	++	#	#	+	+
Neurocan	++	++	+	++	-
Brevican	++++	++++	+++	-	-
Tenascin-R	+++	+++	+++	+++	+
HAPLN1	++	+	+	++	-

Table 3. Semiquantative scoring of PNN staining intensities as -: no staining, +: weak staining, ++: moderate staining, +++: strong staining, ++++: very strong staining. *: MVN MC. #: versican reaction revealed only heavily stained dots, so the presence of PNNs is not clearly recognizable.

5.1.1 Superior vestibular nucleus

Location and position of SVN is indicated schematically on Fig. 6a. Cells of SVN have 24.01 µm diameter in average, ranging between 12,94-57,23 µm. Two thirds of the neurons are medium sized, only a minority is large or giant sized. The neurons are scattered unequally, the larger neurons are located in the central part of the nucleus, whereas the smaller ones are peripheral. The intensity and staining pattern of the reactions showed regional differences within the cross section of SVN, although in the rostrocaudal extension no difference was seen. In the central part of the nucleus PNN was present around the large- and giant sized neurons, with all studied reactions. Staining was most intensive with the anti-aggrecan and anti-brevican reactions, but wasn't as strong with HA, TN-R, WFA, versican, and was the weakest with neurocan, and HAPLN1 reactions (Fig. 6b-i). With aggrecan antibody patch-like

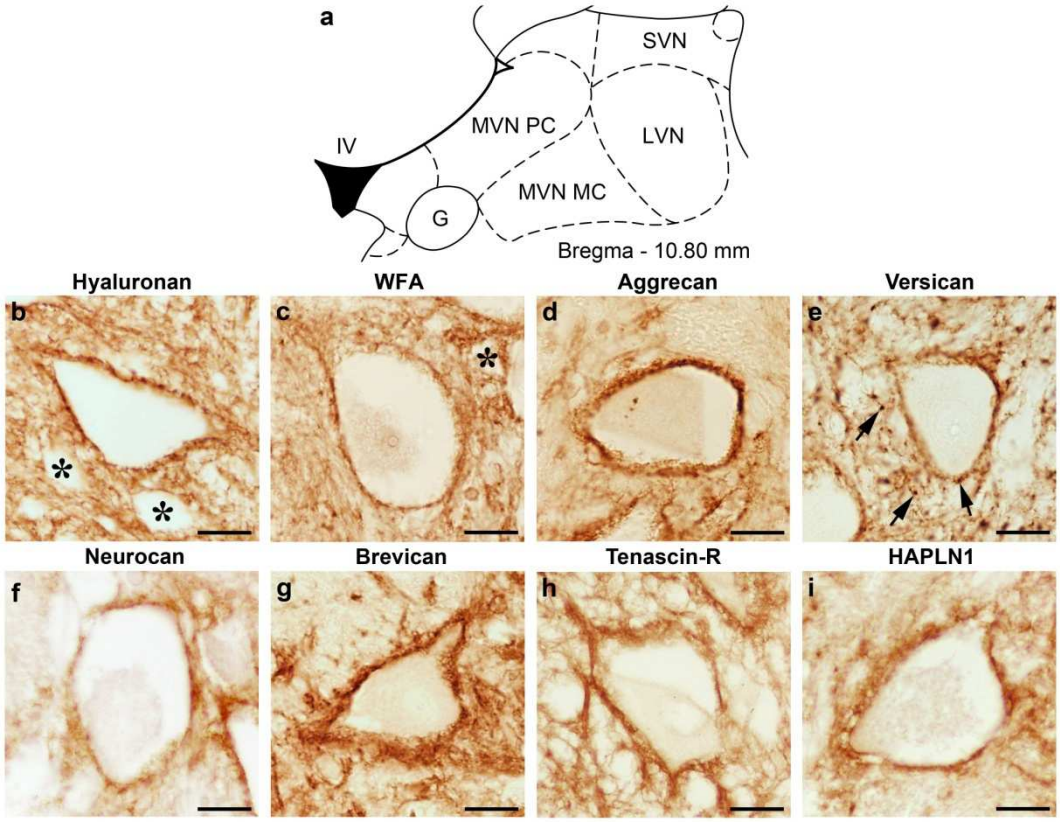

Figure 6. (a) Schematic image shows the position of SVN, MVN MC, MVN PC, and LVN. (b-i) PNN in the superior vestibular nucleus. IV: fourth ventricle. G: genu of facial nerve. Arrows show dot-like condenstaions of versican in the neuropil. *: small-sized neurons. Scale bar 20 µm.

immunoreactive spots were seen in perisomatic location. With the anti-versican reaction, in addition to continuous PNN, we also observed heavily stained dots in the pericellular area (Fig. 6e). The majority of small and medium sized neurons were surrounded by PNNs with variable staining intensity for each reaction, which was experienced both in the central and

peripheral parts of the nucleus, but a minority of these neurons weren't covered by perineuronal ECM condensation (Fig. 6b, c).

In the neuropil, both in the central and peripheral portions of the SVN, a diffuse ECM staining appeared presenting reticular patterning (Fig 6b-i). In case of neurocan and HAPLN1 a weaker staining appeared than at the other reactions. With the versican reaction, similarly to perisomatic areas, heavily stained dots appeared in the neuropil together with reticularly organized pattern (Fig. 6e).

A Neurolucida reconstruction was made to demonstrate the distribution of PNN-bearing neurons (Fig. 9), which indicates that large and giant neurons, positioned centrally in the SVN, bear PNNs. The semiquantitative analysis, demonstrating the staining intensity of PNNs in case of each reaction in the SVN, is shown in Table 3.

5.1.2 Lateral vestibular nucleus

Location and position of LVN is indicated schematically on Fig. 6a. The size of neurons ranges between 12,65-74,88 µm, 34,2 µm average, having 1/10 in small range, and 41% in large or giant sizes. In the rat there is no difference in cell sizes and morphology along the rostrocaudal or cross sectional extent.

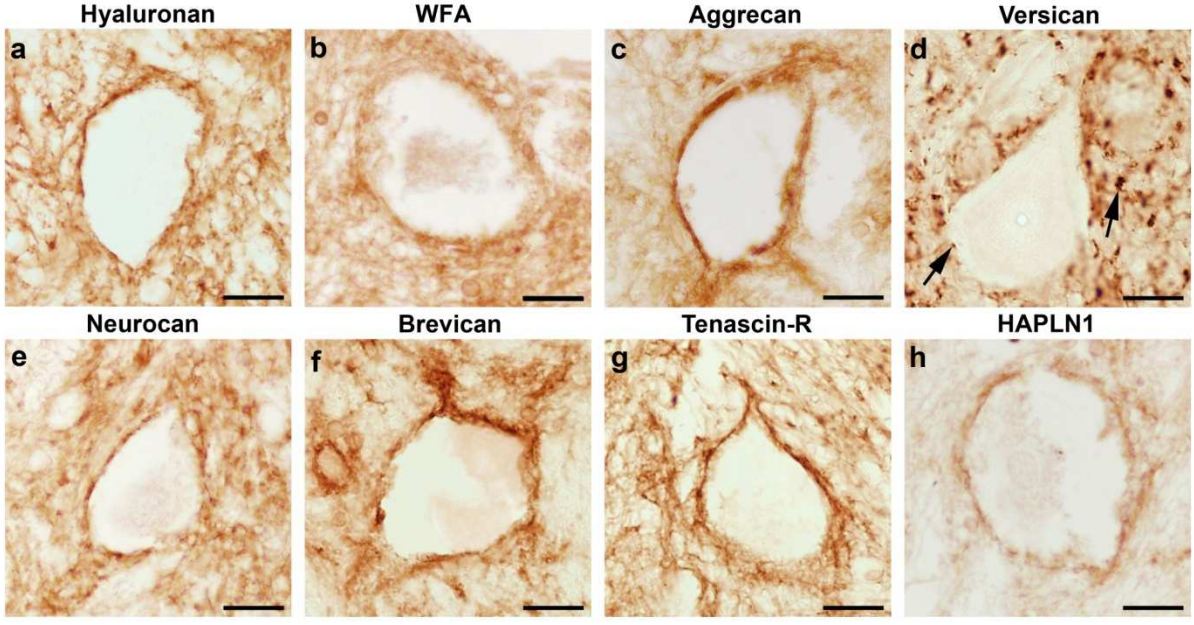

Figure 7. (a-h) PNNs in the lateral vestibular nucleus. (d)Arrows show dot-like condenstaions of versican in the neuropil. Scale bar 20 µm.

Opposite to the regional differences experienced in SVN, in the LVN there wasn't any regional distinction seen in the staining pattern throughout the nucleus. The nucleus is rich in giant and large neurons, which were characteristically surrounded by PNNs (Fig. 7a-h, Table

3). The strongest staining intensity was seen with aggrecan and brevican reactions, as they were the most intense in PNNs from the CSPG family. The hyaluronan, TN-R, WFA and neurocan staining appeared particularly fainter, and the weakest was the HAPLN1, regarding the PNNs. Comparing versican reaction with the one seen in SVN, in LVN a different pattern was seen, in which no continuous perisomatic ring showed, just few heavily stained dots surrounding the soma (Fig. 7d). As seen in SVN, the medium and small sized neurons varied in having or lacking perineuronal nets around their somas, with some of them wearing no PNN (not shown), others showing different staining pattern for the reactions.

Neurolucida reconstruction demonstrates the distribution of PNN-bearing neurons in the LVN (Fig. 9). Reconstructions show the differences in the number of stained PNNs for each of the reaction.

The neuropil also showed net-like reticular appearance. The strongest intensity of reaction was seen with HA, WFA, neurocan, brevican, and TN-R. Fainter staining was observed by using the aggrecan reaction, whereas the least staining intensity occurred with HAPLN1 reaction. By semiquantitative observation the staining intensity showed similar strength in the reactions, except for HAPLN1, which was much fainter (Table 3). There was intense immunoreaction in case of versican showing the characteristic punctuated appearance, being present around the soma and in the neuropil, most probably perisynaptically or in the nodes of Ranvier (Fig. 8d).

5.1.3 Medial vestibular nucleus

MVN is divided into two well distinguishable subpopulations of neurons, forming the dorsomedial parvocellular, and magnocellular ventrolateral parts of the nucleus (Bagnall et al., 2007). The average diameter of cells is 20,50 µm, ranging between 6,88-44,06 µm, nearly half being small, and only few percent of large cells, the rest is medium sized. The parvocellular part, composed of predominantly small

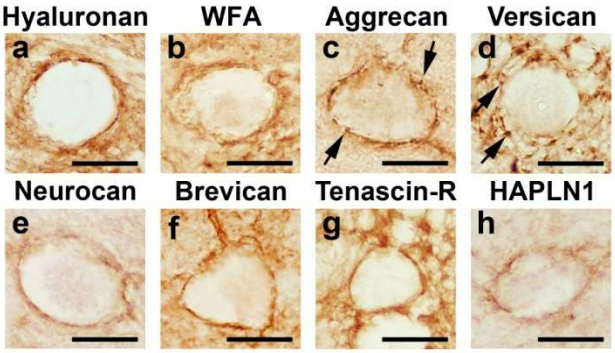

Figure 8. (a-h) PNN in the magnocellular part of medial vestibular nucleus. (c, d) Arrows show dot- or patch-like condenstaions of aggrecan pericellularly, and versican in the neuropil. Scale bar 20 µm.

neurons, is found in the dorsomedial subventricular position, laterally to the facial geniculum

and prepositus hypoglossi nucleus, and the magnocellular part, formed by large and medium sized neurons, lies ventrolaterally to the parvocellular, between the facial geniculum and LVN. Position of the subnuclei is schematically shown on Fig. 6a.

The magnocellular part mostly contains medium- and large-sized neurons, which were surrounded by PNN (Fig. 8a-h), stained strongest for HA, aggrecan, brevican, and TN-R. Slightly weaker staining appeared for WFA and neurocan, the faintest staining occurred with HAPLN1 reaction. As described in LVN, the aggrecan reaction produced some occasionally seen heavily immunoreacive patch like patterns (Fig. 8c), also described earlier. Versican reaction, similarly to the previously described, resulted in dense dot-like staining, localized around cell bodies (Fig. 8d). In the parvocellular part, where mostly small sized neurons are present, cell bodies are rarely covered by PNNs. In those few cases, where PNN was identifiable, HA and TN-R appeared to be positive. Only a few PNN ensheathed neurons were there for aggrecan, brevican and WFA staining, and with neurocan and HAPLN1 no PNN was recognizable.

The Neurolucida reconstructions show the number and distribution of PNN-bearing neurons in the magnocellular- and parvocellular parts, for each reaction. The reconstruction clearly shows the difference in the number of PNN-bearing cells among the MVN MC and MVN PC. To the caudal direction in the magnocellular part, the number of PNNs gradually decrease parallel with the disappearance of large or medium-sized neurons (Fig. 9). Table 3 provides semiquantitative analysis on staining intensity of PNNs in divisions of MVN.

The neuropil staining was also positive for both parts and in all of the reactions with the exception of aggrecan, neurocan and HAPLN1, which showed fainter staining. All reactions were strong in the neuropil, but aggrecan, WFA, neurocan, and HAPLN1 reactions were much fainter in the neuropil of the parvocellular part, in all other reactions the intensity was similar in the two subdivisions. The versican positive dots were present throughout the neuropil of both subdivisions, presenting the intensively stained dot-like structures distant from cell bodies.

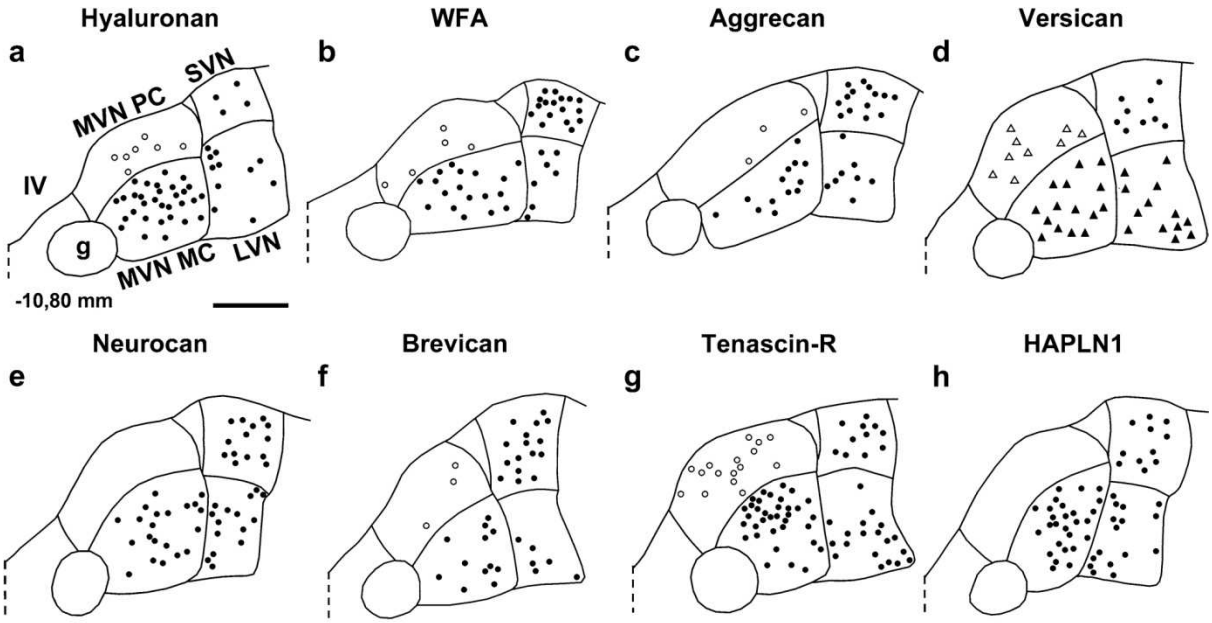

Figure 9. Neurolucida reconstruction showing the distribution of neurons bearing PNN in SVN (dots), LVN (dots), MVN MC (dots), and MVN PC (circles). The dot-like versican labeling is illustrated in LVN and MVN MC with (solid triangles), and in MVN PC (empty triangles). g: genu of facial nerve. IV: fourth ventricle. Scale bar 500 µm.

5.1.4 Descending vestibular nucleus

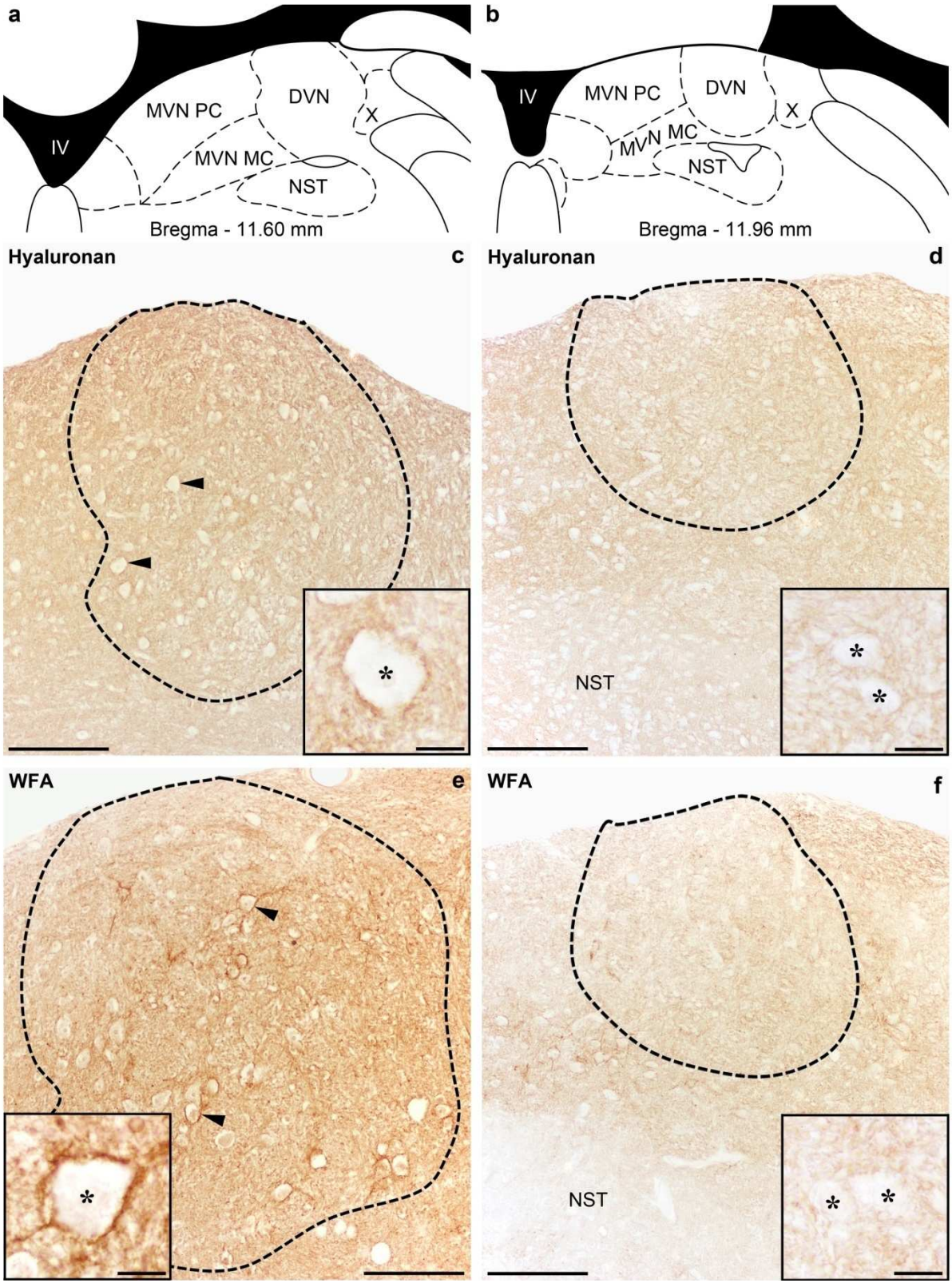

Figure 10: (a, b) Schematic images show the position of rostral and caudal parts DVN. (c-f) Illustrating ECM staining patterns in the rostral and caudal divisions of DVN. *Arrowheads* show characteristic PNN-bearing neurons. *: label neurons in the inserts: PNN bearing neurons in the rostral-, and non-PNN bearing neurons in the caudal parts. *IV*: fourth ventricle. *NST*: nucleus of solitary tract. Scale bar 200 µm (low magnification), 20 µm (insert).

In rostrocaudal extension the DVN can be subdivided into a rostral part containing numerous giant-, large-, and medium-sized neurons, and a caudal part where longitudinally running parallel fiber bundle cross sections occupy the visual field, characteristically, with fewer number of intermitting small- or middle-sized neurons. The neuron sizes are ranging between 10,88-62,77 µm, 25,24 µm in average, assembled of 2/3 medium sized neurons, and

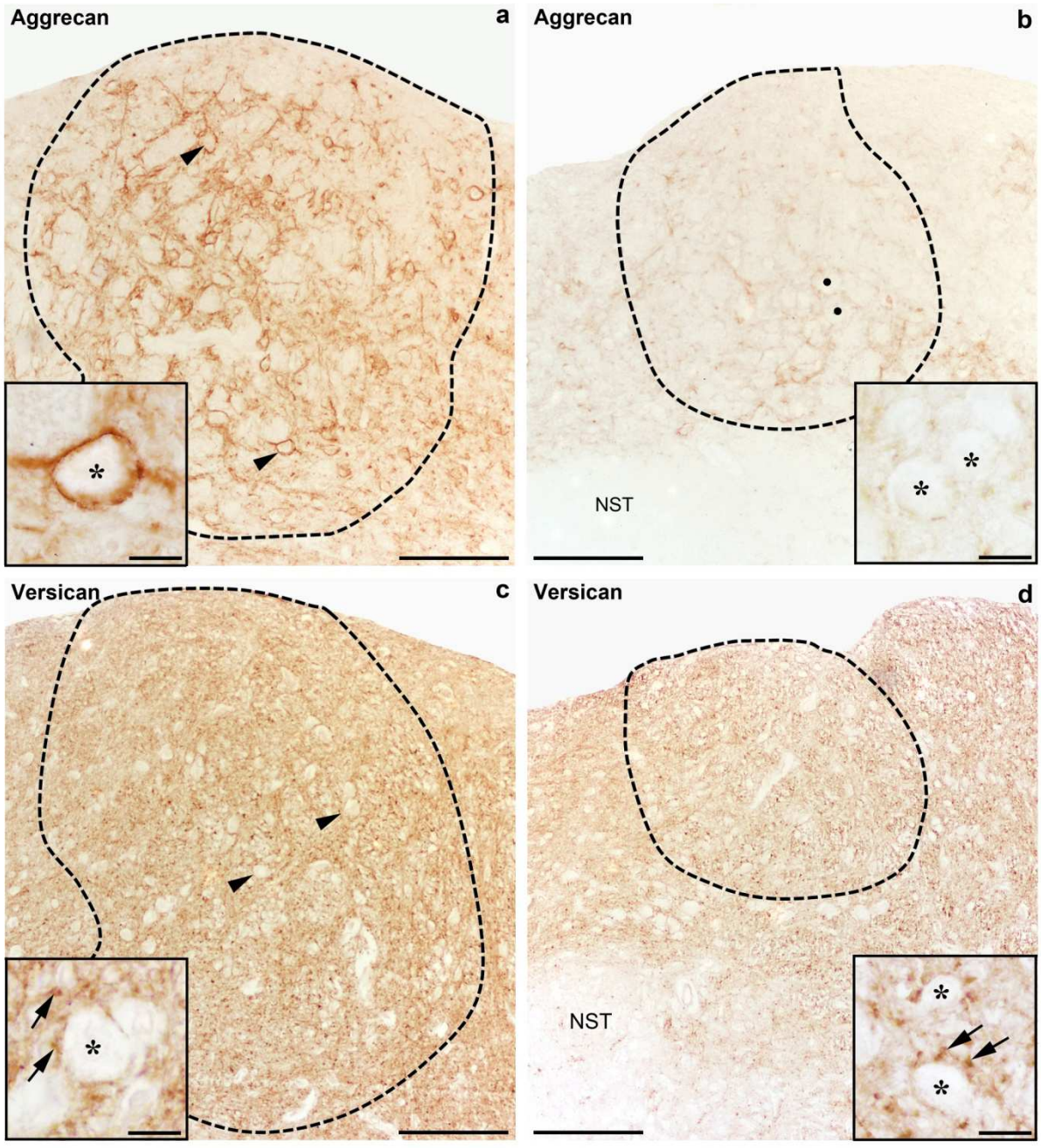

Figure 11: (a-d) Illustrating ECM staining patterns in the rostral and caudal divisions of DVN. *Arrowheads* show PNN-bearing neurons. *: label neurons in the inserts: PNN-bearing neurons in the rostral-, and non-PNN bearing neurons in the caudal parts. (b) *Dots* label longitudinal fascicles. (c-d) *Arrows* show dot-like condensations of versican pericellularly and in the neuropil. *NST*: nucleus of solitary tract. Scale bar 200 µm (low magnification), 20 µm (insert).

1 per ten of large or giant cells. Along the rostrocaudal extension there is great difference in the neuronal morphology, function, and hodology.

The position and dimensions of DVN are schematically shown on Fig. 10a (rostral) and b (caudal). Our results revealed obvious differences between the rostral and caudal parts of DVN in expression of molecules, and concerning the number of PNN-bearing neurons.

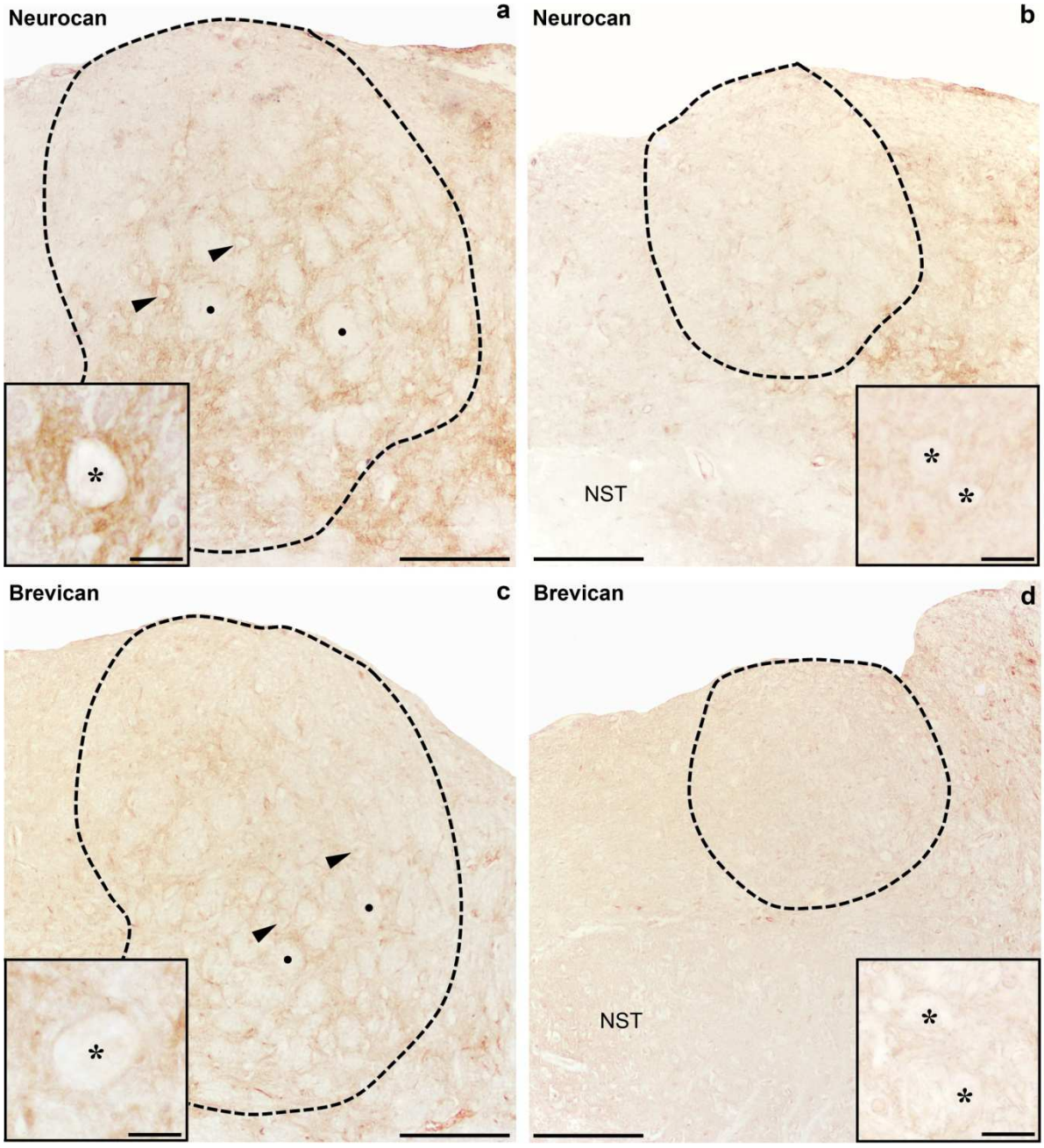

Figure 12: (a-d) Illustrating ECM staining patterns in the rostral and caudal divisions of DVN. *Arrowheads* show PNN-bearing neurons. *: label neurons in the inserts: PNN-bearing neurons in the rostral-, and non-PNN bearing neurons in the caudal parts. (a, c) *Dots* label longitudinal fascicles. *NST*: nucleus of solitary tract. Scale bar 200 µm (low magnification), 20 µm (insert).

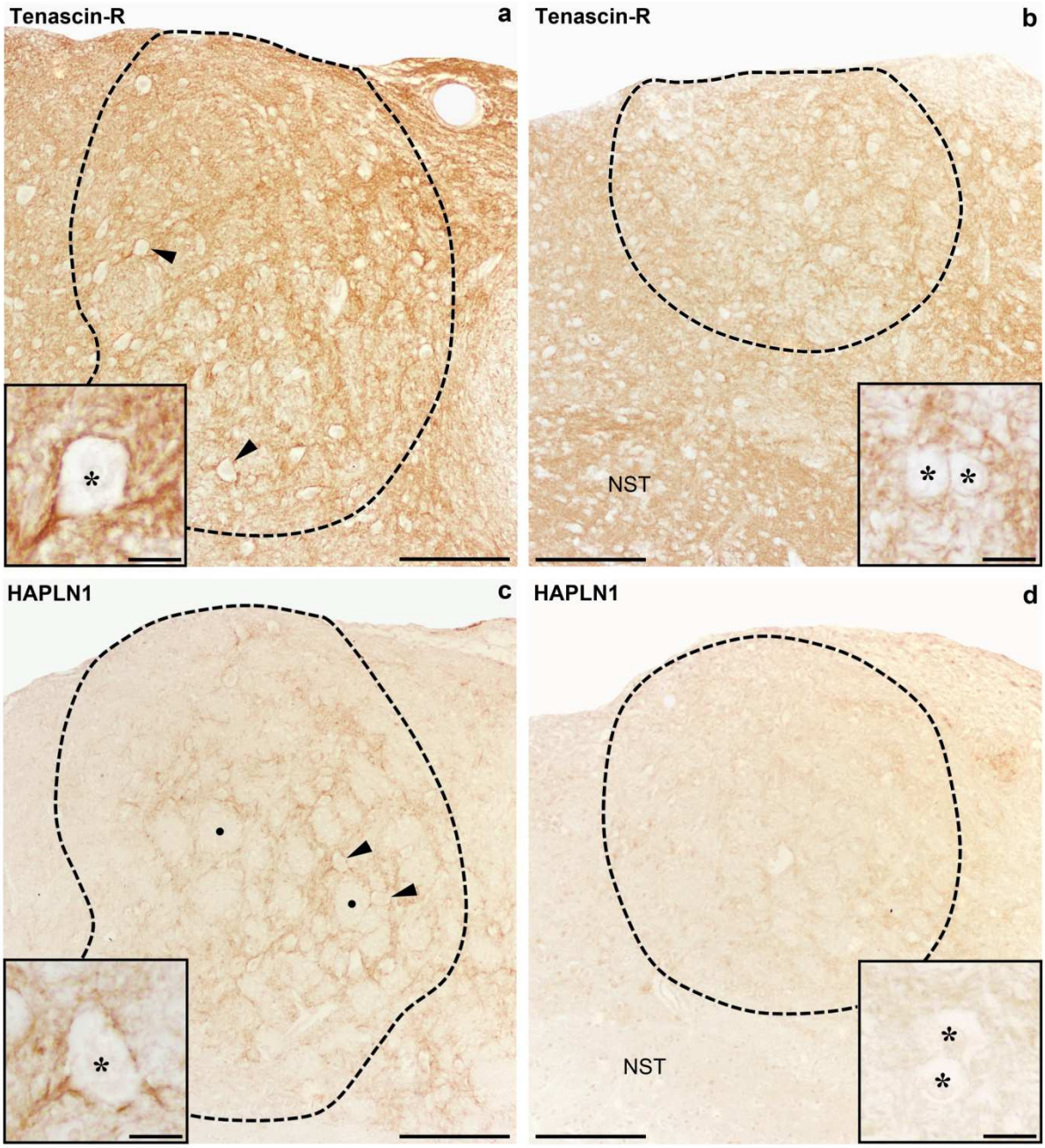

Figure 13: (a-d) Illustrating ECM staining patterns in the rostral and caudal divisions of DVN. *Arrowheads* show PNN-bearing neurons. *: label neurons in the inserts: PNN-bearing neurons in the rostral-, and non-PNN bearing neurons in the caudal parts. (c) *Dots* label longitudinal fascicles. *NST*: nucleus of solitary tract. Scale bar 200 µm (low magnification), 20 µm (insert).

PNNs were widely observed in the rostral part of the nucleus around giant, large, and medium size neurons (Figs. 10-13). The aggrecan and WFA staining produced the strongest staining intensity, then TN-R followed, and the weakest was by HA, neurocan and HAPLN1. Compared to the other nuclei the versican produced much fainter immunostaining, but still with the characteristic dot appearance. The brevican immunoreactions appeared weakest, with no or very faint reaction. The small-sized neurons were mostly not covered by PNN, only the WFA, aggrecan and the TN-R reaction was positive. In the caudal part of the nucleus a very

different ECM distribution and PNN construction was observed. Staining was generally fainter showing the strongest reactions for HA, WFA, versican, and TN-R. PNNs were sporadically visible, exclusively with versican and TN-R reactions, in weak staining intensity. In case of the other reactions, no PNN was observed in the caudal part (Figs. 10-13).

Staining intensity of PNNs in the rostral and caudal parts of DVN were semiquantitatively evaluated in Table 3. A detailed Neurolucida reconstruction was made to visualize the distribution and number of PNN-bearing neurons both in the rostral and caudal part of the nucleus in each reaction (Fig 14).

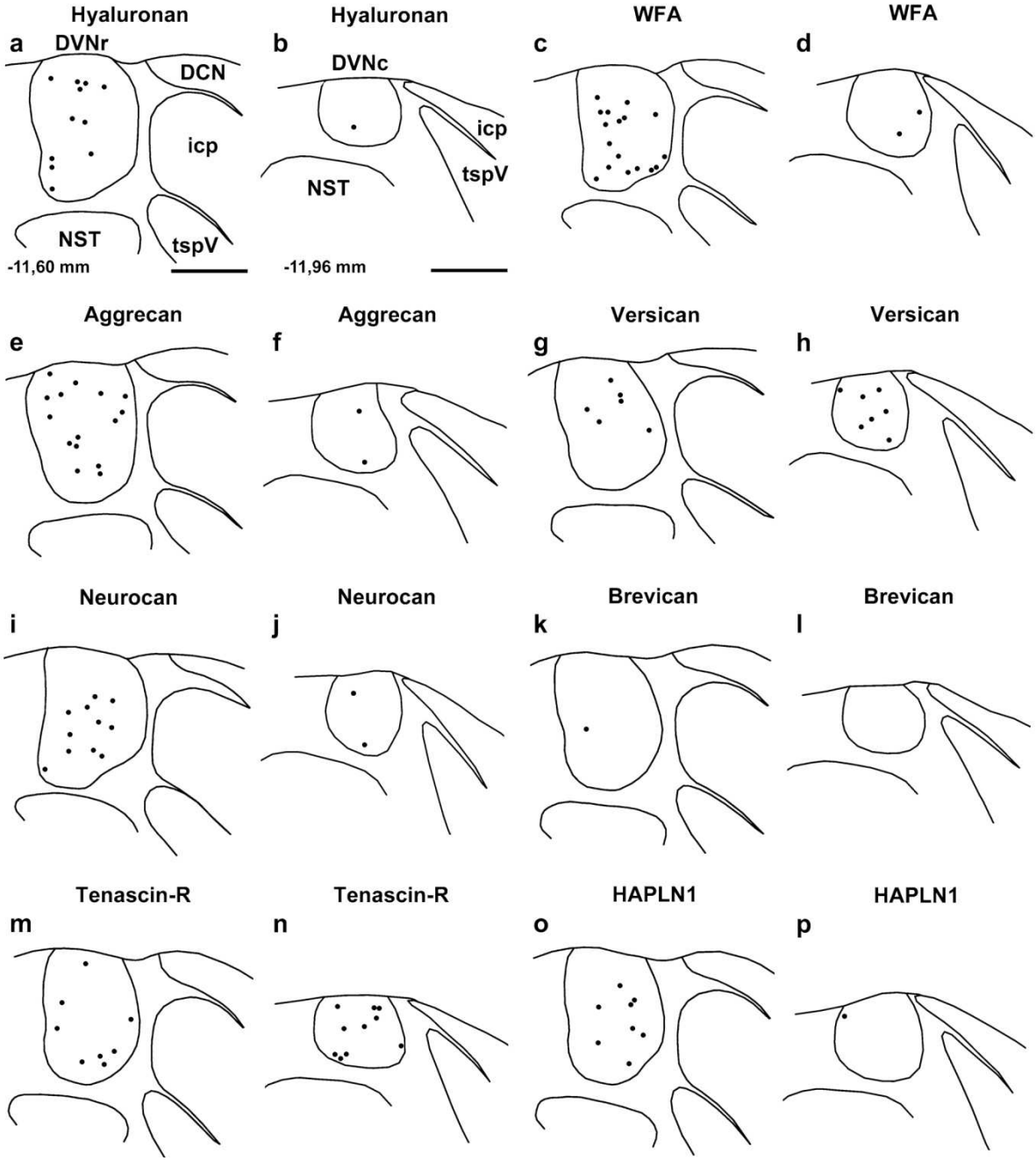

Figure 14. Neurolucida reconstruction showing the distribution of PNN-bearing neurons, in the rostral- and caudal parts of DVN (*dots*).

In the neuropil the staining pattern was determined by the longitudinally running parallel fiber fascicles that are only present in DVN within the VNC (Suarez et al, 1993). The previously described rostral and caudal regional differences in staining pattern of PNNs were identifiable in the neuropil as well. In the rostral part staining inside the fascicles as well as in the interfascicular areas presented strong positivity of reaction for WFA, aggrecan, versican, and TN-R, and slightly fainter for HA. With these reactions fiber bundles can be just hardly distinguished in the neuropil (Fig. 10c, e; Fig. 11a, c, Fig. 13a). On the other hand, neurocan, brevican, and HAPLN1 didn't make staining at territories of fascicles, but did stain the interfascicular areas (Figs. 12a, c; Fig. 13c). The neuropil of the caudal region was generally weaker stained than that of the rostral part. The fascicles and interfascicular areas can only be seen clearly with aggrecan, TN-R and fainter with HAPLN1 reactions. In case of the versican reaction boundaries of fascicular and interfascicular areas were clear, and a punctuated appearance of reaction was present in both places.

5.2 Alterations of perineuronal net staining after unilateral labyrinthectomy in rat

On the first postoperative day HA staining in the PNN almost entirely disappeared on the operated side, but there wasn't severe change seen in the intact side LVN. There was also a decrease in the neuropil staining intensity on the operated side compared to the unoperated one (Fig. 15a, b). On the 3rd day the HA staining in the LVN of the operated side further faded, PNN wasn't recognizable, whereas in the unoperated side the staining intensity was

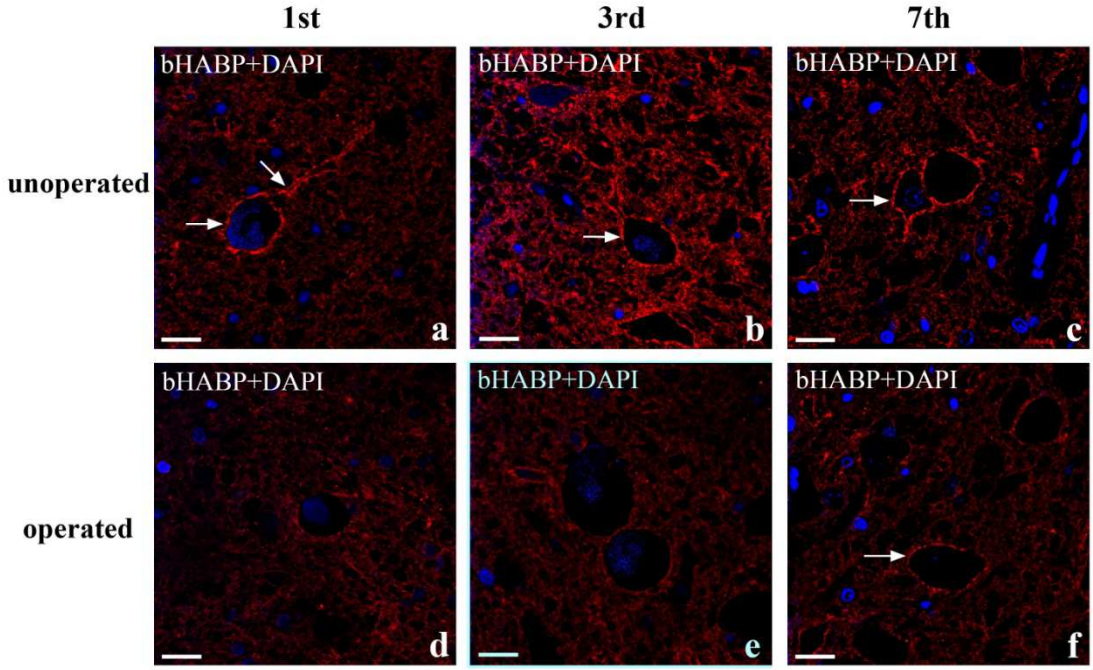

Figure 15. Hyaluronan labeling on unoperated and operated sides of rat LVN following UL, on 1st, 3rd, and 7th survival days. *Arrows* show PNNs. Scale bar 25 µm.

bilaterally compared to the first stage (Fig. 15c, d). After seven days of survival intensity of HA staining in the PNN increased on the operated side, PNNs were recognizable and were rebuilt to appearance close to controls. The neuropil staining still showed increased HA expression on the 7th day, as it was seen in the 3rd postoperative day (Fig. 15e, f).

The staining of CSPGs in the PNN by WFA lectin revealed severe fading of PNN labeling on the operated side, suggesting gradual decrease of CSPG levels in the PNN, whereas on the intact side PNNs were still present (Fig. 16a-f). Intensity of staining was much fainter in the neuropil as well on the operated side, on the 1st postoperative day in the LVN. On the third day after operation the overall staining pattern did not differ from the one seen on first day, regarding both the PNN and neuropil (Fig. 16b, e). By the 7th postoperative day the CSPGs reaccumulated in the PNN and weak staining of neuropil also appeared (Fig. 16f).

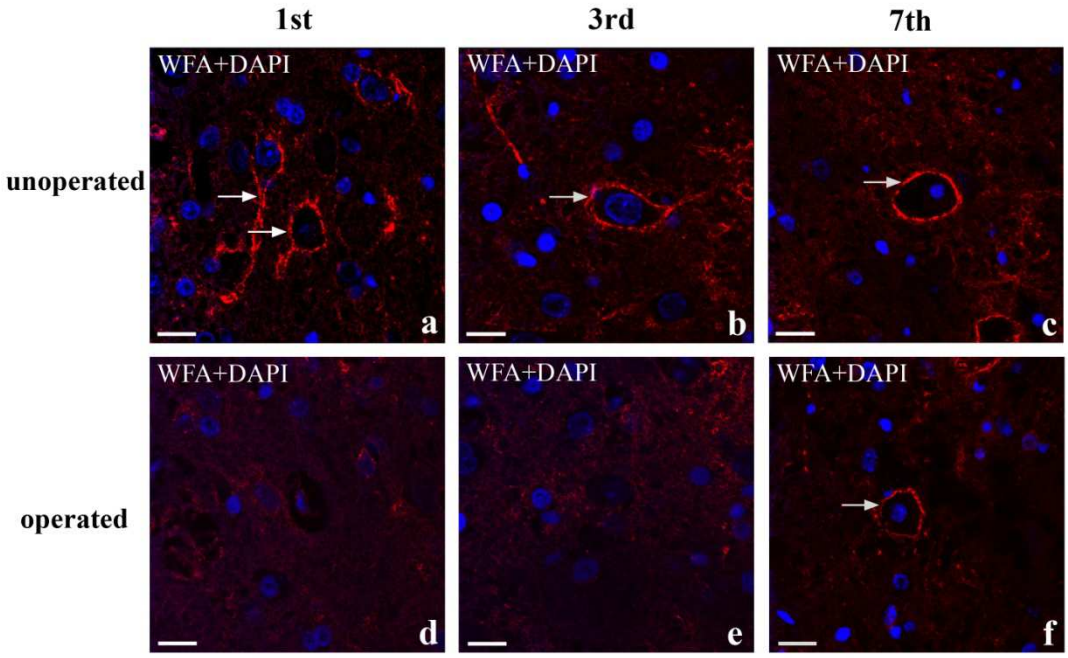

Figure 16. ***WFA*** **labeling on unoperated and operated sides of rat LVN following UL, on 1st, 3rd, and 7th survival days.** ***Arrows*** **show PNNs. Scale bar 25 µm.**

5.3 Distribution of ECM molecules in the vestibular nuclear complex of the frog

The TN-R and aggrecan molecules were not investigated before on frog nervous tissue with the chosen antibodies, therefore WB analysis was made to test specificity (Fig. 17).

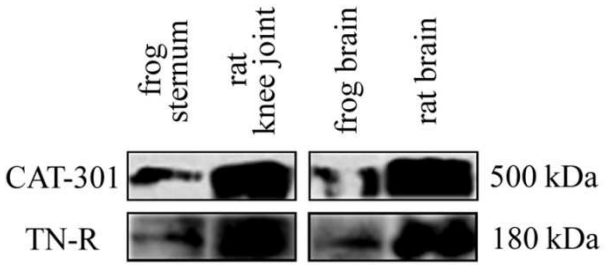

Figure 17. Western blot control on frog and rat brain, and sternal cartilages.

5.3.1 Superior vestibular nucleus

The HA reaction was only moderate or weak around cells of SVN. PNN accumulation forming complete rings over neurons was not observed, just discontinuous focal accumulations over perikaryons (Fig. 18A). The rest of the pericellular area was negative to HA reaction. In the neuropil HA labeling produced a reticular staining pattern with moderate intensity. The TN-R staining was negative, it didn't mark any PNNs in the SVN, even didn't show immunoreactions in the neuropil as well (Fig. 18B). The WFA, as a general marker of CSPGs, revealed no PNN at all in the SVN (Fig. 18C), and even no pericellular labeling was seen. In the neuropil there was a reticular-like patterning throughout the nucleus. With the WFA some ring like structures were observed scattered in the neuropil, with sizes of 1,5-17 µm, which are suspected to be the accumulations of CSPGs in the nodes of Ranvier (Fig.

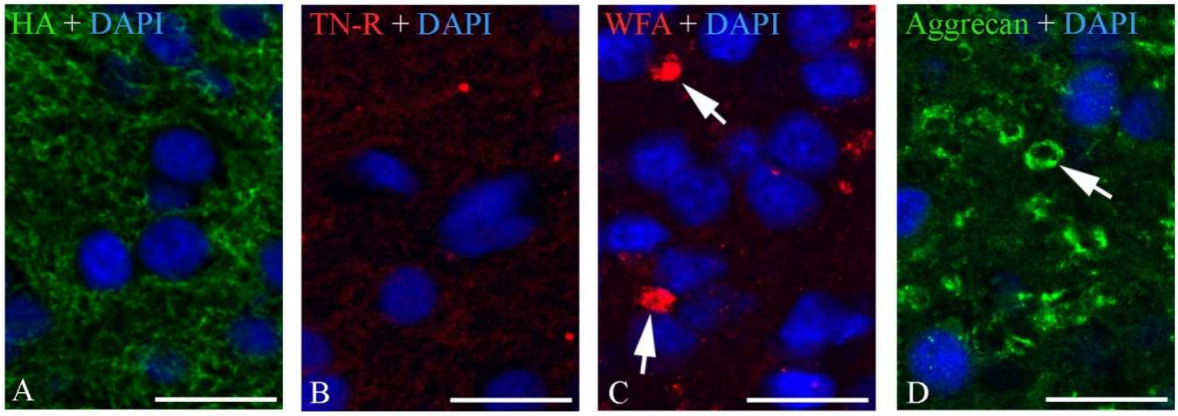

Figure 18. ECM labeling in SVN of the frog. (C, D) *Arrows* show nodal accumulations of aggrecan (CSPGs). Scale bar 20 µm.

18D). To specify the CSPG staining we applied Cat-301 clone aggrecan antibody. It didn't label any PNNs around perikarya of SVN, but in the cytoplasms of neurons several heavily immunoreactive granules showed (Fig. 18D). Similar reaction was recently reported in the cytoplasm of human basal ganglia cells, suggesting the neuronal production of aggrecan (Brückner et al., 2008, Giamanco and Matthews, 2012). In the neuropil Cat-301 showed more intense staining than WFA, with a similar reticular arrangement. Even more clearly visible dot or ring like forms were identified suspected as the nodal accumulations, mentioned earlier.

5.3.2 Lateral vestibular nucleus

Within nuclei of the frog VNC, HA histochemical reaction was the most intense in the LVN (Fig. 19A). Complete ring shape PNNs were only present around neurons of the LVN within the VNC, drawing strong continuous pericellular labeling around somas. In the

neuropil of LVN the HABP had the strongest reaction within the VNC, having the typical reticular organization in which neuronal processes and contacts run.

Compared to HA, TN-R immunoreactions had a fainter and not completely circular PNN condensation labeled around neurons of LVN (Fig. 19B). In the neuropil it showed expression, and among the other nuclei of VNC, staining was the strongest in LVN. The reaction with WFA lectin was generally not very intense, although the strongest was still in the LVN with this labeling (Fig. 19C). No PNN was observed, and in the neuropil the reticular appearance also wasn't visible. Like in the SVN, we could see the dot or ring shape condensations of CSPGs, most probably representing nodal ECM of thick myelinated axons.

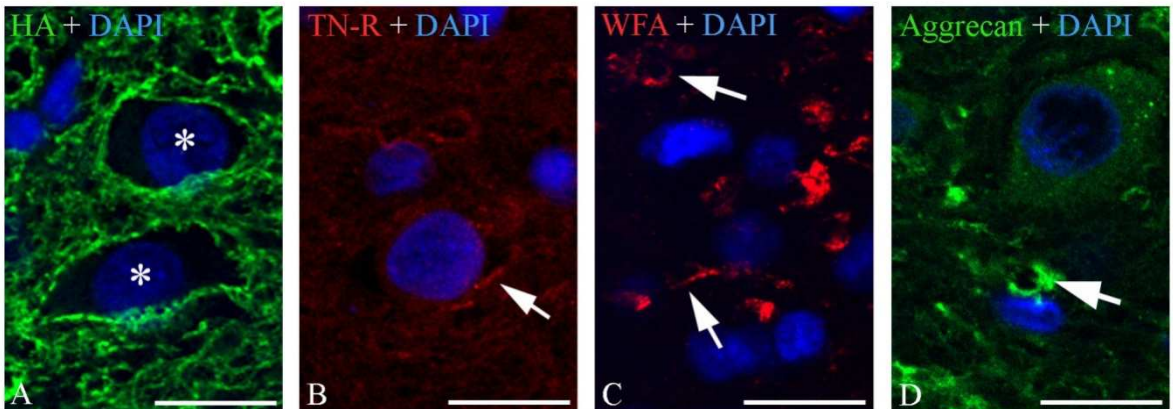

Figure 19. ECM labeling in LVN of the frog. (C, D) *Arrows* show nodal accumulations of aggrecan (CSPGs). * shows PNN-bearing neurons. Scale bar 20 µm.

The aggrecan Cat-301 labeling was similar to the one experienced in SVN (Fig. 19D). Thus the pericellular accumulation was not seen at all, but in the cytoplasm the immunoreactive granular dots presented. Theoretical basis of this phenomenon were detailed above for SVN. The neuropil staining was moderate, containing reticular diffuse staining pattern with dots or ring shaped condensations identified, as described above.

5.3.3 Medial vestibular nucleus

Following the LVN, the MVN showed the strongest labeling for HA (Fig. 20A), as far the pericellular area is concerned. In the pericellular area a discrete condensation was seen, forming PNN well separating from the surrounding neuropil. The PNN was less strongly stained as in case of LVN, even though most of the cells were PNN sheathed. The intensity of the neuropil staining was similar to the one seen in the LVN, but was seemingly stronger compared to SVN or DVN. With TN-R there wasn't any pericellular or characteristic neuropil staining in the MVN (Fig. 20B), and lacked nodal labeling. The neuropil had a diffuse patterning with low immunoreactivity. Labeling of CSPGs by WFA exclusively stained

structures in the neuropil (Fig. 20C). No pericellular signal was detected, and the neuropil had no reticular appearance at all. Just the dots or rings were seen, presumably representing nodal accumulations. In case of aggrecan Cat-301 reaction also no PNN was seen (Fig. 20D). The

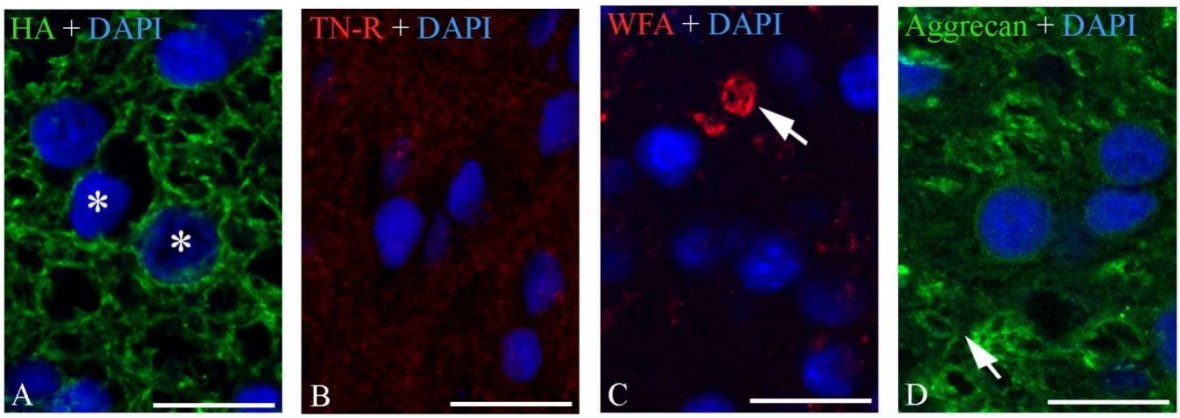

Figure 20. ECM labeling in MVN of the frog. (C, D) *Arrows* show nodal accumulations of aggrecan (CSPGs). * shows PNN-bearing neurons. Scale bar 20 µm.

previously mentioned immunoreactive granules were devoid in the cytoplasm of MVN neurons, although in the neuropil staining for aggrecan was the most intense here among the VNC. The rings and dots, suspectedly being nodes of Ranvier, are numerously represented.

5.3.4 Descending vestibular nucleus

Stained by the HABP there were no PNNs found in the DVN (Fig 21A), and the overall intensity of the reaction revealed lower HA expression in the nucleus. In the neuropil the HA reaction was diffusely distributed, at slightly higher intensity than found in SVN. The TN-R reaction reveled very low or no expression of the molecule either in the pericellular compartment or diffusely in the neuropil (Fig. 21B). With the WFA we could not detect any

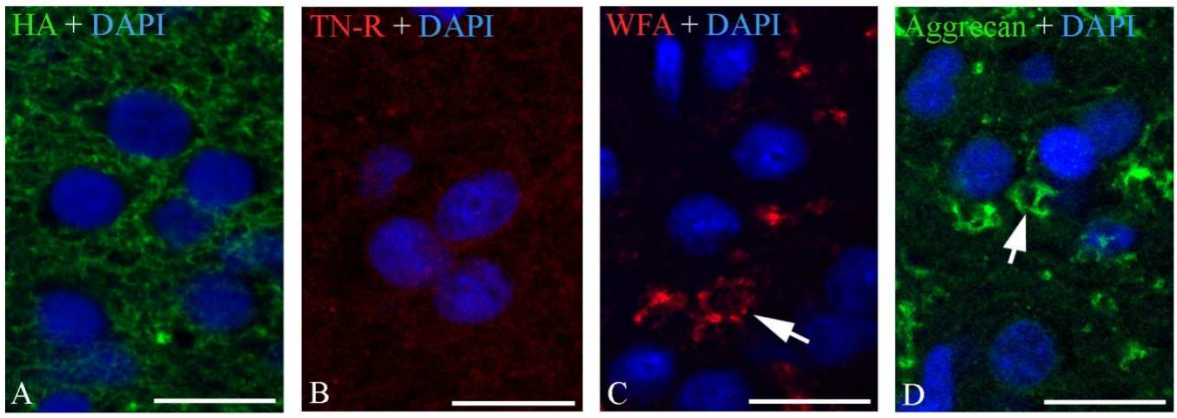

Figure 21. ECM labeling in DVN of the frog. (C, D) *Arrows* show nodal accumulations of aggrecan (CSPGs). Scale bar 20 µm.

signs of pericellular condensation of ECM molecules. In the neuropil we could only see signals of the mentioned dot or ring like structures corresponding to nodes of Ranvier (Fig 21C), confirmed by measuring of the diameters and comparing with axonal diameters. Other than the ring structures no other diffuse or reticular ECM expression was observed. As far as the aggrecan Cat-301 reaction is concerned, no PNN was labeled (Fig. 21D), but a faint cytoplasmic signal can be seen, showing just few faint granules. Heavily immunoreactive spots weren't characteristic in the cytoplasm. As seen for WFA as in all the other nuclei of the VNC, there were the intensively stained rings being most probably the nodal condensations.

6. DISCUSSION

6.1 Introductory words to the Discussion

In the rat brainstem the distribution of extracellular matrix macromolecules were mapped in the individual nuclei of VNC. By using histochemical and immunohistochemical methods we intended to reveal whether there is area and cell type dependent distribution of ECM in the VNC of rat. The widely differing hodological properties of VNC nuclei have long been described, which may also be in relation with ECM composition. Results were summarized in Figures of IHC images, in a Neurolucida reconstruction of the PNN covered neurons, and a Table of semiquantitative assessment scoring of PNN intensities. Explanation of results is presented firstly considering each nucleus of VNC, then later taking each molecule of ECM in count (Chapter **6.2)**.

Unilateral labyrinthectomy is the mechanic damaging of the balance sensory organs in the inner ear, resulting in unilateral deafferentation of the VNC. This is expected to trigger various related processes, including alterations of ECM molecular composition. The previously mapped ECM in the intact VNC will provide comprehensive information for further comparison and other associations explaining the plastic events in the CNS after injuries. During subsequent days of UL alterations of HA and CSPGs were investigated in the lateral vestibular nucleus. Proposed explanations of results is delivered in Chapter **6.3**; considering differing roles of CSPGs and HA, and associations of ECM turnover and improvement of symptoms.

Amphibian species are good model animals because of their relatively simple nervous system, which still reflects the conservativity of systems through evolution. The available data on ECM in the CNS of frog is very poor. Amphibians are evolutionary lower animals, and have the special ability to anatomically and functionally repair their cranial nerves and central pathways after disintegrating injuries. Explanations propose, among many other possible explanations, the very different ECM molecular assembly compared to higher mammalian species. Based on earlier results from our laboratory, the purpose of the present survey on ECM was to provide experimental evidences for later comparative investigations between lesioned mammalian and amphibian species. Results are explained below for each of the detected ECM molecules, in Chapter **6.4**. A comparison is made regarding the detected ECM molecules, hodological properties, and embryonic origins of the corresponding vestibular nuclear areas of rat and frog.

6.2 Distribution of extracellular matrix in the vestibular nuclear complex of the rat

6.2.1 Superior vestibular nucleus

In the SVN the centrally located giant and large neurons were surrounded with PNN, but the medium and small neurons, positioned in the peripheral part of the nucleus, were mostly devoid of PNN coverage. **We concluded that the presence of PNN around neurons in the SVN correlated with neuronal size, consequently experienced throughout the entire SVN. This also may indicate that neurons found in functionally different regions of SVN are associated with different PNN staining patterns.** The large-sized neurons establish inhibitory connections with the oculomotor and trochlear nuclei neurons through the ipsilateral medial longitudinal fasciculus containing glycine (horizontal) or GABA (vertical) inhibitory neurotransmitters (Buttner and Buttner-Ennever 2006). They are critical components forming the vestibulo-ocular reflex, described earlier in cat, rabbit, squirrel monkey, and other mammalian species (Ito et al. 1970; McCrea et al. 1987a; McCrea et al. 1987b; Mitsacos et al. 1983a). Small and medium cells, also called non-ocular neurons, project to the cerebellum and reticular formation, or they are establishing commissural connections with contralateral vestibular nuclei (Mitsacos et al. 1983a; Ladpli and Brodal 1968).

In the neuropil of SVN no regional difference was seen in the rostrocaudal or central to peripheral extension.

6.2.2 Lateral vestibular nucleus

In the rat no regional difference was found regarding the distribution of neuronal sizes throughout any extensions of the nucleus. The LVN contains mostly **large- and giant-sized neurons, which were all ensheathed by thick perineuronal nets, and there was no variability experienced in the PNN staining patterns throughout the nucleus**. The result is rather contradictory, since despite the homogenous cellular arrangement in the nucleus, the rostral and caudal parts have different afferent and efferent connections, which would suggest different molecular assembly of PNN in the two parts. The rostral parts receives afferents mainly from the utricle and *cristae ampullares*, and these neurons project to the oculomotor nuclei, via mono- di-, or even polysynaptic contacts, and most probably are similar physiologically to magnocellular elements of MVN, because of identical projection target areas. These cells also have reciprocal connection with cerebellum. Contrary, the caudal part of LVN doesn’t receive any vestibular afferents, just some spinal and inferior olivary

afferents were reported. The whole nucleus has reciprocal projections to the spinal cord in somatotopical manner: the rostral portion projects into cervical-, and the caudal portion into the lumbosacral segments of the spinal cord (Suarez et al. 1993; Brodal and Brodal 1981; Gacek 1969; McCrea et al. 1987b; McCrea et al. 1987a; Voogd et al. 1991; Bacskai et al. 2002; Pompeiano and Brodal 1957). Interestingly, our study shows that the LVN owns a special character among the vestibular nuclei, where the regionally differing projections of the nucleus don't result differing molecular assembly of the PNN. The possible explanation is still not complete, but it is tempting to assume that the homogenous PNN patterning is due to homogenous membrane properties, firing rates, and neurotransmitter content of the large LVN neurons in rats (Uno et al. 2003; Eugene et al. 2011).

The neuropil showed to be also homogenous throughout the nucleus, possibly a result of the homogenous neuronal distribution.

6.2.3 Medial vestibular nucleus

We found that the **staining patterns of PNNs appeared regionally different in the subdivisions of the MVN. Results also suggest that the differences are due to the cytoarchitectonical and hodological properties of the neurons composing the nucleus**. We found that **PNN ensheathed the large- and medium-sized neurons in the ventrolateral magnocellular portion of the nucleus, with all eight reactions studied, although in various intensities, whereas in the parvocellular part, located periventricularly, no or just few PNNs were labeled.**

Since there are morphologically, hodologically, and thus physiologically different neuron populations composing the MVN, interpreting results demands the identification of neurons according to these parameters. From the several categorizations of MVN neurons we found two relevant for our results, giving opportunity for two possible approaches.

Neurons of MVN were earlier categorized in mouse (Camp et al. 2006; Sekirnjak and du Lac 2006), rat (Johnston et al. 1994; Saito et al. 2008; Takazawa et al. 2004), and guinea pig (Babalian et al. 1997; Babalian and Vidal 2000; Serafin et al. 1991) into two major types. Accordingly the 'type A' neurons found in the parvocellular division, producing GABA, have a regular firing rate. These receive input from the *otolith receptors*, and project to inferior olive. They also have reciprocal connections with spinal cord and cerebellum. The other dominant neurons are the 'type B', located in the magnocellular division of MVN. They have an irregular firing rate, and their neurotransmitters are either glutamate or glycin. Their major inputs are from the *cristae ampullares* and cerebellar efferents, and provide efferents of

vestibulo-ocular and vestibulo-spinal pathways (Eugene et al. 2011; Kodama et al. 2012). 'Type B' neurons are also involved in spatial recognition by being connected to mammillary body (Brown et al. 2005; Shinder and Taube 2010). Considering the localization of distinct neuron groups in MVN, it is likely that 'type B' neurons are surrounded by PNN. On the other hand the 'type A' subpopulation, having rare or no PNN, represent the parvocellular division of MVN, involved in cerebellar, spinal, and perhaps autonomic regulations.

Recently, six distinct groups of neurons were identified in the MVN by Kodama et al. (2012), considering single-cell neurotransmitter, ion channel, and neuronal marker expressions. Thus, three excitatory neuron types were identified (E1-3), expressing glutamate transporter VGluT2. The E1 class comprises of large cells that project to contralateral abducens and oculomotor nuclei, and these provide predominant excitation to motoneurons of extraocular muscles. The E2 profile group contains precerebellar neurons projecting to flocculus through the mossy fibers. These neurons are located periventricularly, in rather caudal position, thus we may consider these being in the MVN PC subdivision. The E3 group isn't believed to operate in VOR, rather suggested to be present in the vestibulo-sympathetic autonomic reflex circuits of spinal cord (Kodama et al. 2012), suggested of being small-sized neurons. There are also three inhibitory neuron types identified (I1-3) by coexpressing genes encoding GABA synthetic enzymes, the GAD65 and -67, and glycine transporter GlyT2 proteins. The glycinergic I1 group was reported to gather premotor interneurons to the ipsilateral oculomotor neurons, innervated by flocculus. They are most probably located in the MVN MC, presumably surrounded by PNN. The I2 neurons are gylcin- and GABAergic and project to the contralateral oculomotor and abducens nuclei, receiving sparse inhibitory synapses on soma from floccular Purkinje cells. They presumably have weak or no PNN. Neurons in I3 group are GABA-ergic neurons, having inhibitory commissural connections between the bilateral MVNs (McElvain et al. 2010), and are located in the middle third of the nucleus. They receive none or weak floccular inhibition and by feedforward inhibition balances excitability of bilateral MVN neurons of VOR (Shin et al. 2012; Kodama et al. 2012). Although associating PNN-bearing and non-PNN-bearing neurons to the single-cell expression profiles extends far beyond our chosen aims, but still most of the neuron groups can be linked by morphology and localization.

Intensities in the subdivisions were different in case of aggrecan, WFA, neurocan, and HAPLN1 reactions, being lower in the MVN PC. Extact physiological reasons are not well understood.

6.2.4 Descending vestibular nucleus

We found in the DVN that there is considerable difference in the staining of ECM pattern between the rostral and caudal parts of the nucleus indicating the different contribution of the rostral and caudal segments of DVN to vestibular integral functions. In the rostral part the most numerous cells are the medium-sized neurons, large and giant cells provide approx. 15 %, and small sized cells are found in low number (Suarez et al. 1993). **PNN was experienced covering the medium-, large-, and giant-sized neurons with all reactions studied, except for brevican**. Small neurons having PNN were sporadically found, being positive only for WFA, aggrecan and TN-R. In the caudal part only 6 % of neurons are large-sized, and the majority are medium or small. **PNNs were rarely seen, consideably with TN-R and as forms of versican accumulations.**

Interpretation of results requires the consideration of the differing connections of rostral and caudal DVN. The above listed properties of the DVN were reported to be common in rabbit, cat, and rat (Porter and Balaban 1997).

In the rostral part of the nucleus the numerous large- and giant-sized neurons have parallel function with the LVN neurons, participating in the balance, posture, and head movements by extended vestibulo-spinal connections, and also by being part of the vestibulo-ocular circuit (Balaban 1996; Kerman et al. 2006; Holstein et al. 2011; McCall and Yates 2011). The vestibulo-oculo-collic reflex circuit neurons are widely spread over DVN, as well as MVN, and provide bifurcating axons projecting to the oculomotor nuclei and to the spinal cord, which are glutamatergic excitatory (Minor et al. 1990). These neurons don’t receive floccular inhibition, but instead, DVN neurons receive excitatory vestibular input from the utricule and saccule, together with LVN, caudal SVN, and nodulus. In the lack of information we may suspect the axons from thiese sources terminate on soma and proximal dendrite segments, thus contributing to PNN formation.

One unexpected phenomenon was the faint brevican staining both in the rostral and caudal parts of DVN. There were regional differences identified in brevican expression in mouse and rat cortical areas and were suspected to be related to differing plastic properties of certain areas (Ajmo et al. 2008). In case of the vestibular nuclei similar conclusion shouldn’t be stated, since the contribution of the individual vestibular nuclei to postlesional recovery is undescribed. In fact, there was strong brevican staining in the SVN, LVN, and MVN, being very strong component of PNNs, thus the absence of brevican could indicate some yet unknown function of brevican in the physiological function of the vestibular system during autonomic adaptation or in postlesional compensation.

The neuropil staining was moderate or weak, but was more intense in the rostral portion then caudally. The characteristic longitudinal fiber bundles were easier to recognize with WFA, aggrecan, versican, and TN-R reactions, because of the ECM molecules accumulating in nodes of Ranvier (Dours-Zimmermann et al. 2009). Fibers originate in the cerebellar vermis, or DVN, or are descending primary vestibular efferents.

6.2.5 Comparison of staining patterns in the rat's VNC - Possible functions of extracellular macromolecules in the rat VNC and further associations

Our work was the first one to provide a coherent description of ECM staining patterns in the VNC of rat. Besides recognizing a number of common regularities characterizing expression patterns of individual ECM building components, **we could find differences within subdivisions of SVN, MVN and DVN,** making comparison possible with rat, monkey, or human (Zimmermann and Dours-Zimmermann 2008; Morawski et al. 2012; Hartig et al. 1999; Carulli et al. 2006; Bruckner et al. 2008). **According to our findings the presence or absence of PNNs correlates with the neuronal sizes.**

Hyaluronan is the backbone of ECM, especially in the PNN formation. It is present from the initial steps of neural development as a permissive guidance molecule for migrating neurons and climbing axon growth cones. HA is an essential component of PNN, without HA PNN assemblies are not reported (Bignami et al. 1993; Kwok et al. 2010). In case of absent hyaluronan synthase enzymes (HAS1-3), the integrity of ECM structure is impaired or even animals are not viable (Kwok et al. 2010; Zimmermann and Dours-Zimmermann 2008). **Throughout the VNC strong or moderate presence of HA was seen in forms of pericellular condensations, diffuse signals in the neuropil.**

Chondroitin sulfate proteoglycans, are essential polyanionic macromolecules of mammalian PNNs (Koppe et al. 1997; Zimmermann and Dours-Zimmermann 2008). The general marker of CSPGs is the *WFA* lectin (Hartig et al. 1992). **Although it recognizes the majority of CSPGs**, having GAG side chains, **including lecticans**, **it provides no further insight to what molecules are specifically present at the area, but only provides additive overview of CSPGs.** *Aggrecan* is belived to have the largest number of chondroitin sulfate and keratan sulfate GAGs on the protein cores, and is the most abundant molecule of PNNs, thus we may expect its considerable influence on WFA staining (Härtig et al. 1992, Matthews et al. 2002).

In the mammalian mature CNS *brevican* is the most common CSPG after aggrecan, being a prominent constituent of the PNN, and shows age dependent dynamics (Frischknecht

and Seidenbecher 2012; Zimmermann and Dours-Zimmermann 2008; Yamaguchi 1996). We found strong brevican staining in the PNNs of in SVN, LVN, and magnocellular part of MVN large neurons, which demonstrates the findings of earlier reports on brevican. **Interestingly WFA staining wasn't similar to brevican reaction intensity.** WFA is able to label approx. 80 % of CSPGs (Giamanco et al. 2010). by N-acetyl galactosamin residues, but brevican has very few or even none CS substituents. Recent ultrastructural studies (Frischknecht and Seidenbecher 2012; Blosa et al. 2013) suggest close but spatially different locations for aggrecan and brevican were described in giant calyciform synaptic terminals of Held, in the trapezoid body. Aggrecan was located in the periphery of the synapse, surrounding it, and presumably preventing neurostransmitter spillover from synaptic cleft, whereas brevican was found inside the cleft separating active zones. Electron microscope studies reported plenty of calyx synapses in the SVN, LVN, and MVN (Matesz 1988; Peusner et al. 1988; Sotelo and Palay 1970), in frog, chicken, and rat, which may suggest the similar function of brevican, as well as aggrecan, perisynaptically. This confirmation may provide physiological explanation for the dynamics or time lapse of neurotransmitter release, reuptake, synaptic stability, etc.

The pericellular area was positive for *neurocan*, although it appeared fainter in all studied areas, compared to other lecticans' staining. The weak staining could be explained by the gradual decrease of full length neurocan postnatally (Zimmermann and Dours-Zimmermann 2008). According to other speculations, full length neurocan is cleaved after birth, forming C-terminal and N-terminal fragments. The applied DSHB 1F6 monoclonal antibody only recognizes the N-terminal fragment that may explain the seen results. We also observed strongly immunolabelled patches sporadically located on the neuronal membrane, and in the neuropil. The earlier could be some perisomatic localized forms, and the latter can be the nodal neurocan (Bekku and Oohashi 2010), forming diffusion barrier and ion trap. **Neurocan** is a nervous tissue specific CSPG, **believed being inhibitory on axon regrowth during tissue remodeling.**

In the adult only the *versican* V2 isoform is present. We detected V2 with the DSHB monoclonal antibody 12C5 clone, which recognizes the hyaluronan binding region of the molecule. Immunostaining has the characteristic punctuate appearance, regerdless of which part of the CNS is studied (Oohashi et al. 2002; Zimmermann and Dours-Zimmermann 2008; Bekku et al. 2009). It is primarily located in the nodes of Ranvier, together with TN-R, HAPLN2, brevican, and phosphacan (Zimmermann and Dours-Zimmermann 2008; Bekku et al. 2009). Electronmicrographic explanations showed that nodal regions of axons in the vestibular nuclei are not only located in the neuropil, but are in close contact with the

neuronal soma (Sotelo and Palay 1970; Matesz 1988). If so, then the sporadic immunopositive dots, embracing the soma, could be either axonal coats around calyciform terminals (Lendvai et al. 2012; Bruckner et al. 2008; Morawski et al. 2012), or could be a versican-relative brevican anchorage of PNN covering the axon initial segment of certain neurons (Dours-Zimmermann et al. 2009). Versican inhibits axon growth/regrowth, plastic reorganizations in the adult CNS, and its expression ascends in the postnatal period (Zimmermann and Dours-Zimmermann 2008). **Its moderate expression in the VNC, especially in the DVN may be one explanation for the system's high level of plasticity.**

The *tenascin-R* is a homotrimeric glycoprotein of the ECM in mammalian species, and is a major contributor of the PNN integrity, and stabilization (Bruckner et al. 2000; Carulli et al. 2006; Deepa et al. 2006; Koppe et al. 1997; Kwok et al. 2010; Wang and Fawcett 2012; Pesheva and Probstmeier 2000). It has special affinity to bind lecticans by its fibronectin domains, especially to brevican. TN-R accumulates in large polymer structures at the nodes of Ranvier (Dours-Zimmermann et al. 2009; Kwok et al. 2011). The biological role of TN-R is divers, sometimes controversial, depending on developmental state, physical form, or molecules collaborating. TN-R's effect on plasticity or repair is not direct, but is mediated by cytokines, or neurotrophic factors. Nevertheless, **TN-R has repellent effect on axon growth,** there is still lack of data on the function of TN-R in the vestibular system.

The role of *hyaluronan and proteoglycan link protein 1* is to fasten anchorage between HA and the G1 domain of CSPGs. Mice lacking link proteins have increased plasticity, resulting the prolonged flexibility of ocular dominance establishment (Carulli et al. 2010). In link protein knock-out mice there was no brevican, versican, hyaluronan labeled in the nodal space, and weak TN-R, suggesting the putative role of link proteins in matrix integrity (Bekku and Oohashi 2010). In the vestibular nuclei the function of HAPLN1 is not completely revealed. We may suspect **higher plasticity in the VNC explained by the weak staining pattern of HAPLN1 throughout each nucleus.**

According to our **general experience** there was striking difference experienced between subnuclei of MVN and DVN, suggesting that **these areas may have higher flexibility for adaptations in the circulatory and respiratory regulation**.

6.3 Unilateral labyrinthectomy in rat results temporary alterations of HA and CSPG staining in the postoperative period

During the histological examinations, PNN wasn't recognizable on the first postoperative day around neurons of LVN, on the operated side of the sections, by using

bHABP and bWFA histochemical reactions. The positivity of both HA and WFA staining returned by 7th postoperative days. **Our experiment revealed that amelioration of symptoms corresponds to the reestablishment of PNNs, suggesting the possible involvement of HA and CSPGs in vestibular compensation.** Earlier and recent studies emphasized the specific presence of lecticans in the rat's CNS, particularly in the VNC (Hagihara et al. 1999). WFA labeling provides only indirect evidence on the impairment of CSPGs during compensation process, which reasons further specifications on molecular components. Our, yet unpublished, data suggests that all lecticans, aggrecan, brevican, neurocan, and versican, are deeply involved in the image seen with WFA.

In the lack of experimental data on the role of ECM in the vestibular compensation and deafferentation induced plasticity of vestibular nuclei, we propose, some explanations how the ECM molecules may contribute to the various mechanism of vestibular compensation. In the acute phase of vestibular compensation axonal sprouting and elongation (de Waele et al. 2000), or establishment of new synaptic connections is questionable, although HA and CSPG decrease could be in favor, because it is the sensory organ and the peripheral process of the vestibular ganglion cells which has been damaged, and no central pathway was cut.

Even though there is, most probably, no axonal rewiring in the VNC during the postoperative period, severe alterations can be expected in synaptic transmission efficacy, triggered by the imbalance of bilateral VNCs. Among intracellular events, changes in the ECM is triggered as well, experienced as the decrease of HA and WFA staining intensities in the PNN. Plastic synaptic modifications for the remodeling of resting membrane potentials demands structural "loosening" of synaptic elements to change physiologically and morphologically to adapt to new circumstances, induced by deafferentation. Studies on spinal cord and cortical injuries suggest similar plastic mechanisms in the background of functions repair. Plastic changes of synapses involve both kinds of alterations, (i) the synaptic plasticity, which is the activity-dependent changes in the efficacy of synaptic transmission accross existing synapses, but these require simultaneous (ii) anatomical plasticity, or structural plasticity, during which a new anatomical arrangement of connections develop either by new synapse formation or modification of existing ones (Fawcett 2002). In this sense experience based learning (Butz et al. 2009), or injuries act similar. The process of natural compensation is also presents in the cerebral cortex or in the spinal cord after strokes or mechanic injuries, during which the perilesional intact nervous circuits are able to take over functions of the lost area. Other experiments on stroke suffered aging rat brains also suggest that even in the aging brain a window of plasticity can be kept open by introducing chondroitinase ABC, by which

prospects of recovery become better (Doidge: The brain that changes itself 2007, Soleman et al. 2012).

HA is synthesized by the membrane bound hyaluronan synthase (HAS) enzymes, having three variation, HAS1, HAS2, and HAS3. Physiological studies suggest that changes of membrane properties of 2nd order vestibular neurons simultaneously alters ECM composition (Shao et al. 2009). If so, we may suggest that changing membrane properties cause change in HAS activity/presence, explaining decrease of HA staining in 1st and 3rd postoperative days. ECM is believed to be activity dependent.

The rapid decrease of CSPG expression, on 1-3 postoperative days, seems more difficult to explain. In the mouse barrel cortex the sensory deprivation didn't alter the aggrecan staining pattern and intensities of PNNs, which stands opposite our results. The possible reason of this obvious difference can be that the vestibular system shows higher plastic characteristics compared to other sensory systems (McCrea 2007).

The turnover of intercellular space macromolecules is also in synchrony with the found results. The turnover of sulfated GAGs is approximately 24 h in the brain, by the rapid facilitation of extracellular MMPs, and rapid decrease of synthetic enzyme activities (Rauch 2007). Similarly, the half life of HA in the intercellular space ranges between less than 1 to several days, which is in accordance with the experienced results after UL (Fraser et al. 1997). In the background of improvement of postlesional symptoms we mainly suspect those plastic events which progress intracellularly by altering the physiology of neurons to a new equilibrium state that influences the ECM molecular assembly by means of temporary HA and CSPG decrease.

In the past decade, a surprising neurogenesis was mentioned in the VNC, after unilateral vestibular neurectomy in cat. Results show a peak of neurogenesis at 3 days post UL, which gradually decreases until 30 days. Among microglia and astroglia cells, GABAergic neurons develop in medium and small sizes (Tighilet et al. 2007). In our experiment **HA was found to increase its expression in the neuropil after UL, which may provide a permissive environment for axonal pathfinding, or synaptogenesis.**

6.4 Function of extracellular matrix molecules in the vestibular nuclei of the frog

The common waterfrog, classified below mammals on the phylogenetic tree, is suspected to show a different assembly of matrix molecules in the same vestibular system, especially regarding PNNs. In many of the mammalian, marsupial, avian, or lower species the composition of ECM was described in various CNS areas (Bertolotto et al. 1996; Becker et al.

2000; Becker et al. 1999; Becker et al. 2004; Morawski et al. 2009; Gáti et al. 2010a, b). There is some data available on ECM composition in the vestibular nuclei of rat, mouse, Madagascan tenrecs (Afroteria). Their common feature is that CSPGs are found in the PNNs of vestibular neurons (Bertolotto et al. 1996; Deepa et al. 2006; Hagihara et al. 1999; Costa et al. 2007; Morawski et al. 2010), but those clades are phylogenetically higher.

Our work showed great contrast to reports on placental or marsupial mammalian species, or avian, and could be compared to our recent study on rat vestibular nuclei. In frog, PNNs were seen around large neurons of LVN and MVN, showing positivity only for HA, and less considerably TN-R labeling, whereas, in the DVN and SVN none of the examined ECM components had pericellular accumulation. Based on additionally performed IHC investigations, we may suggest that PNN assembly in **the vestibular nuclei of the frog, are devoid of CSPGs**.

ECM deposits accumulate in the nodes of Ranvier of thick myelinated axons. The molecular assembly of mammalian nodal ECM contains versican, brevican, phosphacan of the CSPGs, TN-R, link proteins, and HA (Dours-Zimmermann et al. 2009; Cicanic et al. 2012; Bekku et al. 2009; Bekku and Oohashi 2010). In the frog we found similar ring-like structures in the neuropil of vestibular nuclei, whith diameters up to 17 μm, or smaller, most probably representing the nodal ECM accumulation of thick vestibular axons (Reichenberger and Dieringer 1994; Birinyi et al. 2001; Honrubia et al. 1981), which are primary vestibular afferent fibers. The possible function of those nodal ECM deposits are same as those described in higher vertebrates.

6.4.1 Vestibular nuclei with different hodological properties exhibit different extracellular matrix assembly

Since there was varying molecular composition of ECM seen in the individual vestibular nuclei of the frog, we may suspect these differences being in correlation with the differing functional connections of each nucleus. Evaluation of results is not easy, as there has not been a selective fiber tracing performed on non-mammalian frogs, except for the LVN in our laboratory (Matesz et al. 2002). Nevertheless, we can refer to earlier data collected in mammalian species, reasoned simply by the evolutionarily conserved morphofunctional organization of the vestibular system. As described in the rat, SVN projects predominantly to motoneurons of eye movement nuclei, and is involved in the VOR (GABAergic) (Straka and Dieringer 2004; Buttmer and Buttner-Ennever 2006). DVN and MVN are involved in the control of head and eye movement during body displacement (gylcinergic), but their caudal

part establishes widespread vestibulo-autonomic connections with autonomic brainstem- and spinal areas. The LVN is the main source of medial longitudinal fasciculus fibers, both in mammals and frogs, and control head and eye movements upon vestibular stimulus. Although similar segregation of neuron subpopulations within each nucleus wasn't seen in the frog's VNC, that regional differences in the differing connections of the individual vestibular nuclei also can be reasons of PNN presence or absence.

The HA rich PNNs were only experienced in the LVN and occasionally in the MVN, which is tempting to underline earlier remarks that these two nuclei are primarily involved areas in restoration of damaged vestibular function (Halasi et al. 2007). In amphibians not only functional compensation happens after vestibular damage, but the HA rich milieu can promote anatomical repair as well, by axonal sprouting and neurogenesis, that will newly establish synaptic contacts (Halasi et al. 2007). In mammalian species similar considerable neurogenetic progress wasn't reported so far. In the compensation process, the role of commissural connections is especially important. Among the nuclei, SVN and DVN establishes majority of the bilateral connection, followed by the MVN and LVN, reported in cat and frog (Ito et al. 1985; Malinvaud et al. 2010).

Funtions and connections, thus physiological activity of neurons is determined by their embryonic origin, in the case of VNC the rhombomeric origins. In the frog brainstem the SVN develops from rhombomere 1/2, LVN develops from rhombomere 3/4, the majority of MVN and DVN from rhombomere 5/8, and the efferent vestibular neurons develop from rhombomere 4, which is common in vertebrates (Simon and Lumsden 1993; Fritsch et al. 1997; Straka et al. 2001). The description of rhombomere specific ECM expression pattern is still an unexploited field.

6.5 Composition and suspected function of ECM in the frog and rat vestibular system

Important recognition of our results is that in the common water frog's ECM, with special regard on the PNNs seen in MVN and LVN, **we could only detect HA, with lesser expression of TN-R, but no considerable appearance of CSPGs were experienced**. In strong contrast to mammals, neurogenesis in amphibians possibly exists in the adult vestibular nuclei, taken over from recent studies experiencing similar progresses in amphibian midbrain and medullary auditory centers (Simmons et al. 2006). The HA rich, but CSPG poor milieu provides permitting environment for new neuronal divisions, cell migration and connection into existing circuits.

After vestibular neurectomy of the common water frog (Halasi et al. 2007), it was found that HA deposits in the perineuronal spaces decreased on the operated side, then were rebuild from the third postlesional week, and the newly regrowing axons from the vestibular ganglion established functional connections with the deafferented vestibular neurons in the brainstem, supported by HA deposits. Supporting this result, in the neural stem cell niche a HA enrichment was found (Preston and Sherman, 2011; Pajenda et al. 2013), which is permitting axonal through-growth. Experimental removal of non-permissive CSPGs from glial scar has similar effect on axon growth.

The largest contrast of ECM molecular composition occurred in case of CSPGs in frogs, in relation to mammalian species. Our results indirectly support the inhibitory effect of CSPGs in LVN of rat after UL. The structural state of synapses is highly supported by the anchoring CSPG structural elements, so changes in the synaptic transmission demands breakdown of ECM meshwork in order to change morphology at the same time. The possible reasons why only low expression of CSPGs could be seen in the forg vestibular nuclei may be: **1**) Plasticity of the system is required to accommodate to seasonal, thus hormonal-temperature-metabolic changes, terrain and prey variabilities, being continuously prepared for environmental impacts. **2**) Evolutionary steps under mammalians suggest that there has to be a certain evolution of different CNS systems, also reflecting in ECM composition. **3**) Yet unidentified molecular composition of ECM is present, which may not be grabbed by antibodies presently available. Although WFA lectin and a number of antibodies were tested during investigation to recognize any possible sulfated or unsulfated GAGs of CSPGs. **4**) Other, yet unknown factors.

Parallel with findings on CSPGs there was a lack of TN-R in the PNNs of vestibular neurons in the frog, but some immunoreactive patches occurred in the neuropil. TN-R is an inhibitory molecule, and the same restricting effect was described in zebrafish (Becker et al. 2004), salamander (Becker et al. 1999), and mice (Becker et al. 2000), which means a range in phylogenetical levels below and above frogs. Consequently, the TN-R free PNNs of frog vestibular neurons could be providing a permissive background for growing axons during anatomical recovery and functional repair, following injuries.

7. FINAL CONCLUSIONS and FUTURE PERSPECTIVES

The presented scientific findings seem to support the previously proposed functions and properties of the ECM. Our work provides a morphological basis of the expressed ECM molecules in the intact vestibular nuclei of the rat and frog, as well as of changes of HA and CSPGs after deafferentation by UL. Consequences and future perspectives of these studies are summarized below.

By using morphological methods in the intact rat VNC, a detailed description on the molecular organization and regional distribution of ECM was given in all nuclei and subnuclei. We have recognized that besides HA, as a key framework of ECM, the different lecticans are expressed in considerable, but very area dependent amounts. In our study both condensed and diffuse forms of ECM were present in the VNC of rat, confirming reports on other parts of CNS. Our other important recognition is that presence of perineuronal nets is associated with the neuronal size, meaning that giant and large cells are ensheathed by strong PNN condensation, but around medium and small neurons PNN is mostly missing. Further striking finding is that considerable differences showed in ECM staining patterns between areas of VNC having different afferent and efferent connections. Thus, we may conclude that regional differences shown in staining patterns correlates with cytoarchitecture, hodological and functional characters of each vestibular nucleus, including their subnuclei. Although belonging to basic research, these data can initiate a new approach for the classification of vestibular neurons. ECM, more specifically PNN, is a product of neurons and glia, highly influenced by functional properties of the neurons, and vice-versa. Based on our findings so far, a consequent mapping on co-localization of matrix molecules with ion channels, neurotransmitter receptors, presynaptic terminals must be made. Thus a closer aspect on function may be obtained on each ECM molecule, and a more precise classification of vestibular neurons.

Results of UL in rat have shown a number of consequences. It was the first study performed in the vestibular system, showing the changes of HA and CSPGs staining patterns in LVN. This suggests the possible involvement of ECM molecules in plastic events of the vestibular system. In firm connection, the temporal progress of postural deficits and repair of

close-to-normal balance function follows the re-establishment of perineuronal nets in the LVN. Although further ultrastructural confirmation is needed to localize different CSPGs perisynaptically or in the synaptic cleft, we may suspect the involvement of aggrecan and brevican, the two most abundant contributors of WFA staining, to be involved in synaptic activity alterations and re-establishment of a new synaptic discharge balance, around large calyciform axon terminals. This is in harmony with earlier findings on the role of ECM functional repair after lesions of CNS, or even experience-based learning. These data is still not detailed enough to substract appropriate functional conclusions for individual ECM molecules, and for what happens in the other nuclei of VNC. The results of an already ongoing project will soon provide deeper insight into the time course and role of lecticans, TN-R, and link proteins during vestibular compensation. The theoretical background knowledge, we can obtain from these experiments can later cooperate in developing new therapeutic methods for vestibular disorders, yet incurable. The further very important message of this study is that the adult brain cannot be considered “hardwired”, as thought in past times. What’s more, neural circuits have great, but hidden potentials in changing themselves, to compensate and restore functions after a number of neurological or psychiatric disorders (Doidge: The brain that changes itself, 2007).

In the common water frog (*Rana esculenta*), our work was the first to describe the molecular composition of ECM in the VNC. This enables evolutionary comparison of taxons, still considering the relatively conserved organization of the vestibular system. The most important result is that PNNs, exclusively found in the frog’s LVN and MVN, demonstrated only HA positivity. Despite the extended case of IHC reactions against various CSPGs, TN-R, and link proteins, we couldn’t detect considerable signals in the PNNs. This result is in strong contrast to findings in rat VNC, where CSPGS, TN-R, and HAPLN1 was present. However, similarly to observations in rat, a strict regional segregation was seen between nuclei of VNC, which also corresponded with functional and connection specificities, or even with embryological origin of nuclei. It is also known that the amphibian CNS has better regenerative and plastic capability than mammals, but the theoretical background of it is not well explored, so far. The HA dominant, low CSPG and TN-R containing matrix could be one explanation. To provide wider explanations on why only HA builds PNNs, the knowledge on detailed afferent and efferent connections of VNC nuclei is required, and perhaps lesion experiments, and biochemical confirmation.

8. SUMMARY

We described for the first time the molecular composition and distribution of extracellular matrix (ECM) in the vestibular nuclear complex. Observations were carried out on intact and unilaterally labyrinthectomized rats, and on intact common water frogs.

Our main findings:

- In the vestibular nuclei of the rat, ECM molecules are expressed in an area dependent manner. All forms of ECM are present in rat's vestibular nuclei; diffusely in the neuropil, or in condensed forms as perineuronal net (PNN) or axonal coats, and accumulation in nodes of Ranvier.
- Formation of perineuronal nets is in association with the neuronal size, suggesting that giant and large neurons are ensheated, while medium and small neurons are mostly not covered by perineuronal accumulation of ECM.
- Considerable staining differences were seen, including both neuropil and perineuronal net patterns, between parts of the vestibular nuclei having different afferent and efferent connections. Thus, regional differences correlate with cytoarchitecture, hodological, and functional characters of each vestibular nucleus, and their subnuclei.
- In the rat severe alterations in staining patterns of hyaluronan and chondroitin sulfate proteoglycans occur around neurons of lateral vestibular nucleus following unilateral labyrinthectomy. This finding proves the possible role of ECM molecules in the induction of postlesional disorders.
- The temporal onset of functional and behavioral progress after unilateral labyrinthectomy corresponds with the time course of perineuronal net reestablishment, which suggests the role of matrix turnover in plastic changes of neuronal circuits and compensatory processes.
- In the frog vestibular nuclear complex perineuronal nets are only accumulated around neurons of lateral and medial vestibular nucleus. They are built only by hyaluronan, and devoid of chondroitin sulfate proteoglycans and glycoproteins, enabling better plastic and regenerative properties.
- Parallel with findings in rat, regional difference characterizes the expression of matrix molecules in frog's vestibular nuclei, associating with functional and connection properties.

9. ÖSSZEFOGLALÁS

Jelen munka az első morfológiai összefoglalás, amely az extracellularis matrix (ECM) molekuláris összetételének vizsgálatát és eloszlásának feltérképezést tűzte ki célul a vestibularis magkomplexumban. Vizsgálatainkat ép és labyrinthus irtott patkányokon, valamint ép kecskebékákon (*Rana esculenta*) végeztük.

Eredményeink alapján a legfontosabb következtetéseink:

- Patkány vestibularis magkomplexumában az ECM molekulák regionális megoszlást mutatnak. Az ECM valamennyi ismert megjelenési formáit leírtuk a patkány vestibularis magjaiban: diffúzan a neuropilben, és kondenzált formában, mint ’perineuronalis net’ (PNN) és ún. ’axonal coat’, ill. nodalis ECM a Ranvier féle befűződések körül.
- A PNN kialakulása neuron mérettől függő, az óriás- és nagyméretű neuronokat erős PNN veszi körül, míg a közepes- és kisméretű neuronok körül nagyrészt nem alakul ki PNN.
- Jelentős különbségek mutatkoztak a neuropil és PNN-ek jelölődési mintázatában a vestibularis magkomplexum különböző afferens és efferens kapcsolatokkal rendelkező régiói között. Megállapítottuk, hogy a regionális különbségek korrelálnak az adott mag cytoarchitektonikai, hodológiai, és funkcionális jellemzőivel.
- Patkányban féloldali labyrinthusirtást követően a hyaluronsav és chondroitin sulfat proteoglycanok jelölődésének jelentős csökkenését tapasztaltuk a sérült oldali *nucl. vestibularis lateralis* neuronjait borító PNN-ben. A megfigyeltek alapján feltételezzük az ECM jelentős változását a vestibularis léziót követő tünetek kialakulása során.
- Labyrinthus irtását követő tünetek rendeződésének időbeli lefolyása megfelel a perineuronalis hálók újbóli kiépülésének idejével, amiből következtethetünk az ECM turnover szerepére az idegrendszer plasztikus változásaiban, és a tünetek kompenzálódásában.
- Béka vestibularis magkomplexumában kizárólag a lateralis és medialis magokban jellemző a PNN. Felépítésükben csak a hyaluronsav vesz részt, viszont chondroitin sulfat proteoglycanok nincsenek jelen. Ezen ECM összetétel alátámasztja a béka vestibularis rendszer nagyfokú plaszticitási és regenerációs képességeit/lehetőségeit.
- Béka vestibularis magkomplexumában, patkányhoz hasonlóan, karakterisztikus regionális különbségek láthatók az ECM molekuláris összetételét és a jelölődés mintázatát tekintve, amely összefüggésbe hozható az területek funkcionális és kapcsolati jellemzőivel.

10. REFERENCES

Aboitiz F, Zamorano F (2013) Neural progenitors, patterning and ecology in neocortical origins. Frontiers in Neuroanatomy 7.

Ajmo JM, Eakin AK, Hamel MG, Gottschall PE (2008) Discordant localization of WFA reactivity and brevican/ADAMTS-derived fragment in rodent brain. BMC Neurosci 9:14.

Alilain WJ, Horn KP, Hu HM, Dick TE, Silver J (2011) Functional regeneration of respiratory pathways after spinal cord injury. Nature 475 (7355):196-U195.

Anlar B, Gunel-Ozcan A (2012) Tenascin-R: Role in the central nervous system. International Journal of Biochemistry & Cell Biology 44 (9):1385-1389.

Babalian A, Vibert N, Assie G, Serafin M, Muhlethaler M, Vidal PP (1997) Central vestibular networks in the guinea-pig: functional characterization in the isolated whole brain in vitro. Neuroscience 81 (2):405-426.

Babalian AL, Vidal PP (2000) Floccular modulation of vestibuloocular pathways and cerebellum-related plasticity: An in vitro whole brain study. J Neurophysiol 84 (5):2514-2528

Bacskai T, Szekely G, Matesz C (2002) Ascending and descending projections of the lateral vestibular nucleus in the rat. Acta Biol Hung 53 (1-2):7-21

Bagnall MW, Stevens RJ, du Lac S (2007) Transgenic mouse lines subdivide medial vestibular nucleus neurons into discrete, neurochemically distinct populations. J Neurosci 27 (9):2318-2330.

Balaban CD (1996) Vestibular nucleus projections to the parabrachial nucleus in rabbits: Implications for vestibular influences on the autonomic nervous system. Experimental Brain Research 108 (3):367-381

Balaban CD, Beryozkin G (1994) Vestibular Nucleus Projections to Nucleus-Tractus-Solitarius and the Dorsal Motor Nucleus of the Vagus Nerve - Potential Substrates for Vestibule-Autonomic Interactions. Experimental Brain Research 98 (2):200-212

Bausch SB, He S, Petrova Y, Wang XM, McNamara JO (2006) Plasticity of both excitatory and inhibitory synapses is associated with seizures induced by removal of chronic blockade of activity in cultured hippocampus. J Neurophysiol 96 (4):2151-2167.

Becker CG, Becker T, Meyer RL, Schachner M (1999) Tenascin-R inhibits the growth of optic fibers in vitro but is rapidly eliminated during nerve regeneration in the salamander Pleurodeles waltl. J Neurosci 19 (2):813-827

Becker CG, Schweitzer J, Feldner J, Schachner M, Becker T (2004) Tenascin-R as a repellent guidance molecule for newly growing and regenerating optic axons in adult zebrafish. Mol Cell Neurosci 26 (3):376-389.

Becker T, Anliker B, Becker CG, Taylor J, Schachner M, Meyer RL, Bartsch U (2000) Tenascin-R inhibits regrowth of optic fibers in vitro and persists in the optic nerve of mice after injury. Glia 29 (4):330-346.

Beggah AT, Dours-Zimmermann MT, Barras FM, Brosius A, Zimmermann DR, Zurn AD (2005) Lesion-induced differential expression and cell association of neurocan, brevican, versican V1 and V2 in the mouse dorsal root entry zone. Neuroscience 133 (3):749-762.

Bekku Y, Vargová L, Goto Y, Vorísek I, Dmytrenko L, Narasaki M, Ohtsuka A, Fässler R, Ninomiya Y, Syková E, Oohashi T (2010) Bral1: its role in diffusion barrier formation and conduction velocity in the CNS.
J Neurosci. 30(8):3113-23

Bekku Y, Oohashi T (2010) Neurocan contributes to the molecular heterogeneity of the perinodal ECM. Archives of Histology and Cytology 73 (2):95-102

Bekku Y, Rauch U, Ninomiya Y, Oohashi T (2009) Brevican distinctively assembles extracellular components at the large diameter nodes of Ranvier in the CNS. J Neurochem 108 (5):1266-1276.

Bertolotto A, Manzardo E, Guglielmone R (1996) Immunohistochemical mapping of perineuronal nets containing chondroitin unsulfated proteoglycan in the rat central nervous system. Cell Tissue Res 283 (2):283-295

Bignami A, Hosley M, Dahl D (1993) Hyaluronic acid and hyaluronic acid-binding proteins in brain extracellular matrix. Anat Embryol (Berl) 188 (5):419-433

Birinyi A, Straka H, Matesz C, Dieringer N (2001) Location of dye-coupled second order and of efferent vestibular neurons labeled from individual semicircular canal or otolith organs in the frog. Brain Research 921 (1-2):44-59.

Blosa M, Sonntag M, Bruckner G, Jager C, Seeger G, Matthews RT, Rubsamen R, Arendt T, Morawski M (2013) Unique Features of Extracellular Matrix in the Mouse Medial Nucleus of Trapezoid Body - Implications for Physiological Functions. Neuroscience 228:215-234.

Bradbury EJ, Moon LDF, Popat RJ, King VR, Bennett GS, Patel PN, Fawcett JW, McMahon SB (2002) Chondroitinase ABC promotes functional recovery after spinal cord injury. Nature 416 (6881):636-640.

Brodal P, Brodal A (1981) The Olivocerebellar Projection in the Monkey - Experimental Studies with the Method of Retrograde Tracing of Horseradish-Peroxidase. Journal of Comparative Neurology 201 (3):375-393.

Brown JE, Card JP, Yates BJ (2005) Polysynaptic pathways from the vestibular nuclei to the lateral mammillary nucleus of the rat: substrates for vestibular input to head direction cells. Experimental Brain Research 161 (1):47-61.

Bruckner G, Grosche J, Schmidt S, Hartig W, Margolis RU, Delpech B, Seidenbecher CI, Czaniera R, Schachner M (2000) Postnatal development of perineuronal nets in wild-type mice and in a mutant deficient in tenascin-R. J Comp Neurol 428 (4):616-629.

Bruckner G, Morawski M, Arendt T (2008) Aggrecan-based extracellular matrix is an integral part of the human basal ganglia circuit. Neuroscience 151 (2):489-504.

Buttmer U, Buttner-Ennever JA (2006) Present concepts of oculomotor organization. Neuroanatomy of the Oculomotor System 151:1-42.

Butz M, Worgotter F, van Ooyen A (2009) Activity-dependent structural plasticity. Brain Research Reviews 60 (2):287-305.

Camp AJ, Callister RJ, Brichta AM (2006) Inhibitory synaptic transmission differs in mouse type A and B medial vestibular nucleus neurons in vitro. J Neurophysiol 95 (5):3208-3218

Carbonetto S (1984) The Extracellular-Matrix of the Nervous-System. Trends in Neurosciences 7 (10):382-387.

Carpenter MB (1967) Central connections of the vestibular system. Arch Otolaryngol 85 (5):517-520

Carulli D, Pizzorusso T, Kwok JCF, Putignano E, Poli A, Forostyak S, Andrews MR, Deepa SS, Glant TT, Fawcett JW (2010) Animals lacking link protein have attenuated perineuronal nets and persistent plasticity. Brain 133:2331-2347.

Carulli D, Rhodes KE, Brown DJ, Bonnert TP, Pollack SJ, Oliver K, Strata P, Fawcett JW (2006) Composition of perineuronal nets in the adult rat cerebellum and the cellular origin of their components. J Comp Neurol 494 (4):559-577.

Celio MR, Spreafico R, De Biasi S, Vitellaro-Zuccarello L (1998) Perineuronal nets: past and present. Trends Neurosci 21 (12):510-515.

Chandran PL, Horkay F (2012) Aggrecan, an unusual polyelectrolyte: Review of solution behavior and physiological implications. Acta Biomaterialia 8 (1):3-12

Chaturvedi M, Kaczmarek L (2014) MMP-9 Inhibition: a Therapeutic Strategy in Ischemic Stroke. Molecular Neurobiology 49 (1):563-573.

Chklovskii DB, Mel BW, Svoboda K (2004) Cortical rewiring and information storage. Nature 431 (7010):782-788.

Cicanic M, Sykova E, Vargova L (2012) Bral1: "Superglue" for the extracellular matrix in the brain white matter. International Journal of Biochemistry & Cell Biology 44 (4):596-599.

Colognato H, Yurchenco PD (2000) Form and function: The laminin family of heterotrimers. Developmental Dynamics 218 (2):213-234.

Costa C, Tortosa R, Domenech A, Vidal E, Pumarola M, Bassols A (2007) Mapping of aggrecan, hyaluronic acid, heparan sulphate proteoglycans and aquaporin 4 in the central nervous system of the mouse. J Chem Neuroanat 33 (3):111-123.

Curthoys IS, Halmagyi GM (1995) Vestibular compensation: a review of the oculomotor, neural, and clinical consequences of unilateral vestibular loss. J Vestib Res 5 (2):67-107.

Curthoys IS, Halmagyi GM (1999) Vestibular compensation. Adv Otorhinolaryngol 55:82-110

Darlington CL, Smith PF (2000) Molecular mechanisms of recovery from vestibular damage in mammals: recent advances. Prog Neurobiol 62 (3):313-325.

Deepa SS, Carulli D, Galtrey C, Rhodes K, Fukuda J, Mikami T, Sugahara K, Fawcett JW (2006) Composition of perineuronal net extracellular matrix in rat brain: a different disaccharide composition for the net-associated proteoglycans. J Biol Chem 281 (26):17789-17800.

de Waele C, Loquet G, Campos Torres A, Vidal PP (2000) Lack of growth-associated protein-43 reemergence or of growth-associated protein-43 mRNA modulation in deafferented vestibular nuclei during the first 6 weeks after unilateral inner ear lesion. Exp Brain Res32(4):464-75

Dieringer N (1995) 'Vestibular compensation': neural plasticity and its relations to functional recovery after labyrinthine lesions in frogs and other vertebrates. Prog Neurobiol 46 (2-3):97-129

Dityatev A, Fellin T (2008) Extracellular matrix in plasticity and epileptogenesis. Neuron Glia Biology 4:235-247.

Dityatev A, Rusakov DA (2011) Molecular signals of plasticity at the tetrapartite synapse. Current Opinion in Neurobiology 21 (2):353-359.

Dityatev A, Schachner M (2003) Extracellular matrix molecules and synaptic plasticity. Nat Rev Neurosci 4 (6):456-468.

Dityatev A, Schachner M (2006) The extracellular matrix and synapses. Cell and Tissue Research 326 (2):647-654.
Dityatev A, Schachner M, Sonderegger P (2010) The dual role of the extracellular matrix in synaptic plasticity and homeostasis. Nature Reviews Neuroscience 11 (11):735-746.
Donevan AH, MacDonald JA, Brennan PA, Rose PK (1992) Morphology of single vestibulospinal collaterals in the upper cervical spinal cord of the cat. II. Collaterals originating from axons outside the ventral funiculi. J Comp Neurol 322 (3):343-359.
Dours-Zimmermann MT, Maurer K, Rauch U, Stoffel W, Fassler R, Zimmermann DR (2009) Versican V2 Assembles the Extracellular Matrix Surrounding the Nodes of Ranvier in the CNS. Journal of Neuroscience 29 (24):7731-7742.
Dutheil S, Escoffier G, Gharbi A, Watabe I, Tighilet B GABA(A) receptor agonist and antagonist alter vestibular compensation and different steps of reactive neurogenesis in deafferented vestibular nuclei of adult cats. J Neurosci 33 (39):15555-15566.
Dutheil S, Lacour M, Tighilet B [Discovering a new functional neurogenic zone: the vestibular nuclei of the brainstem]. Med Sci (Paris) 27 (6-7):605-613.
Dutia MB (2010) Mechanisms of vestibular compensation: recent advances. Current Opinion in Otolaryngology & Head and Neck Surgery 18 (5):420-424.
Epema AH, Gerrits NM, Voogd J (1988) Commissural and Intrinsic Connections of the Vestibular Nuclei in the Rabbit - a Retrograde Labeling Study. Experimental Brain Research 71 (1):129-146
Eugene D, Idoux E, Beraneck M, Moore LE, Vidal PP (2011) Intrinsic membrane properties of central vestibular neurons in rodents. Experimental Brain Research 210 (3-4):423-436.
Faissner A, Heck N, Dobbertin A, Garwood J (2006) DSD-1-proteoeycan/phosphacan and receptor protein tyrosine phosphatase-beta isoforms during development and regeneration of neural tissues. Brain Repair 557:25-53
Fanardjian VV, Manvelyan LR, Zakarian VL, Pogossian VI, Nasoyan AM (1999) Electrophysiological properties of the somatotopic organization of the vestibulospinal system in the frog. Neuroscience 94 (3):845-857.
Fawcett J (2002) Repair of spinal cord injuries: where are we, where are we going? Spinal Cord 40 (12):615-623.
Fraser JRE, Laurent TC, Laurent UBG (1997) Hyaluronan: Its nature, distribution, functions and turnover. Journal of Internal Medicine 242 (1):27-33.
Friedlander DR, Milev P, Karthikeyan L, Margolis RK, Margolis RU, Grumet M (1994) Neuronal Chondroitin Sulfate Proteoglycan Neurocan Binds to the Neural Cell-Adhesion Molecules Ng-Cam/L1/Nile and N-Cam, and Inhibits Neuronal Adhesion and Neurite Outgrowth. Journal of Cell Biology 125 (3):669-680.
Frischknecht R, Heine M, Perrais D, Seidenbecher CI, Choquet D, Gundelfinger ED (2009) Brain extracellular matrix affects AMPA receptor lateral mobility and short-term synaptic plasticity. Nature Neuroscience 12 (7):897-U115.
Frischknecht R, Seidenbecher CI (2012) Brevican: A key proteoglycan in the perisynaptic extracellular matrix of the brain. International Journal of Biochemistry & Cell Biology 44 (7):1051-1054.
Fritsch M, Reichenbach HD, Wolf E, Brem G (1997) Development rate of in vitro fertilized oocytes with fresh and cryopreserved semen of the same bulls. Reproduction in Domestic Animals 32 (1-2):91-91
Gacek RR (1969) The course and central termination of first order neurons supplying vestibular endorgans in the cat. Acta Otolaryngol Suppl 254:1-66
Galtrey CM, Asher RA, Nothias F, Fawcett JW (2007) Promoting plasticity in the spinal cord with chondroitinase improves functional recovery after peripheral nerve repair. Brain 130:926-939.
Galtrey CM, Fawcett JW (2007a) The role of chondroitin sulfate proteoglycans in regeneration and plasticity in the central nervous system. Brain Res Rev 54 (1):1-18.
Galtrey CM, Fawcett JW (2007b) The role of chondroitin sulfate proteoglycans in regeneration and plasticity in the central nervous system. Brain Research Reviews 54 (1):1-18.
Galtrey CM, Kwok JCF, Carulli D, Rhodes KE, Fawcett JW (2008) Distribution and synthesis of extracellular matrix proteoglycans, hyaluronan, link proteins and tenascin-R in the rat spinal cord. European Journal of Neuroscience 27 (6):1373-1390.
Gáti G, Morwski M, Lendvai D, Matthews RT, Jäger C, Zachar G, Arendt T, Alpár A (2010) Chondroitin sulphate proteoglycan-based perineuronal net establishment is largely activity-dependent in chick visual system. J Chem. Neuroanatomy 40:243-247.
Gáti G, Morawski M, Lendvai D, Jäger C, Négyessy L, Arendt T, Alpár A. (2010) Distribution and classification of aggrecan-based extracellular matrix in the thalamus of the rat. J Neurosci. Research 88(15):3257-66
Gherardini L, Gennaro M, Pizzorusso T Perilesional Treatment with Chondroitinase ABC and Motor Training Promote Functional Recovery After Stroke in Rats. Cereb Cortex.

Giamanco KA, Morawski M, Matthews RT (2010) Perineuronal Net Formation and Structure in Aggrecan Knockout Mice. Neuroscience 170 (4):1314-1327.
Grimpe B, Silver J (2004) A novel DNA enzyme reduces glycosaminoglycan chains in the glial scar and allows microtransplanted dorsal root ganglia axons to regenerate beyond lesions in the spinal cord. J Neurosci 24 (6):1393-1397.
Hagihara K, Miura R, Kosaki R, Berglund E, Ranscht B, Yamaguchi Y (1999) Immunohistochemical evidence for the brevican-tenascin-R interaction: Colocalization in perineuronal nets suggests a physiological role for the interaction in the adult rat brain. Journal of Comparative Neurology 410 (2):256-264
Halasi G, Bacskai T, Matesz C (2005) Connections of the superior vestibular nucleus with the oculomotor and red nuclei in the rat: an electron microscopic study. Brain Res Bull 66 (4-6):532-535.
Halasi G, Wolf E, Bacskai T, Szekely G, Modis L, Szigeti ZM, Meszar Z, Felszeghy S, Matesz C (2007) The effect of vestibular nerve section on the expression of the hyaluronan in the frog, Rana esculenta. Brain Struct Funct 212 (3-4):321-334.
Hall CL, Turley EA (1995) Hyaluronan: RHAMM mediated cell locomotion and signaling in tumorigenesis. Journal of Neuro-Oncology 26 (3):221-229.
Hamilton SR, Fard SF, Paiwand FF, Tolg C, Veiseh M, Wang C, McCarthy JB, Bissell MJ, Koropatnick J, Turley EA (2007) The hyaluronan receptors CD44 and Rhamm (CD168) form complexes with ERK1,2 that sustain high basal motility in breast cancer cells. Journal of Biological Chemistry 282 (22):16667-16680.
Hartig W, Brauer K, Bruckner G (1992) Wisteria floribunda agglutinin-labelled nets surround parvalbumin-containing neurons. Neuroreport 3 (10):869-872
Hartig W, Derouiche A, Welt K, Brauer K, Grosche J, Mader M, Reichenbach A, Bruckner G (1999) Cortical neurons immunoreactive for the potassium channel Kv3.1b subunit are predominantly surrounded by perineuronal nets presumed as a buffering system for cations. Brain Research 842 (1):15-29.
Highstein SM (1971) Organization of the inhibitory and excitatory vestibulo-ocular reflex pathways to the third and fourth nuclei in rabbit. Brain Res 32 (1):218-224. doi:0006-8993(71)90169-7 [pii]
Hill JJ, Jin KL, Mao XO, Xie L, Greenberg DA (2012) Intracerebral chondroitinase ABC and heparan sulfate proteoglycan glypican improve outcome from chronic stroke in rats. Proceedings of the National Academy of Sciences of the United States of America 109 (23):9155-9160. doi:DOI 10.1073/pnas.1205697109
Holstege G (1988) Brainstem-spinal cord projections in the cat, related to control of head and axial movements. Rev Oculomot Res 2:431-470
Holstein GR, Friedrich VL, Kang T, Kukielka E, Martinelli GP (2011) Direct Projections from the Caudal Vestibular Nuclei to the Ventrolateral Medulla in the Rat. Neuroscience 175:104-117.
Honrubia V, Sitko S, Kimm J, Betts W, Schwartz I (1981) Physiological and anatomical characteristics of primary vestibular afferent neurons in the bullfrog. Int J Neurosci 15 (4):197-206
Hubbard SR, Gnanasambandan K (2013) Structure and activation of MuSK, a receptor tyrosine kinase central to neuromuscular junction formation. Biochimica Et Biophysica Acta-Proteins and Proteomics 1834 (10):2166-2169.
Hurtado A, Podinin H, Oudega M, Grimpe B (2008) Deoxyribozyme-mediated knockdown of xylosyltransferase-1 mRNA promotes axon growth in the adult rat spinal cord. Brain 131:2596-2605. doi:Doi 10.1093/Brain/Awn206
Ito J, Matsuoka I, Sasa M, Takaori S (1985) Commissural and ipsilateral internuclear connection of vestibular nuclear complex of the cat. Brain Res 341 (1):73-81.
Ito M, Highstein SM, Tsuchiya T (1970) The postsynaptic inhibition of rabbit oculomotor neurones by secondary vestibular impulses and its blockage by picrotoxin. Brain Res 17 (3):520-523.
Jian BJ, Acernese AW, Lorenzo J, Card JP, Yates BJ (2005) Afferent pathways to the region of the vestibular nuclei that participates in cardiovascular and respiratory control. Brain Res 1044 (2):241-250.
Johnston AR, MacLeod NK, Dutia MB (1994) Ionic conductances contributing to spike repolarization and after-potentials in rat medial vestibular nucleus neurones. J Physiol 481 (Pt 1):61-77
Kerman IA, Akil H, Watson SJ (2006) Rostral elements of sympatho-motor circuitry: A virally mediated transsynaptic tracing study. Journal of Neuroscience 26 (13):3423-3433.
Khaing ZZ, Milman BD, Vanscoy JE, Seidlits SK, Grill RJ, Schmidt CE High molecular weight hyaluronic acid limits astrocyte activation and scar formation after spinal cord injury. J Neural Eng 8 (4):046033.
Kilcoyne M, Sharma S, McDevitt N, O'Leary C, Joshi L, McMahon SS (2012) Neuronal glycosylation differentials in normal, injured and chondroitinase-treated environments. Biochemical and Biophysical Research Communications 420 (3):616-622.
Knapska E, Lioudyno V, Kiryk A, Mikosz M, Gorkiewicz T, Michaluk P, Gawlak M, Chaturvedi M, Mochol G, Balcerzyk M, Wojcik DK, Wilczynski GM, Kaczmarek L (2013) Reward Learning Requires Activity of Matrix Metalloproteinase-9 in the Central Amygdala. Journal of Neuroscience 33 (36):14591-14600.

Kodama T, Guerrero S, Shin M, Moghadam S, Faulstich M, du Lac S (2012) Neuronal Classification and Marker Gene Identification via Single-Cell Expression Profiling of Brainstem Vestibular Neurons Subserving Cerebellar Learning. Journal of Neuroscience 32 (23):7819-7831.

Koppe G, Bruckner G, Brauer K, Hartig W, Bigl V (1997) Developmental patterns of proteoglycan-containing extracellular matrix in perineuronal nets and neuropil of the postnatal rat brain. Cell Tissue Res 288 (1):33-41

Kwok JCF, Afshari F, Garcia-Alias G, Fawcett J (2008) Proteoglycans in the central nervous system: Plasticity, regeneration and their stimulation with chondroitinase ABC. Restorative Neurology and Neuroscience 26 (2-3):131-145

Kwok JCF, Carulli D, Fawcett JW (2010) In vitro modeling of perineuronal nets: hyaluronan synthase and link protein are necessary for their formation and integrity. Journal of Neurochemistry 114 (5):1447-1459.

Kwok JCF, Dick G, Wang DF, Fawcett JW (2011) Extracellular Matrix and Perineuronal Nets in CNS Repair. Developmental Neurobiology 71 (11):1073-1089.

Ladpli R, Brodal A (1968) Experimental studies of commissural and reticular formation projections from the vestibular nuclei in the cat. Brain Res 8 (1):65-96.

Lendvai D, Morawski M, Bruckner G, Negyessy L, Baksa G, Glasz T, Patonay L, Matthews RT, Arendt T, Alpar A (2012) Perisynaptic Aggrecan-Based Extracellular Matrix Coats in the Human Lateral Geniculate Body Devoid of Perineuronal Nets. Journal of Neuroscience Research 90 (2):376-387.

Leonova EI, Galzitskaya OV (2013) Structure and functions of syndecans in vertebrates. Biochemistry-Moscow 78 (10):1071-1085.

Li H, Godfrey DA, Rubin AM (1999) Astrocyte reaction in the rat vestibular nuclei after unilateral removal of Scarpa's ganglion. Ann Otol Rhinol Laryngol 108 (2):181-188

Lin CM, Lin JW, Chen YC, Shen HH, Wei L, Yeh YS, Chiang YH, Shih R, Chiu PL, Hung KS, Yang LY, Chiu WT (2009) Hyaluronic acid inhibits the glial scar formation after brain damage with tissue loss in rats. Surg Neurol 72 Suppl 2:S50-54.

Lindwall C, Olsson M, Osman AM, Kuhn HG, Curtis MA (2013) Selective expression of hyaluronan and receptor for hyaluronan mediated motility (Rhamm) in the adult mouse subventricular zone and rostral migratory stream and in ischemic cortex. Brain Research 1503:62-77.

Lau LW, Cua R, Keough MB, Haylock-Jacobs S, Yonf WV (2013) Pathophysiology of the brain extracellular matrix: a new target for remyelination. Nat. Reviews vol. 14: 722-729.

Malinvaud D, Vassias I, Reichenberger I, Rossert C, Straka H (2010) Functional Organization of Vestibular Commissural Connections in Frog. Journal of Neuroscience 30 (9):3310-3325.

Margolis RK, Margolis RU, Preti C, Lai D (1975) Distribution and metabolism of glycoproteins and glycosaminoglycans in subcellular fractions of brain. Biochemistry 14 (22):4797-4804

Margolis RU, Margolis RK (1997) Chondroitin sulfate proteoglycans as mediators of axon growth and pathfinding. Cell Tissue Res 290 (2):343-348

Massey JM, Hubscher CH, Wagoner MR, Decker JA, Amps J, Silver J, Onifer SM (2006) Chondroitinase ABC digestion of the perineuronal net promotes functional collateral sprouting in the cuneate nucleus after cervical spinal cord injury. Journal of Neuroscience 26 (16):4406-4414.

Matesz C (1979) Central Projection of the VIIIth-Cranial Nerve in the Frog. Neuroscience 4 (12):2061

Matesz C (1988) Fine structure of the primary afferent vestibulocochlear terminals in the frog. Acta Biol Hung 39 (2-3):267-277

Matesz C, Kulik A, Bacskai T (2002) Ascending and descending projections of the lateral vestibular nucleus in the frog Rana esculenta. J Comp Neurol 444 (2):115-128.

Matesz C, Nagy E, Kulik A, Tonkol A (1997) Projections of the medial and superior vestibular nuclei to the brainstem and spinal cord in the rat. Neurobiology (Bp) 5 (4):489-493

Matthews RT, Kelly GM, Zerillo CA, Gray G, Tiemeyer M, Hockfield S (2002) Aggrecan glycoforms contribute to the molecular heterogeneity of perineuronal nets. J Neurosci 22(17):7536-47.

Maurel P, Rauch U, Flad M, Margolis RK, Margolis RU (1994) Phosphacan, a Chondroitin Sulfate Proteoglycan of Brain That Interacts with Neurons and Neural Cell-Adhesion Molecules, Is an Extracellular Variant of a Receptor-Type Protein-Tyrosine-Phosphatase. Proceedings of the National Academy of Sciences of the United States of America 91 (7):2512-2516.

McCall AA, Yates BJ Compensation following bilateral vestibular damage. Front Neurol 2:88.

McCrea RA, Strassman A, Highstein SM (1987a) Anatomical and physiological characteristics of vestibular neurons mediating the vertical vestibulo-ocular reflexes of the squirrel monkey. J Comp Neurol 264 (4):571-594.

McCrea RA, Strassman A, May E, Highstein SM (1987b) Anatomical and physiological characteristics of vestibular neurons mediating the horizontal vestibulo-ocular reflex of the squirrel monkey. J Comp Neurol 264 (4):547-570.

McCrea SM (2007) Measurement of recovery after traumatic brain injury: A cognitive-neuropsychological comparison of the WAIS-R with the Cognitive Assessment System (CAS) in a single case of atypical language lateralization. Applied Neuropsychology 14 (4):296-304

McElvain LE, Bagnall MW, Sakatos A, du Lac S (2010) Bidirectional Plasticity Gated by Hyperpolarization Controls the Gain of Postsynaptic Firing Responses at Central Vestibular Nerve Synapses. Neuron 68 (4):763-775.

Meland MN, Herndon ME, Stipp CS (2010) Expression of alpha 5 Integrin Rescues Fibronectin Responsiveness in NT2N CNS Neuronal Cells. Journal of Neuroscience Research 88 (1):222-232.

Mentlein R, Hattermann K, Held-Feindt J (2011) Proteases Involved in Glioma Invasion. Glia 59:S40-S40

Michaluk P, Mikasova L, Groc L, Frischknecht R, Choquet D, Kaczmarek L (2009) Matrix Metalloproteinase-9 Controls NMDA Receptor Surface Diffusion through Integrin beta 1 Signaling. Journal of Neuroscience 29 (18):6007-6012.

Michaluk P, Wawrzyniak M, Alot P, Szczot M, Wyrembek P, Mercik K, Medvedev N, Wilczek E, De Roo M, Zuschratter W, Muller D, Wilczynski GM, Mozrzymas JW, Stewart MG, Kaczmarek L, Wlodarczyk J (2011) Influence of matrix metalloproteinase MMP-9 on dendritic spine morphology. Journal of Cell Science 124 (19):3369-3380.

Minor LB, Mccrea RA, Goldberg JM (1990) Dual Projections of Secondary Vestibular Axons in the Medial Longitudinal Fasciculus to Extraocular Motor Nuclei and the Spinal-Cord of the Squirrel-Monkey. Experimental Brain Research 83 (1):9-21

Mitsacos A, Reisine H, Highstein SM (1983a) The superior vestibular nucleus: an intracellular HRP study in the cat. I. Vestibulo-ocular neurons. J Comp Neurol 215 (1):78-91.

Mitsacos A, Reisine H, Highstein SM (1983b) The superior vestibular nucleus: an intracellular HRP study in the cat. II. Non-vestibulo-ocular neurons. J Comp Neurol 215 (1):92-107.

Montgomery NM (1988) Projections of the Vestibular and Cerebellar Nuclei in Rana-Pipiens. Brain Behavior and Evolution 31 (2):82-95.

Moon LD, Asher RA, Fawcett JW (2003) Limited growth of severed CNS axons after treatment of adult rat brain with hyaluronidase. J Neurosci Res 71 (1):23-37.

Morawski M, Alpar A, Bruckner G, Fiedler A, Jager C, Gati G, Stieler JT, Arendt T (2009) Chondroitin sulfate proteoglycan-based extracellular matrix in chicken (Gallus domesticus) brain. Brain Research 1275:10-23.

Morawski M, Bruckner G, Arendt T, Matthews RT (2012) Aggrecan: Beyond cartilage and into the brain. International Journal of Biochemistry & Cell Biology 44 (5):690-693. doi:DOI 10.1016/j.biocel.2012.01.010

Morawski M, Bruckner G, Jager C, Seeger G, Kunzle H, Arendt T (2010) Aggrecan-Based Extracellular Matrix Shows Unique Cortical Features and Conserved Subcortical Principles of Mammalian Brain Organization in the Madagascan Lesser Hedgehog Tenrec (Echinops Telfairi Martin, 1838). Neuroscience 165 (3):831-849.

Morita S, Oohira A, Miyata S (2010) Activity-Dependent Remodeling of Chondroitin Sulfate Proteoglycans Extracellular Matrix in the Hypothalamo-Neurohypophysial System. Neuroscience 166 (4):1068-1082.

Nagy V, Bozdagi O, Matynia A, Balcerzyk M, Okulski P, Dzwonek J, Costa RM, Silva AJ, Kaczmarek L, Huntley GW (2006) Matrix metalloproteinase-9 is required for hippocampal late-phase long-term potentiation and memory. Journal of Neuroscience 26 (7):1923-1934.

Newman A, Kuruvilla A, Pereda A, Honrubia V (1986) Regeneration of the eight cranial nerve. I. Anatomic verification in the bullfrog. Laryngoscope 96 (5):484-493

Oohashi T, Hirakawa S, Bekku Y, Rauch U, Zimmermann DR, Su WD, Ohtsuka A, Murakami T, Ninomiya Y (2002) Bral1, a brain-specific link protein, colocalizing with the versican V2 isoform at the nodes of Ranvier in developing and adult, mouse central nervous systems. Molecular and Cellular Neuroscience 19 (1):43-57.

Oohira A, Matsui F, Tokita Y, Yamauchi S, Aono S (2000) Molecular interactions of neural chondroitin sulfate proteoglycans in the brain development. Archives of Biochemistry and Biophysics 374 (1):24-34.

Opdam P, Kemali M, Nieuwenhuys R (1976) Topological Analysis of Brain-Stem of Frogs Rana-Esculenta and Rana-Catesbeiana. Journal of Comparative Neurology 165 (3):307-331. doi:DOI 10.1002/cne.901650304

Pajenda G, Pajer K, Marton G, Hegyi P, Redl H, Nogradi A (2013) Rescue of injured motoneurones by grafted neuroectodermal stem cells: Effect of the location of graft. Restorative Neurology and Neuroscience 31 (3):263-274.

Pesheva P, Probstmeier R (2000) The yin and yang of tenascin-R in CNS development and pathology. Prog Neurobiol 61 (5):465-493.

Peterson BW, Coulter JD (1977) New Long Spinal Projection from Vestibular Nuclei in Cat. Brain Research 122 (2):351-356

Peusner KD, Lindberg NH, Mansfield PF (1988) Ultrastructural study of calycine synaptic endings of colossal vestibular fibers in the cristae ampullares of the developing chick. Int J Dev Neurosci 6 (3):267-283
Pizzorusso T, Medini P, Berardi N, Chierzi S, Fawcett JW, Maffei L (2002) Reactivation of ocular dominance plasticity in the adult visual cortex. Science 298 (5596):1248-1251.
Pompeiano O, Brodal A (1957) Spinovestibular fibers in the cat; an experimental study. J Comp Neurol 108 (3):353-381
Porter JD, Balaban CD (1997) Connections between the vestibular nuclei and brain stem regions that mediate autonomic function in the rat. Journal of Vestibular Research-Equilibrium & Orientation 7 (1):63-76
Precht W, Llinas R (1969) Functional organization of the vestibular afferents to the cerebellar cortex of frog and cat. Exp Brain Res 9 (1):30-52
Precht W, Shimazu H, Markham CH (1966) A mechanism of central compensation of vestibular function following hemilabyrinthectomy. J Neurophysiol 29 (6):996-1010
Preston M, Sherman LS Neural stem cell niches: roles for the hyaluronan-based extracellular matrix. Front Biosci (Schol Ed) 3:1165-1179.
Racz E, Bacskai T, Halasi G, Kovacs E, Matesz C (2006) Organization of dye-coupled cerebellar granule cells labeled from afferent vestibular and dorsal root fibers in the frog Rana esculenta. Journal of Comparative Neurology 496 (3):382-394.
Rauch U (2007) Brain matrix: structure, turnover and necessity. International Journal of Experimental Pathology 88 (6):A81-A81
Rauch U, Feng K, Zhou XH (2001) Neurocan: a brain chondroitin sulfate proteoglycan. Cellular and Molecular Life Sciences 58 (12-13):1842-1856.
Rauch U, Grimpe B, Kulbe G, Arnoldammer I, Beier DR, Fassler R (1995) Structure and Chromosomal Localization of the Mouse Neurocan Gene. Genomics 28 (3):405-410.
Reichenberger I, Dieringer N (1994) Size-related colocalization of glycine and glutamate immunoreactivity in frog and rat vestibular afferents. J Comp Neurol 349 (4):603-614.
Rhodes KE, Fawcett JW (2004) Chondroitin sulphate proteoglycans: preventing plasticity or protecting the CNS? J Anat 204 (1):33-48.
Ris L, de Waele C, Serafin M, Vidal PP, Godaux E (1995) Neuronal activity in the ipsilateral vestibular nucleus following unilateral labyrinthectomy in the alert guinea pig. J Neurophysiol 74 (5):2087-2099
Ris L, Godaux E (1998) Neuronal activity in the vestibular nuclei after contralateral or bilateral labyrinthectomy in the alert guinea pig. J Neurophysiol 80 (5):2352-2367
Ruggiero DA, Mtui EP, Otake K, Anwar M (1996) Vestibular afferents to the dorsal vagal complex: substrate for vestibular-autonomic interactions in the rat. Brain Res 743 (1-2):294-302.
Ruigrok TJ, Voogd J (1990) Cerebellar nucleo-olivary projections in the rat: an anterograde tracing study with Phaseolus vulgaris-leucoagglutinin (PHA-L). J Comp Neurol 298 (3):315-333.
Rutka JT, Apodaca G, Stern R, Rosenblum M (1988) The extracellular matrix of the central and peripheral nervous systems: structure and function. J Neurosurg 69 (2):155-170.
Saito Y, Takazawa T, Ozawa S (2008) Relationship between afterhyperpolarization profiles and the regularity of spontaneous firings in rat medial vestibular nucleus neurons. Eur J Neurosci 28 (2):288-298.
Sanes JR (1989) Extracellular-Matrix Molecules That Influence Neural Development. Annual Review of Neuroscience 12:491-516. doi:DOI 10.1146/annurev.neuro.12.1.491
Schmalfeldt M, Bandtlow CE, Dours-Zimmermann MT, Winterhalter KH, Zimmermann DR (2000) Brain derived versican V2 is a potent inhibitor of axonal growth. Journal of Cell Science 113 (5):807-816
Schwartz NB, Domowicz M (2004) Proteoglycans in brain development. Glycoconj J 21 (6):329-341.
Seil JT, Webster TJ (2010) Electrically active nanomaterials as improved neural tissue regeneration scaffolds. Wiley Interdisciplinary Reviews-Nanomedicine and Nanobiotechnology 2 (6):635-647.
Sekirnjak C, du Lac S (2006) Physiological and anatomical properties of mouse medial vestibular nucleus neurons projecting to the oculomotor nucleus. J Neurophysiol 95 (5):3012-3023.
Serafin M, de Waele C, Khateb A, Vidal PP, Muhlethaler M (1991) Medial vestibular nucleus in the guinea-pig. I. Intrinsic membrane properties in brainstem slices. Exp Brain Res 84 (2):417-425
Shao M, Popratiloff A, Hirsch JC, Peusner KD (2009) Presynaptic and postsynaptic ion channel expression in vestibular nuclei neurons after unilateral vestibular deafferentation. Journal of Vestibular Research-Equilibrium & Orientation 19 (5-6):191-200.
Sharma H, Alilain WJ, Sadhu A, Silver J (2012) Treatments to restore respiratory function after spinal cord injury and their implications for regeneration, plasticity and adaptation. Experimental Neurology 235 (1):18-25.
Shin BS, Oh SY, Kim JS, Kim TW, Seo MW, Lee H, Park YA (2012) Cervical and ocular vestibular-evoked myogenic potentials in acute vestibular neuritis. Clinical Neurophysiology 123 (2):369-375.
Shinder ME, Taube JS (2010) Differentiating ascending vestibular pathways to the cortex involved in spatial cognition. Journal of Vestibular Research-Equilibrium & Orientation 20 (1-2):3-23.

Shiroyama T, Kayahara T, Yasui Y, Nomura J, Nakano K (1999) Projections of the vestibular nuclei to the thalamus in the rat: A Phaseolus vulgaris leucoagglutinin study. Journal of Comparative Neurology 407 (3):318-332

Simmons AM, Chapman JA, Brown RA (2006) Developmental changes in cell proliferation in the auditory midbrain of the bullfrog, Rana catesbeiana. Journal of Neurobiology 66 (11):1212-1224.

Simon H, Lumsden A (1993) Rhombomere-Specific Origin of the Contralateral Vestibulo-Acoustic Efferent Neurons and Their Migration across the Embryonic Midline. Neuron 11 (2):209-220.

Smith PF, Curthoys IS (1989) Mechanisms of recovery following unilateral labyrinthectomy: a review. Brain Res Brain Res Rev 14 (2):155-180

Smith PF, Darlington CL (1991) Neurochemical mechanisms of recovery from peripheral vestibular lesions (vestibular compensation). Brain Res Brain Res Rev 16 (2):117-133

Soleman S, Yip PK, Duricki DA, Moon LDF (2012) Delayed treatment with chondroitinase ABC promotes sensorimotor recovery and plasticity after stroke in aged rats. Brain 135:1210-1223.

Sotelo C, Palay SL (1970) The fine structure of the later vestibular nucleus in the rat. II. Synaptic organization. Brain Res 18 (1):93-115

Sperry RW (1945) The problem of central nervous reorganization after nerve regeneration and muscle transposition. Q Rev Biol 20:311-369

Straka H, Baker R, Gilland E (2001) Rhombomeric organization of vestibular pathways in larval frogs. Journal of Comparative Neurology 437 (1):42-55.

Straka H, Dieringer N (1993) Electrophysiological and Pharmacological Characterization of Vestibular Inputs to Identified Frog Abducens Motoneurons and Internuclear Neurons Invitro. European Journal of Neuroscience 5 (3):251-260.

Straka H, Dieringer N (2004) Basic organization principles of the VOR: lessons from frogs. Progress in Neurobiology 73 (4):259-309.

Straka H, Vibert N, Vidal PP, Moore LE, Dutia MB (2005) Intrinsic membrane properties of vertebrate vestibular neurons: function, development and plasticity. Prog Neurobiol 76 (6):349-392.

Suarez C, Delrey CG, Tolivia J, Llorente JL, Diaz C, Navarro A, Gomez J (1993) Morphometric Analysis of the Vestibular Complex in the Rat. Laryngoscope 103 (7):762-773

Svensson G, Awad W, Hakansson M, Mani K, Logan DT (2012) Crystal Structure of N-Glycosylated Human Glypican-1 Core Protein STRUCTURE OF TWO LOOPS EVOLUTIONARILY CONSERVED IN VERTEBRATE GLYPICAN-1. Journal of Biological Chemistry 287 (17):14040-14051.

Sykova E, Nicholson C (2008) Diffusion in brain extracellular space. Physiol Rev 88 (4):1277-1340.

Takazawa T, Saito Y, Tsuzuki K, Ozawa S (2004) Membrane and firing properties of glutamatergic and GABAergic neurons in the rat medial vestibular nucleus. J Neurophysiol 92 (5):3106-3120.

Tani E, Ametani T (1971) Extracellular distribution of ruthenium red-positive substance in the cerebral cortex. J Ultrastruct Res 34 (1):1-14

Tighilet B, Brezun JM, Sylvie GD, Gaubert C, Lacour M (2007) New neurons in the vestibular nuclei complex after unilateral vestibular neurectomy in the adult cat. Eur J Neurosci 25 (1):47-58.

Uno A, Idoux E, Beraneck M, Vidal PP, Moore LE, Wilson VJ, Vibert N (2003) Static and dynamic membrane properties of lateral vestibular nucleus neurons in guinea pig brain stem slices. J Neurophysiol 90 (3):1689-1703.

Vibert N, De Waele C, Serafin M, Babalian A, Muhlethaler M, Vidal PP (1997) The vestibular system as a model of sensorimotor transformations. A combined in vivo and in vitro approach to study the cellular mechanisms of gaze and posture stabilization in mammals. Prog Neurobiol 51 (3):243-286. doi:S0301-0082(96)00057-3 [pii]

Vibert N, Serafin M, Crambes O, Vidal PP, Muhlethaler M (1995) Dopaminergic agonists have both presynaptic and postsynaptic effects on the guinea-pig's medial vestibular nucleus neurons. Eur J Neurosci 7 (4):555-562

Vidal PP, de Waele C, Vibert N, Muhlethaler M (1998) Vestibular compensation revisited. Otolaryngol Head Neck Surg 119 (1):34-42.

Vigetti D, Karousou E, Viola M, Deleonibus S, De Luca G, Passi A (2014) Hyaluronan: Biosynthesis and signaling. Biochem. et Biophys. Acta doi:org/10.1016/j.bbagen.2014.02.001

Vitellaro-Zuccarello L, De Biasi S, Spreafico R (1998) One hundred years of Golgi's "perineuronal net": history of a denied structure. Ital J Neurol Sci 19 (4):249-253

Voogd, J. 1998. Vestibular nuclei. In: Nieuwenhuys R, ten Donkelaar HJ, Nicholson C. editors. The Central Nervous System of Vertebrates Vol. 3. Berlin Heidelberg: Springer pp 1832-1837

Voogd J, Epema AH, Rubertone JA (1991) Cerebello-Vestibular Connections of the Anterior Vermis - a Retrograde Tracer Study in Different Mammals Including Primates. Archives Italiennes De Biologie 129 (1):3-19

Voogd J, Gerrits NM (1998) Olivocerebellar projection and compartmental organization of the monkey cerebellum. European Journal of Neuroscience 10:304-304

Wakao N, Imagama S, Zhang H, Tauchi R, Muramoto A, Natori T, Takeshita S, Ishiguro N, Matsuyama Y, Kadomatsu K (2011) Hyaluronan oligosaccharides promote functional recovery after spinal cord injury in rats. Neuroscience Letters 488 (3):299-304.

Wang DF, Fawcett J (2012) The perineuronal net and the control of CNS plasticity. Cell and Tissue Research 349 (1):147-160.

Wang DF, Ichiyama RM, Zhao RR, Andrews MR, Fawcett JW (2011) Chondroitinase Combined with Rehabilitation Promotes Recovery of Forelimb Function in Rats with Chronic Spinal Cord Injury. Journal of Neuroscience 31 (25):9332-9344.

Weigel PH, Hascall VC, Tammi M (1997) Hyaluronan synthases. J Biol Chem 272 (22):13997-14000

Wight TN (2002) Versican: a versatile extracellular matrix proteoglycan in cell biology. Current Opinion in Cell Biology 14 (5):617-623.

Yamaguchi Y (1996) Brevican: a major proteoglycan in adult brain. Perspect Dev Neurobiol 3 (4):307-317

Yong VW (2005) Metalloproteinases: Mediators of pathology and regeneration in the CNS. Nature Reviews Neuroscience 6 (12):931-944.

Zakon H, Capranica RR (1981) An anatomical and physiological study of regeneration of the eighth nerve in the leopard frog. Brain Res 209 (2):325-338.

Zhao RR, Fawcett JW (2013) Combination treatment with chondroitinase ABC in spinal cord injury-breaking the barrier. Neuroscience Bulletin 29 (4):477-483.

Zimmermann DR, Dours-Zimmermann MT (2008) Extracellular matrix of the central nervous system: from neglect to challenge. Histochem Cell Biol 130 (4):635-653.

11. LIST of PUBLICATIONS

UNIVERSITY OF DEBRECEN
UNIVERSITY AND NATIONAL LIBRARY
PUBLICATIONS

DEENK
www.lib.unideb.hu

Register number: DEENKÉTK/245/2014.
Item number:
Subject: Ph.D. List of Publications

Candidate: Botond Ágoston Gaál
Neptun ID: SNBEKV
Doctoral School: Doctoral School of Dental Sciences
Mtmt ID: 10037882

List of publications related to the dissertation

1. **Gaál, B.**, Rácz, É., Juhász, T., Holló, K., Matesz, C.: Distribution of extracellular matrix macromolecules in the vestibular nuclei and cerebellum of the frog, Rana esculenta. *Neuroscience. 258*, 162-173, 2014.
   DOI: http://dx.doi.org/10.1016/j.neuroscience.2013.10.080
   IF:3.327 (2013)

2. Rácz, É., **Gaál, B.**, Kecskés, S., Matesz, C.: Molecular composition of extracellular matrix in the vestibular nuclei of the rat.
   Brain Struct. Funct. 219 (4), 1385-1403, 2014.
   DOI: http://dx.doi.org/10.1007/s00429-013-0575-x
   IF:4.567 (2013)

3. Deák, Á., Bácskai, T., **Gaál, B.**, Rácz, É., Matesz, K.: Effect of unilateral labyrinthectomy on the molecular composition of perineuronal nets in the lateral vestibular nucleus of the rat.
   Neurosci. Lett. 513 (1), 1-5, 2012.
   DOI: http://dx.doi.org/10.1016/j.neulet.2012.01.076
   IF:2.026

Total IF of journals (all publications): 9,92
Total IF of journals (publications related to the dissertation): 9,92

The Candidate's publication data submitted to the iDEa Tudóstér have been validated by DEENK on the basis of Web of Science, Scopus and Journal Citation Report (Impact Factor) databases.

09 September, 2014

H- 4032 Debrecen, Egyetem tér 1. ¤ E-mail publikaciok@lib.unideb.hu

12. KEYWORDS

extracellular matrix
perineuronal net
rat vestibular system
labyrinthectomy
frog vestibular system
vestibular compensation
neural plasticity
chondroitin sulfate proteoglycans
hyaluronan
tenascin-R

12. TÁRGYSZAVAK

extracellularis matrix
perineuronalis net
patkány vestibularis rendszer
béka vestibularis rendszer
labyrinthus irtás
vestibularis compensatio
idegi plaszticitás
chondroitin sulfat proteoglycanok
hyaluronsav
tenascin-R

13. ACKNOWLEDGEMENTS

The work, providing basis for the present thesis, was completely made in the Department of Anatomy, Histology, and Embryology, Faculty of Medicine, University of Debrecen. As an agricultural engineer it is a very special privilege for me to meet the PhD requirements of medical science. For this great opportunity I would like say special thank you to all who contributed to this PhD work.

Most importantly, I would like to express my highest gratefulness to my supervisor, Prof. Dr. Klára Matesz, for the endless support in scientific career and in person, motivation, scientific and technical consultations, confidence, and for creating such friendly and inspiring atmosphere in the lab, which is at least as important as scientific standards.

I would like to say special thank you to Prof. Dr. Miklós Antal, chairman of the Anatomy Department, for granting me opportunity in research and education. Academic teaching of anatomy became an important goal to me, and has given me countless wonderful experiences. I never want to forget the support given by Prof. Dr. László Módis, in conventional histological staining, immunohistochemistry, and scientific brainstorming, but before these the personal confidence, friendly chats, and motivation, inevitable for personality progress.

This work couldn't have come true without the contribution of Dr. Zoltán Mészár assistant professor and Dr. Éva Rácz assistant lecturer. From them I could learn details of histological preparation, immunohistochemistry, microsurgery, biochemical methods, image editing, and had many scientific discussions. Besides official duties, we became very good friends.

For the technical assistance I'm very thankful to Ms. Tímea Horváth, professionally managing the laboratory, and giving sophisticated technical solutions, even in the most challenging periods. For the first steps of my lab work I am also very thankful to Mrs. Erzsébet Gregori, Dr. Tímea Bácskai, and Dr. Ádám Deák, and at present Ms. Szilvia Kecskés, Dr. András Birinyi, and Dr. Tamás Juhász. I am also very thankful to all other members of the department for the kind help, continuously provided.

And at last, but above all, I am the most grateful for my dear parents, Prof. Dr. Botond Gaál theologian and Dr. Mária Czeglédy pediatric dentist, for the love and support during my studies and future career.

14. FINANCIAL SUPPORT

MTA-TKI 11008

MTA-TKI 255

OTKA Bridging Fund

OTKA K 67641

TÁMOP-4.2.4B/2-11/1-2012-0001 Campus Hungary

TÁMOP 4.2.2/B-10/1-2010-0024 Scholarship for Predoctors

TÁMOP 4.2.4. A/2-11-1-2012-0001: This research was supported by the **European Union** and the **State of Hungary, co-financed by the European Social Fund** in the framework of TÁMOP 4.2.4. A/2-11-1-2012-0001 'National Excellence Program'.

15. SUPPLEMENTARY MATERIAL